Comparison of a Computational Method for Correcting the Humidity Influence with the Use of a Low-Cost Aerosol Dryer on a SDS011 Low-Cost PM-Sensor

Bernd Laquai (Intisys Engineering Services Stuttgart)

Bianca Kroseberg (cand. B.Sc. Phys. University of Regensburg)

May 1st, 2021

Abstract

The first topic in the course of this work was to analyse data of a sensor node in the OK Lab air quality network that uses a SDS011 low-cost PM sensor and a low-cost temperature/humidity sensor with respect to the humidity influence. This sensor node was located close to a governmental measurement station for air quality in Munich Lothstrasse, which we used as reference. Based on the PM and humidity data collected, we tried to correct the humidity influence on the low-cost sensor. The correction was based on a growth model fit to the ratio between low-cost sensor and reference data. The second topic was to compare the computationally corrected results to results obtained from a Twin-SDS measurement box containing one SDS011 equipped with a low-cost thermal dryer and another SDS011 without thermal dryer. The measurement box was operated during various field measurements and during a co-location measurement in Munich. Particularly, hygroscopic growth events and fog events were analysed and compared to the computational correction method. By accident also two Sahara dust events were captured and analysed. The results gave additional insight into error mechanisms related to the SDS011 low-cost sensor. For the co-location experiment, the constructed Twin-SDS measurement box was operated near the governmental measurement station in Munich, Lothstrasse. For the co-location measurement period, a comparison of the dryer efficiency to the professional equipment was done.

The results revealed that the SDS011 low-cost sensor data can be corrected for hygroscopic growth of PM2.5 with a growth model obtained by the help of reference equipment and using humidity data of an accurate humidity sensor only under certain conditions. The computational correction is limited to one location and a short timeframe under the condition that the hygroscopic properties of the aerosol remain stable. Additionally, a highly accurate humidity sensor suitable for outdoor use is required. A low-cost indoor humidity sensor as used in the sensor network is not sufficient. In contrast to the computational correction, the use of a thermal dryer showed a high efficiency to correct the influence of hygroscopic growth and even fog events, independent of location or time, without the need of reference equipment once being calibrated. However, the control of the dryer requires the modification of the SDS011 sensor by adding a humidity sensor into the exhaust chamber. It also would make a potential network sensor node more bulky and more costly. Nevertheless, it could be shown that the use of a thermal dryer significantly improves the data quality of the SDS011 low-cost PM sensor and achieves an excellent matching to the reference equipment of a governmental measurement station.

Introduction

PM measurements in citizen science networks

In the European Union, cities are forced by legislation to monitor air quality in terms of PM measurements at the most polluted spots using the gravimetric measurement method. The city authorities need to determine these spots and install costly and sensitive instrumentation. In practice, cities in Germany determine a few very polluted spots and do not only install gravimetric measurement equipment but also “suitable” laser scattering instruments equipped with aerosol dryers as well as other sensors for obtaining instantaneous results. This allows fast reporting of PM data combined with meteorological data and data from other pollutants. The containers where the instruments are placed must fulfil precisely defined conditions and must be secured against vandalism and theft. The support effort for these measurement containers is tremendous. Therefore, the number of spots where monitoring is performed is extremely limited.

Despite the governmental measurements many citizens are concerned about air quality in their vicinity. The air is perceived as the “food” that will cause negative health effects most quickly when quality is bad. The fact that the cities do not perform continuous measurements of air quality data over the whole urban space but only at a few very polluted spots appears frightening. On the other hand, it is partly understood that cost would be prohibitively high when the spatial and temporal distribution of PM concentration in a city would be measured with professional equipment. At this point, citizen scientists had the idea to create a network of low-cost PM sensor nodes connected to the internet as an example of an IOT (Internet of things) application, to fill this gap. This approach became possible since mainly manufacturers in Asia provided cheap laser scattering PM sensors to the electronic component market as well as IOT microcontrollers capable to connect to the internet. The construction of a sensor node just requires that both components are combined and operated in the gardens or the balconies of residential homes. Data collection was organized by small expert communities that have the expertise to operate data collection servers and to visualize the data on the Internet. Interestingly, such networks quickly grew all over the world and provided insight into air quality of the urban and even rural space.

In the scientific community and in the governmental authorities, the data collection by citizen scientists who are not always skilled in particle physics also raised the question on the quality of the data measured by low-cost sensors. However, the increasing awareness from the media on those projects put some pressure on politicians as well as on professionals to deal with the quality of the data. It became apparent that the sensors really reached a high quality for some periods but not always and under all conditions. Therefore, Universities but also the authorities started programs to assess the actual performance of the low-cost sensors. The outcome was that mainly the humidity influence in terms of fog and hygroscopic growth causes a major data quality issue. However, it also became apparent that if this issue could be solved, a low-cost sensor network could be very beneficially for society as well as for research. This understanding also fuelled this work. The idea is to improve the PM sensor node and the data processing such that the influence of humidity can be avoided or corrected, and a network can be constructed yielding data in a similar way as before but with much higher quality.

OK Lab Network

Lufdaten.info /1/ is one of the largest citizen science networks for measuring air pollution. Early 2021 it collected data from thousands of network nodes mainly distributed in Europe but also worldwide. The sensor node was developed by the OK Lab Stuttgart in Germany and consists of the low-cost laser-scattering PM sensor SDS011 from Nova Fitness (http://www.inovafitness.com) and a low-cost temperature and humidity sensor of type DHT22, both controlled by an ESP8266 IOT-controller

(NodeMCU). A great advantage of this network is its high spatial coverage which would never be possible with costly professional equipment. It is therefore able to visualize regionally distributed aerosol concentrations and their movement across the continent.

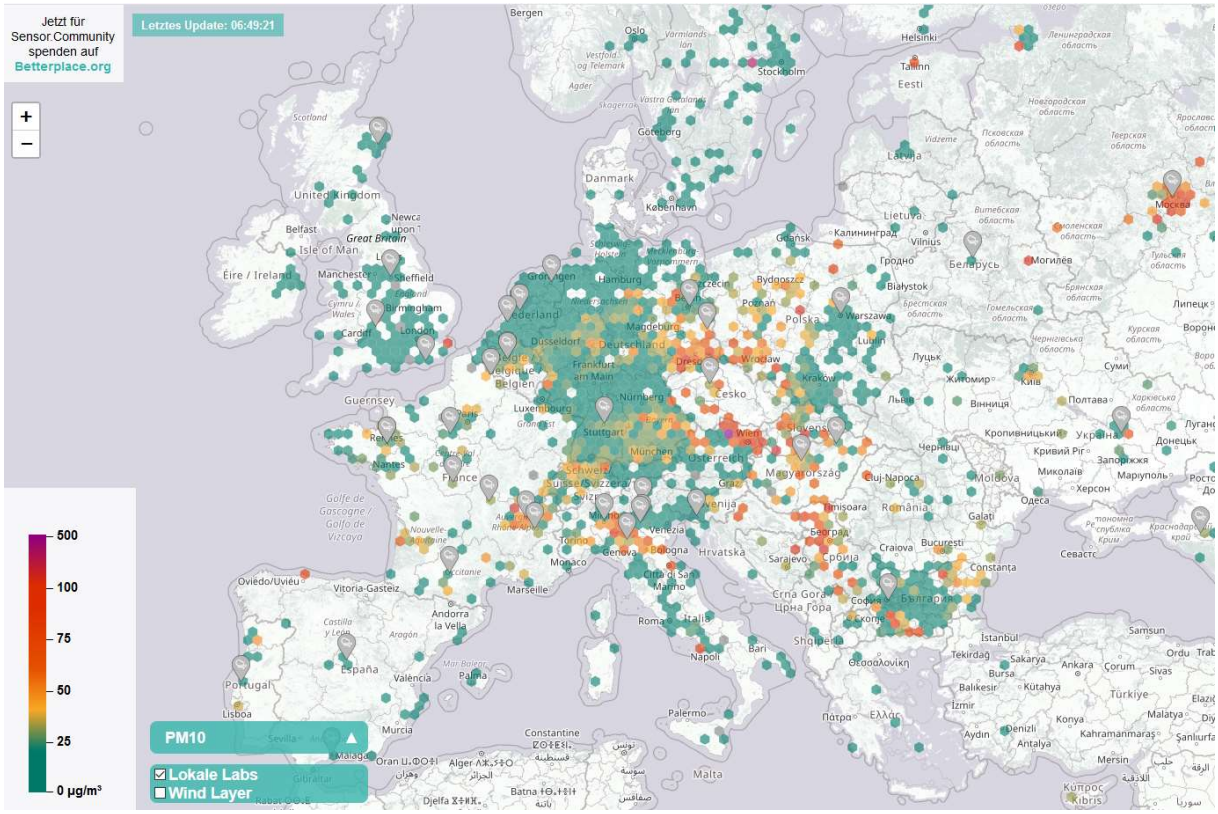

Figure 1:Georeferenced mapping of PM data gathered by the Luftdaten.info sensor network

Unfortunately, the use of low-cost sensors also showed significant disadvantages, already after the first few hundred of sensor nodes had been installed. Various sources of measurement errors were identified that lead to significant differences in the PM measurement results with respect to professional equipment used by the governmental authorities for monitoring particulate matter according to the European legislation. The European legislation requires the measurement of particulate matter in outdoor air with a focus to PM10 and the use of the gravimetric measurement method.

The SDS011 sensor is a PM2.5 sensor originally developed for the control of air conditioning systems. Since it works based on the laser-scattering principle, it is sensitive to any kind of aerosol, regardless of being composed of wet droplets, humid salt crystals or dry particles. Therefore, during periods of fog or high relative humidity, its PM measurement results cannot be compared to a gravimetric measurement method that collects dust on a filter disc and determines its dry mass by weighting it in the lab. The fact that the SDS011 device also outputs a data value named PM10 mislead the citizen science community to the assumption, the sensor can indeed detect particles up to 10um diameter. Detailed investigations of the SDS011 sensor using monodisperse particles of different size clearly revealed that the sensor is not able to detect particles larger than 5um /2/, /3/, /4/. Thus, the PM10 data output of the SDS011 sensor is assumed to be an estimation based on the particle distribution measured in a smaller size range. Both effects, the humidity sensitivity of the laser-scattering principle as well as the inability to detect large particles are the two dominant sources of measurement inaccuracy in the SDS011 PM10 output values.

There was some hope, that at least the humidity influence (not the impact of fog) can be easily mitigated since the sensor node is equipped with a temperature and humidity sensor. In the beginning an AM2302 (DHT22 type) sensor from Aosong, China was used for this purpose. It later was replaced by a higher quality BME280 sensor from Bosch. Since the growth effect of particles that contain hygroscopic salts is well understood and various models had already been developed to describe this effect /6-9/, /11/, the idea was to compensate the hygroscopic growth effect under high humidity conditions with postprocessing based on such a growth model. However, both types of temperature/humidity sensors used by the OK Lab are specified for indoor use only. Consequently, most of the temperature/humidity sensors used by the sensor nodes became defective over time (mostly just the humidity sensor not the temperature sensor) due to the wet water content in the outdoor air (fog, spray water) that contaminated the humidity sensor surface. When turning on the relative humidity data layer on the luftdaten.info map, this effect becomes visible immediately: most of the sensor nodes show a dark blue colour which means they got stuck at 99% relative humidity even during dry weather conditions.

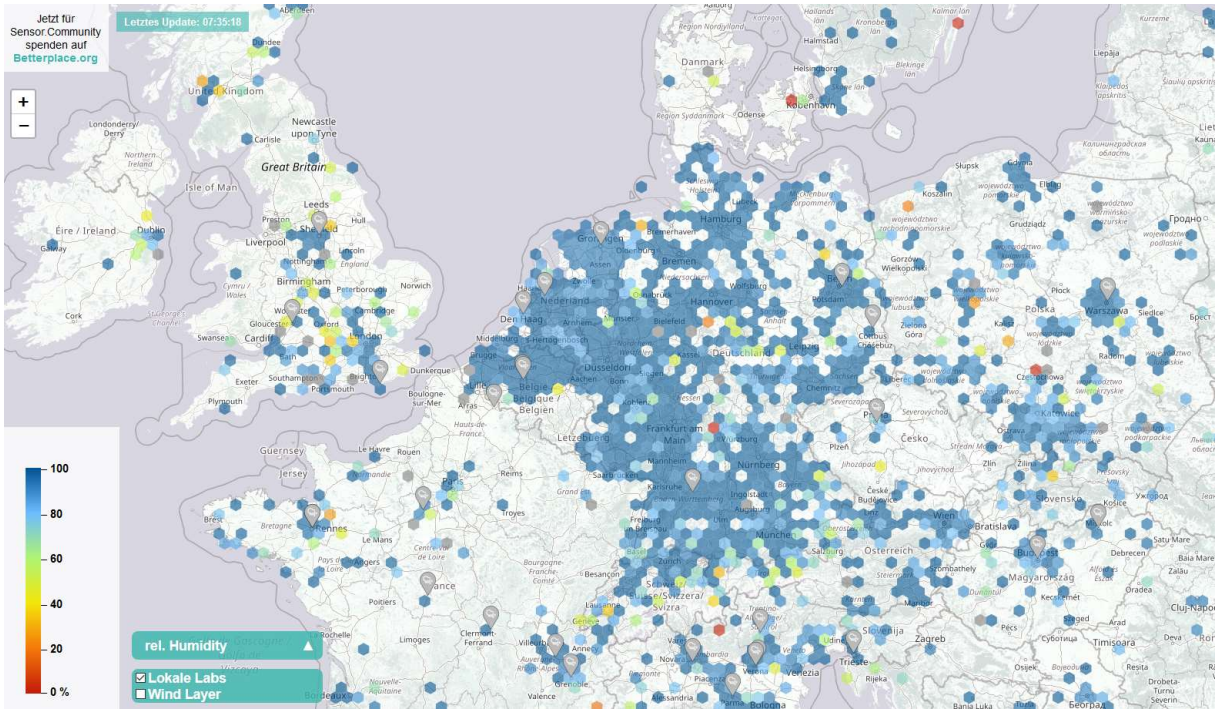

Figure 2: Corresponding humidity data layer of the luftdaten.info sensor network

Even though thousands of sensors are already installed in the network and hardly can be changed anymore, it is worthwhile to investigate the options of improvement for a next generation low-cost sensor node to achieve a higher measurement accuracy. From a cost perspective, the use of a different PM sensor other than the SD011 however, is not an attractive option since the other sensors in the same cost range (e.g., the Sensirion SPS30 or the Plantower 1003) show the same limitations with respect to large particle sizes and the humidity influence. The Alphasense OPC-N3 or OPC-R1 lower-cost sensors can detect particles beyond 10um but their cost is significantly higher (more than 100 Euro) and suffer from the humidity influence too. Therefore, they are most likely not an option to replace the SDS011 in a network with many sensor nodes. Consequently, a future low-cost PM sensor node must focus to a PM2.5 measurement only, regardless of the low-cost sensor manufacturer.

Construction of the OK lab Sensor

The OK lab sensor was designed with the focus to minimize the cost of a sensor node in a network and to have it easily assembled by unskilled citizen scientists without much effort in a short amount of

time. At this point in time, the humidity influence was unknown to the chief designer of the sensor node. The SDS011 selected as PM-sensor was available at around 20$ from various Chinese suppliers. The controller selected for the OK Lab sensor node was the cheap WLAN IOT controller ESP8266 from Espressif (China) available at a cost of about 5$ from Chinese suppliers. Even though this would have been sufficient to already create a PM measurement network node, the designer additionally added an AM2302 (DHT22 type) temperature/humidity sensor from Aosong (China) to the microcontroller. The reason was the low-cost (less than 5$), the availability of vacant pins on the controller to read out the sensor and the idea to create an option to investigate the relationship of PM values and temperature or humidity.

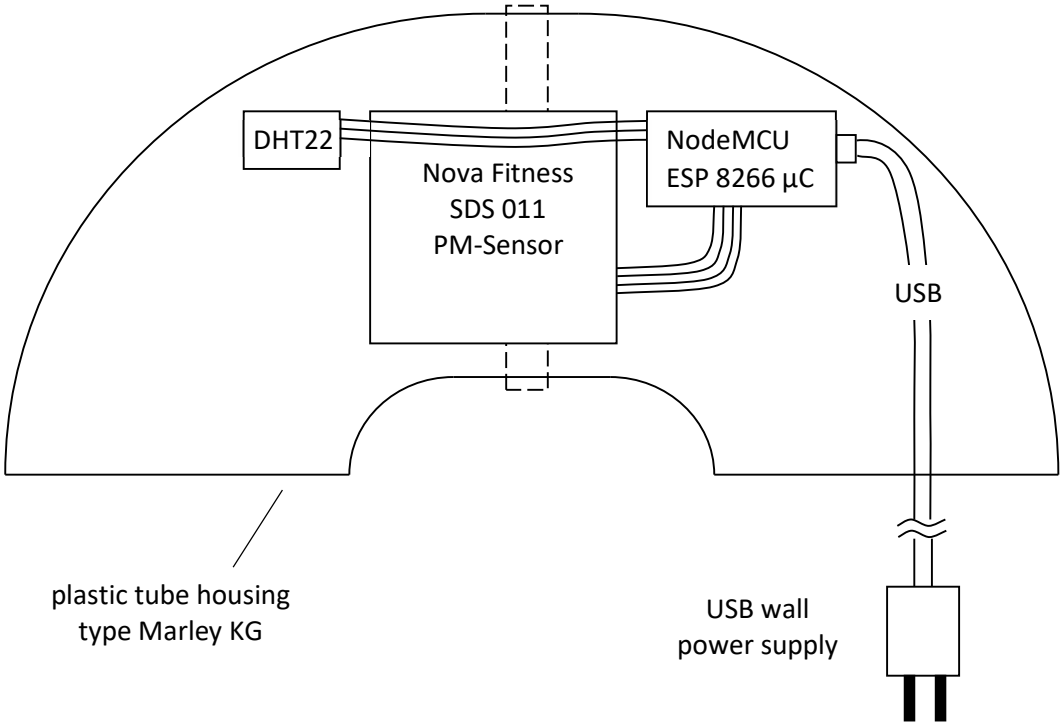

Figure 3: Construction concept of the OK lab sensor node (luftdaten.info)

However, a high risk with this design concept was, that neither the PM sensor nor the temperature/humidity sensor are specified for outdoor use, where fog may occur, and the ambient air may have a substantial wet water content. Condensing conditions for gaseous water vapor thus may cause strong measurement inaccuracy or even destroy a sensor.

As from the perspective of today, a remedy for the humidity influence two options appears attractive:

1) Correction by postprocessing with data from a humidity sensor
2) Correction using a low-cost aerosol dryer

Both options have been investigated in this work and were compared against each other.

Inaccuracies of Low-Cost PM-Sensors

Fog and hygroscopic growth

Most of the low-cost PM-sensors use the laser scattering principle for measurement of particulate matter (PM). The device measures the scattered light of a laser to count the number of particles per time interval and to determine the size (aerodynamic diameter) of the particles, assuming a certain light refractive index. From the diameter the mass can be estimated assuming a standard density of

the particle material (e.g., the density of water) and assuming a spherical shape. Using a given algorithm, and the frequency of occurrence of a certain particle mass, the mass information can be transformed into a PM concentration value. This measurement principle, however, is independent of the particle being composed of a solid material as in dust or being a water droplet around a condensation nucleus in a wet aerosol like fog, haze, or mist.

Most legal regulations on air quality, however, define limit values for PM based on a gravimetric measurement method where only the dry mass is weighted under a controlled temperature of 19-21°C and a humidity of 45-50% (ÖNORM EN 12341:2014 as an example). The problem that a scattering light sensor cannot distinguish between a dry dust or a wet aerosol induces an error in PM measurements when particles contain water. This error can get large during fog episodes or during episodes with a higher humidity when hygroscopic particles absorb the humidity.

Fog episodes occur when the ambient temperature gets close to the dew point and relative humidity gets close to 100% due to condensation of water vapour in the presence of condensation nuclei. Condensation nuclei can be for example ultra-fine particles normally not visible to laser scattering measurement devices. Often, fog builds-up at greater heights in the atmosphere where the air is cooler and then sinks to ground replacing warmer air. Since the water droplets will not vaporize such quickly, the relative humidity can stay significantly smaller than 100% despite the presence of fog. Such an effect may simply increase the wet water content in air without substantially increasing relative humidity. Under such conditions the laser scattering measurement devices that are not equipped with any means for humidity correction simply measure the PM including the mass of the water around smaller solid particles or around condensation nuclei. The error can get exceptionally large, since fog droplets can have diameters broadly distributed between hundreds of nanometres and tens of micrometres and their mass is proportional to the 3rd power of the diameter.

In contrast, hygroscopic growth of environmental particles starts significantly above the dew point, typically when relative humidity increases above 60-70%. Depending on location and season, environmental particles may contain various hygroscopic salts in various concentrations such as sodium chloride or ammonium sulphate. The hygroscopicity of salts is described by their deliquescence and efflorescence points and show a hysteresis in the so called humidogram. Both points depend on the size of the particles /5/, /6/. Smaller particles tend to absorb water at smaller relative humidity than larger particles /5/. The deliquescence and efflorescence points of composite particles additionally are also influenced by their material composition ratios.

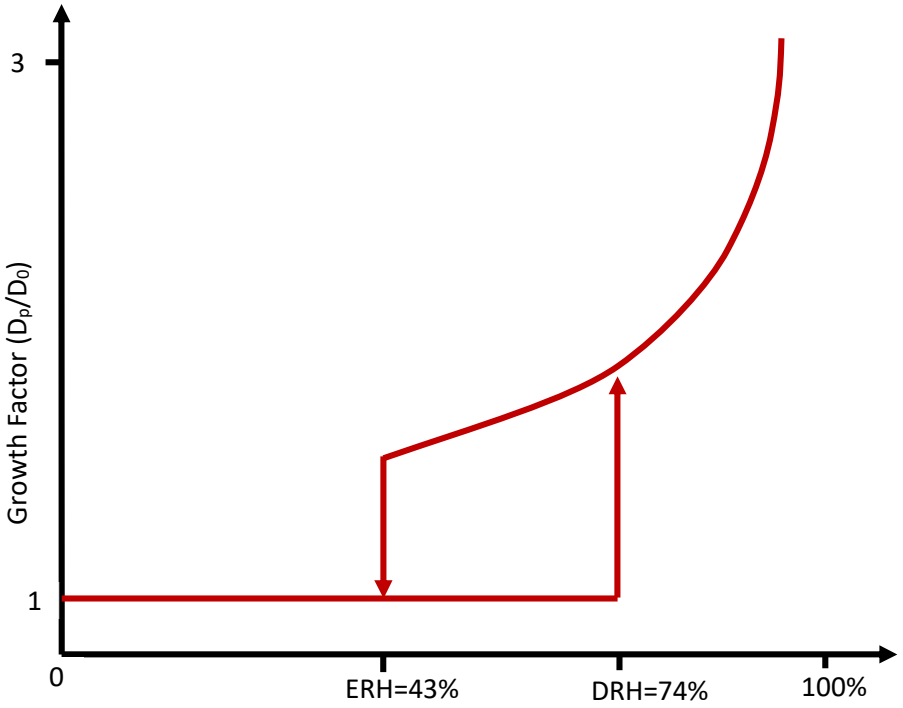

Figure 4: Typical hygroscopic growth function of pure 100nm sodium chloride crystals with their characteristic efflorescence (ERH) and deliquescence (DRH) points /1/

Various growth models have been developed that try to describe the gross growth behaviour of particle composition ratios as they occur in environment. These growth models do not show up with the hysteresis of individual efflorescence and deliquescence but show continuous curves. Nevertheless, it seems to be important for the design of an aerosol dryer that recrystallization may require a relative humidity below 50% due to the hysteresis visible in the humidogram.

When measurement errors occur with low-cost PM sensors purely by hygroscopic growth another effect must be considered. Low-cost PM sensors have difficulties to detect particles with diameters smaller than 0.5um. However, the number concentration of particles with diameters smaller than 0.5um, e.g., from building heating and from combustion engines of vehicles in urban environment, are extremely high. Even with professional equipment, these particles do not contribute much to PM10 and even not to PM2.5 due to their extremely small mass, therefore their initial contribution to the error of low-cost sensors is small. However, in presence of hygroscopic growth, these particles suddenly become visible to the low-cost sensors due to their growth and show up with significant mass contribution. Consequently, the PM increase may become exceptional when exceeding a given humidity threshold. Nevertheless, the assumption of this work is, that hygroscopically grown particles can be reverted to their dry size with less energy in comparison to the energy required to evaporate water droplets during a typical fog event, simply since they are typically smaller in their size compared to fog droplets.

Fog events and hygroscopic growth can occur jointly and may form haze, mist, or smog. Therefore, during field measurements it is often just the sheer intensity and the abruptness or smoothness of mass concentration variation over time that allows to differentiate between pure fog and pure hygroscopic growth events. Fog typically shows strong variations of mass concentration over a short time whereas hygroscopic growth shows only small amounts of variation due to the smaller particle size and spatially more homogeneous distribution.

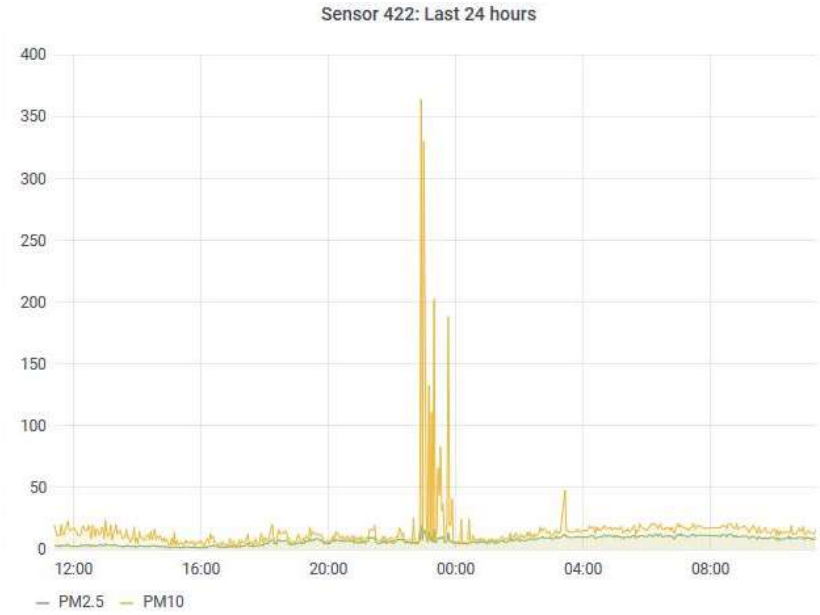

Figure 5: A typical fog event as reported by the OK Lab sensor node 422 in a suburb of Stuttgart (source: luftdaten.info), the graph shows PM in ug/m³.

Other sources of errors

Humidity and fog influence is the most dominant error source for laser scattering PM-measurement devices regardless of their cost. However, low-cost devices are affected more due to their small thermal mass and small thermal self-heating compared to professional equipment. However, it is not the only source of error. As it was shown in various publications such as /2/, /3/, /4/, small low-cost PM devices are typically designed to measure PM2.5 even so they may also output a value named PM10. When mono-disperse particles with diameters greater than 5um are used to test the sensitivity of a low-cost device, the detection limitation for larger particles quickly becomes visible. It also becomes evident that the PM10 value is a kind of estimation value based on the detection of smaller particle sizes. In fact, the values output as PM10 are not fully correlated to the PM2.5 value, therefore particle sizes greater than 2.5um still seem to be detected. The assumption is that a standard mass distribution over size is used for extrapolation to PM10. Consequently, in presence of dust with a particle mass distribution with a centre of gravity close to 10um, the PM10 values of typical low-cost PM sensor fabricated in Asia at a cost of less than 50$ substantially underestimate the results of a gravimetric measurement. This type of error source appears as the second important one.

The reason for maintaining such a sensor design goal by the Asian manufacturers is mostly legislation and cost. PM10 plays much less role for the assessment of air quality in Asia and in the US compared to Europe. The cost and complexity for development and manufacturing of a PM10 capable sensor is much higher due to the much higher settling velocity and the much higher inertial behaviour of large particles. Therefore, estimating values for PM10 using a firmware algorithm is a cheap option to sell such devices also to the European market.

Further error sources of low-cost sensors are the less precise control of the sample flow rate when using cheap simple fans for such a PM sensor or the uncontrolled laser power not considering the aging of the laser source in comparison to the more costly PM sensors manufactured outside of Asia or those that are used in professional equipment.

Computational Correction Method

After having identified the large impact of humidity on the SDS011 PM-sensor, the idea to compensate the humidity influence based on a computational postprocessing by using the relative humidity data of the humidity sensor available in the OK Lab sensor node popped up quickly. As soon as the dependency of the growth factor on humidity in terms of a growth function model is determined, at least the hygroscopic growth of particles could be compensated by applying an inverse growth function to the measured PM-data.

Hygroscopic growth models

To describe the overall effect of hygroscopic growth on the particle mass regardless of the composition and size of particles, many growth models were developed by various aerosol researchers. A well-known and simple growth model was developed and later refined by Hänel /8/, /6/. It is based on the particle extinction coefficient. Others are described in /9/.

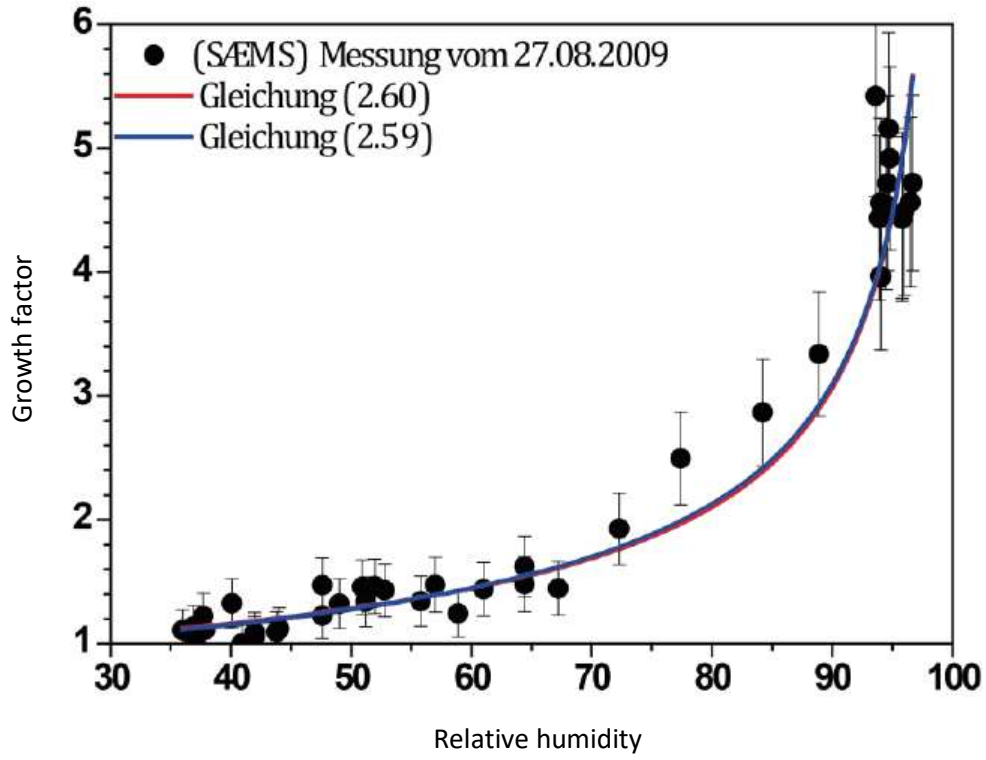

Figure 6: Two growth function models according to Hänel (blue and red curve) fitted into measurement data (source /6/)

The simple model developed by Hänel was used in this work to investigate the option to correct PM measurement data. Data of an example OK Lab sensor node located in Munich near to a governmental reference station were used to extract the model parameters and to fit the growth function to the data. The extracted model function was inverted to later compensate the measured ambient PM values reported by the SDS011 low-cost sensor and to arrive at dry PM values in case of hygroscopic growth. To deploy the inverse growth function to measurement data, the humidity must be known. This data can be taken from a humidity sensor that is operated in parallel to the PM- sensor. Both, the PM data as well as the humidity data are stored and are accessible on the OK Lab servers for analysis of each sensor node.

Humidity measurement

The computational correction of the humidity influence on hygroscopic particles requires the measurement of the humidity in parallel to the PM-values. However, the measurement of humidity is

also afflicted with an error that typically is, for most of the semiconductor sensors, the larger the closer the relative humidity gets to 100%. A key problem in this respect is, that the hygroscopic growth function shows up with a pole close to RH=100%. Hygroscopic growth occurs between 70% and 100% of relative humidity and there the steepness of the growth function increases dramatically towards the value of RH=100%. The humidity measurement error contributes with the derivative of the growth function to the increase of the particle diameter which tends towards infinity close to the 100% point:

$$\Delta D_p = \Delta RH * \frac{\partial GF}{\partial RH}$$

Eq. 1

This error propagation effect gets further aggravated for the particle mass since it is proportional to the third power of the particle diameter D_p. Therefore, it is imperative to use a precise humidity sensor. The AM2302 (DHT22) sensor seems not to meet these accuracy requirements.

However, much more than the accuracy of the humidity sensor as specified in the data sheet of the OK Lab humidity sensor, the problem of irreversible degradation of the sensor is an issue when the sensor gets exposed to wet water content in the air for a longer time. An analysis of many of the AM2302 (DHT22) sensors used in the OK Lab sensor nodes showed that the characteristic of measured values versus real values shifts towards a constant 100% value under the repeated influence of wet water and corrosive salts. To visualize this effect, all the OK Lab DHT sensors located in the urban area of Munich on May 18, 2020 (a sunny and dry day) were extracted for the night (0:00h) and for the noon (12:00h). A professional weather station in Munich (MingaWeda.de) showed a relative humidity of 75% at night and about 30% during daytime. It can be seen clearly that most of the OK Lab sensors show RH = 99.9% at night, whereas at noon, under the influence of the solar irradiation, the humidity is in the midrange. The histogram in Figure 7 shows the frequency of occurrence of the respective RH values. The high number of sensors that show up with RH close to 100% at night becomes obvious. Assuming those showing 100% being no longer working reliably, 83 out of 134 sensors in Munich are defective. Given this situation only a small fraction of the OK Lab sensor nodes can potentially be corrected using the built-in humidity sensor.

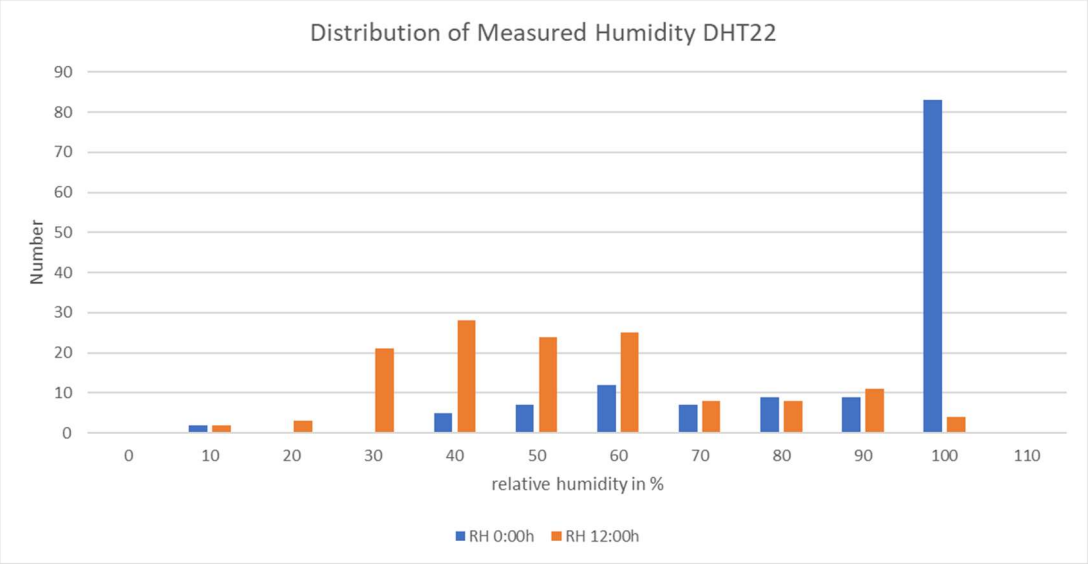

Figure 7: Distribution of the humidity values of 134 active OK lab sensors in Munich at midnight (blue) and at noon (orange) on a day with low humidity (18.5.2020), the majority of sensors show a RH value of 99.9% at midnight

This issue could be removed for a future sensor design, since more accurate and more robust temperature/humidity sensors are available, however only at higher cost. Outdoor capable humidity

sensors are protected for example by a membrane against wet water and dust such as in the case of the HYT221 sensor from IST AG, Switzerland. If the electrical pins are protected against corrosion, this sensor is suitable for being used in outdoor ambient air.

Figure 8: The outdoor capable temperature/humidity sensor HYT221 covered with a protective membrane against wet water and dust

Such a sensor would most likely provide more reliable and accurate humidity data and could be used for a computational correction of the humidity influence. Nevertheless, in this work an OK Lab sensor was selected, for which the built-in AM2303 (DHT22) sensor still reported plausible data during the time frame analysed for humidity correction attempts.

OK Lab Sensor analysis for November and December 2020 in Munich, Lothstrasse

Even though governmental authorities must perform the legally required PM measurements using time consuming gravimetry in laboratories, they often use professional laser-scattering PM measurement equipment (e.g., such as the Palas Fidas 200) to get instant measurement results. To be as close as possible to gravimetric results, these laser-scattering instruments are equipped with controlled aerosol drying systems that dry the air prior to entering the particle measurement chamber. The aerosol drying in professional equipment is often controlled in a way that the results are maximally matching the gravimetric measurements. This does not always mean that the growth effect or fog events are completely compensated, since also care must be taken not to vaporize highly volatile hydrocarbon or organic components of particles that also contribute to a gravimetric result.

Even though it appeared reasonable to construct a low-cost thermal aerosol dryer that would be an option to at least mitigate the hygroscopic growth effect, such a low-cost dryer may substantially increase the cost of a sensor node and would make it bulkier than just the exchange of the humidity sensor to an improved version. Therefore, it seemed to be worthwhile to first investigate the option of a computational correction using humidity measurement data and compare the result to a governmental measurement station with a professional aerosol dryer.

In Germany, the state government of Bavaria publishes PM data on an hourly basis for all the governmental stations (Landesamt für Umwelt, LfU, www.lfu.bayern.de). The high temporal resolution of these data allows a detailed analysis of even fast changing humidity events. An OK Lab sensor node with a functional humidity sensor in immediate vicinity to a professional LfU reference measurement station in Munich was identified. The OK Lab sensor node with id 7687 (Hochschule München Lothstrasse) is directly located nearby the LfU station München/Lothstrasse (N 48.15455°, E 11.55466°). This governmental measurement station was taken as the reference for the evaluation of the OK Lab sensor node #7687. The respective humidity sensor of type AM2303 (DHT22) in this sensor node has the id 7688.

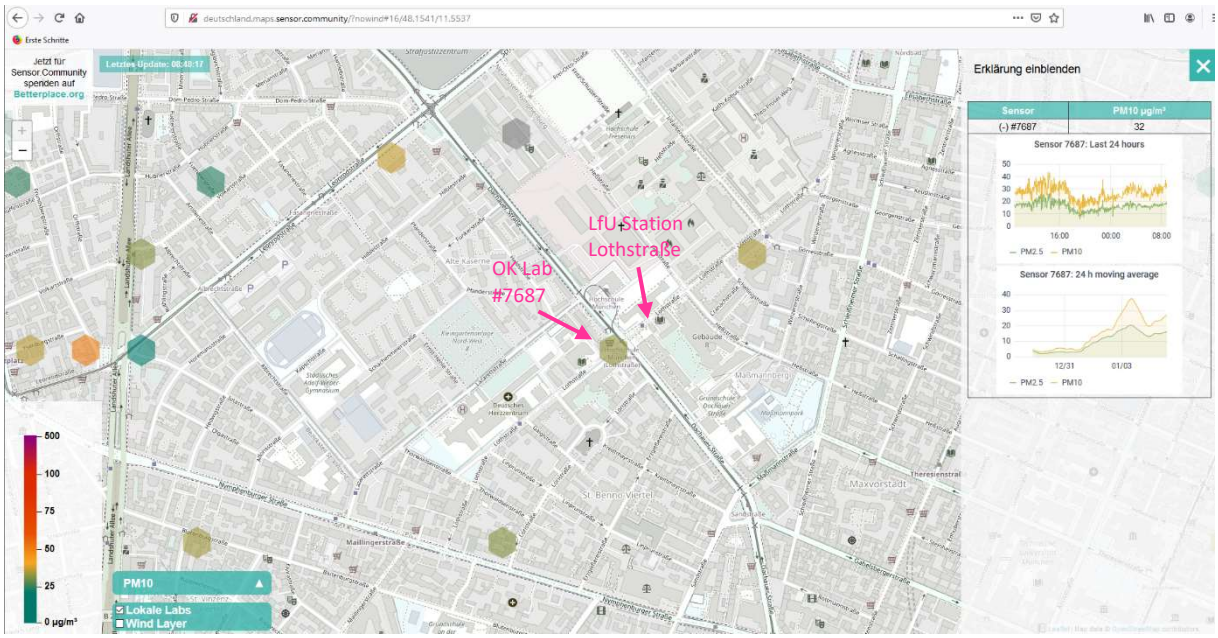

Figure 9: Location of OK Lab Sensor #7687 and location of the LfU station Lothstrasse, Munich

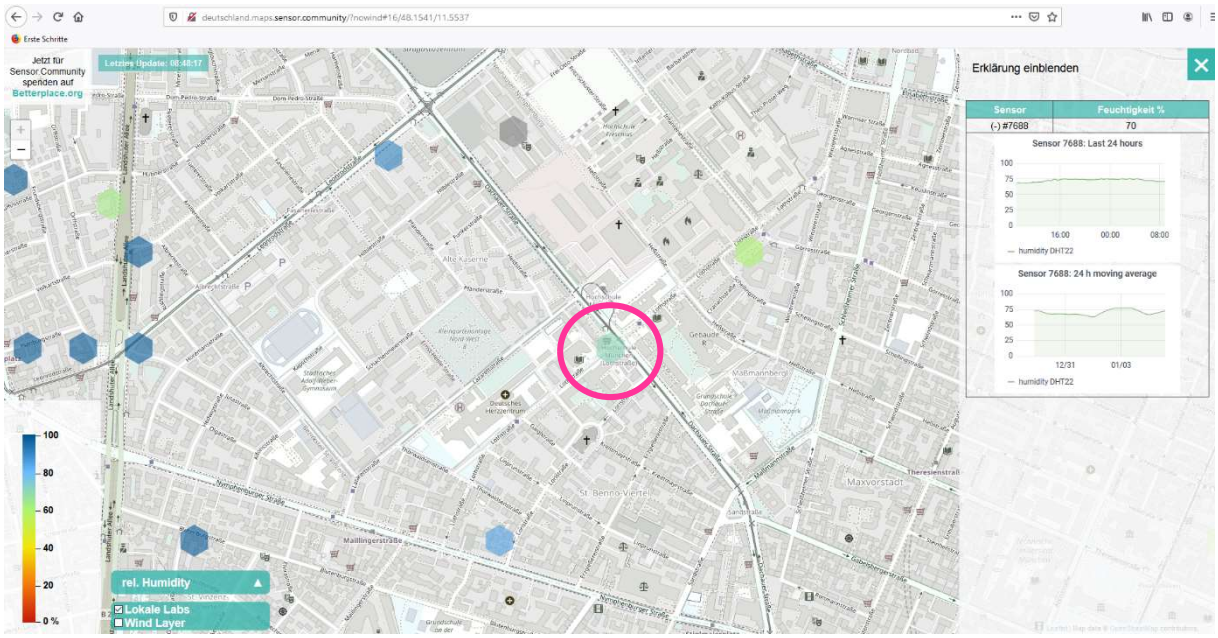

Figure 10: OK Lab temperature/humidity Sensor #7688 (DHT22)

Figure 11: LfU station in front of the "Hochschule München" (picture source: Google street view)

The OK Lab sensor #7687 for PM10 and PM2.5 paired with the AM2302 (DHT22) humidity sensor #7688 is active since April 2020 and data are permanently archived to the luftdaten.info database /10/. During summer 2020 several interruptions occurred and in August 2020 implausible PM values were measured. However, from autumn 2020 on, the sensor worked stable and yielded plausible data for both PM and humidity. As an exemplary case the month of November 2020 was selected for analysis, due to a high humidity phase from 3.11.-12.11.20 as indicated in the weather data from MingWeda.de shown in Figure 12.

For November 2020, the data of the OK Lab sensor and the LfU reference were analysed with respect to PM10 and PM2.5 and a humidity correction according to the Hänel hygroscopic growth model was applied. Figure 13a shows the measured PM10 data of the LfU reference station as well as the OK Lab PM10 data of the SDS sensor and the humidity data as measured with the AM2302(DHT22) humidity sensor inside the OK Lab sensor node before the correction was applied. Figure 13b shows the same graph with the corrected SDS PM10 data.

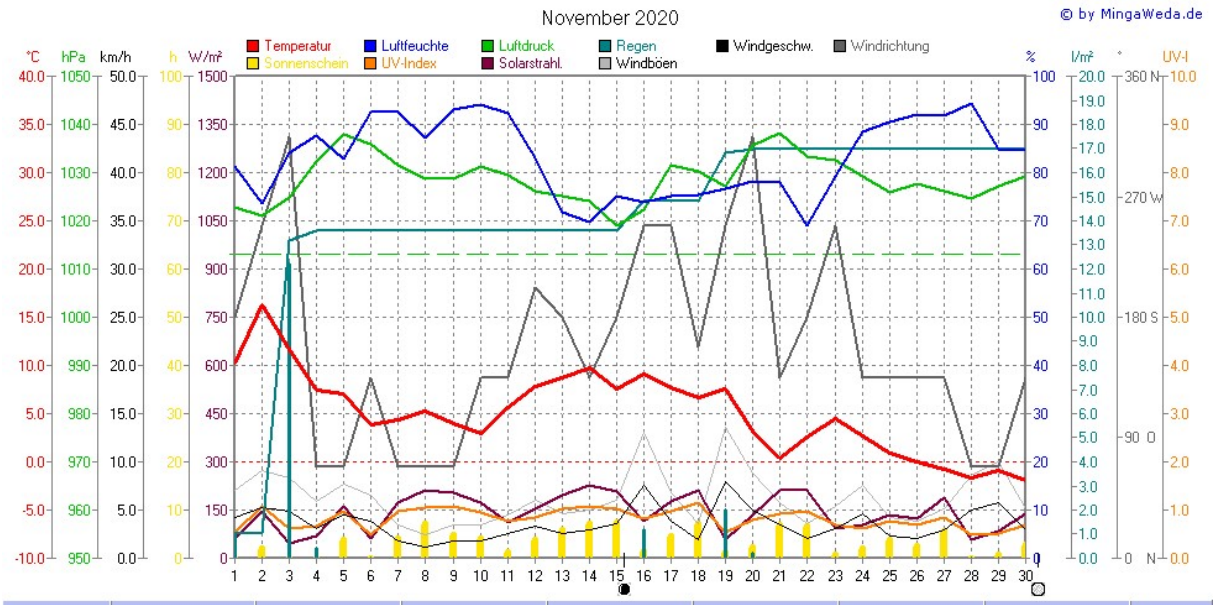

Sensor	Temperatur	°C	Luftfeuchte	%	Luftdruck	hPa	Windgeschw.km/h	Windböen	km/h	Regen	l/m²	UV-Index	UV-I
MinWert	30.11. 05:59	-3.8	22.11. 14:01	38.0	15.11. 21:38	1015.4	01.11. 01:02	0.0	01.11. 01:02	0.0	Regentage: 6		01.11. 00:00	0.0
MaxWert	02.11. 14:28	20.9	07.11. 04:42	96.0	21.11. 02:52	1040.1	19.11. 16W-SW	27.6	19.11. 16W-SW	48.3	03.11. 07:19	12.2	02.11. 12:18	2.3
Durchschnitt		5.09		83.1		1028.7		3.6		6.3	Gesamt:	17.0		0.8

Figure 12: Weather data from Munich for November 2020 (source: MingWeda.de), the blue line indicates the humidity

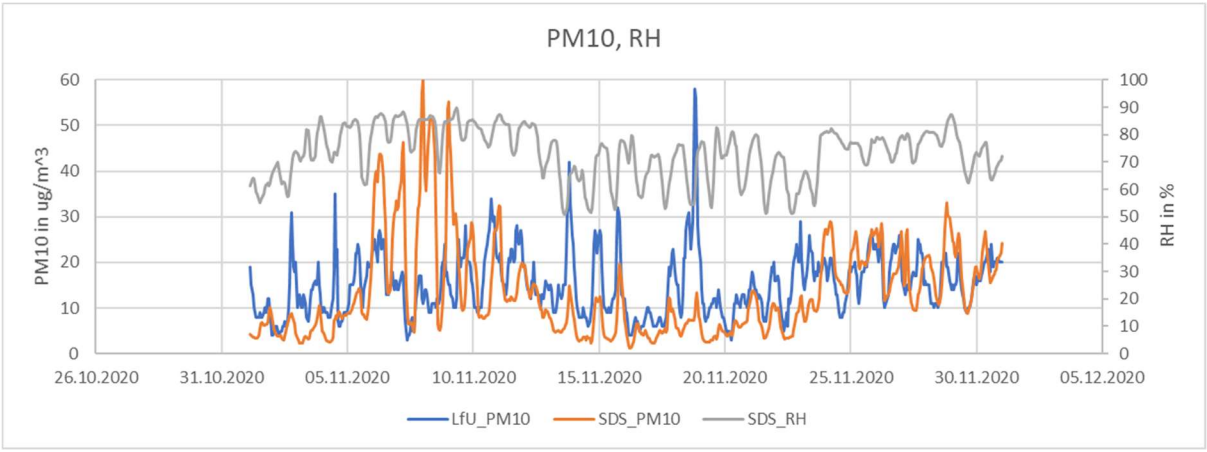

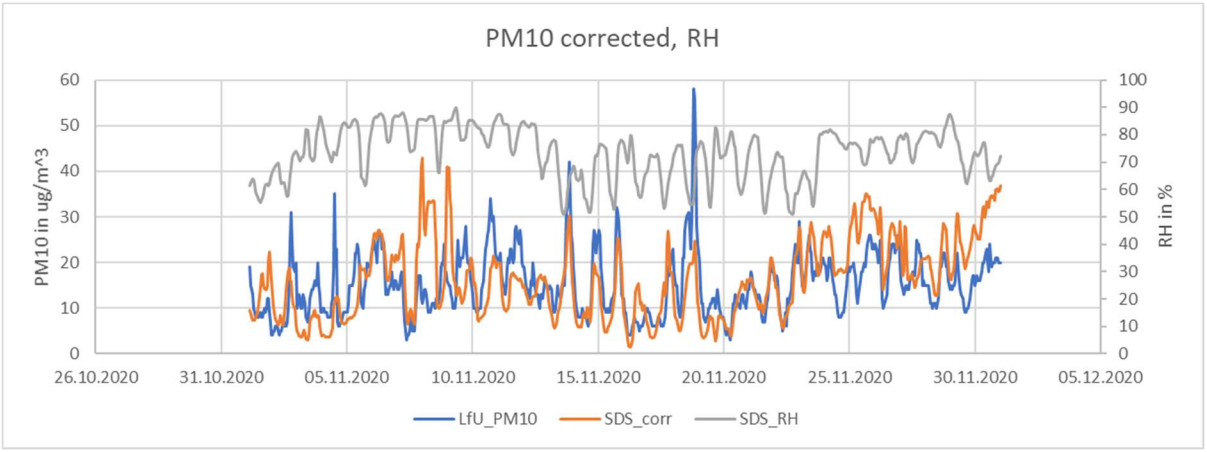

Figure 13a, b: PM10 and humidity data of the OK Lab Sensor #7687 (orange) and the LfU station (blue) before (a) and after (b) humidity correction during November 2020

As it can be seen, a high humidity phase ranging from 3.11. – 12.11.20 occurred with relative humidity values up to 85% as measured by the OK Lab sensor. During this phase, the OK Lab PM10 values exceeded the PM10 values of the LfU reference station by far. Between 14.11. and 19.11.20 however, the situation reverses, and the OK Lab sensor yielded smaller PM10 values compared to the LfU reference. During this phase, the humidity seen by the OK Lab sensor was lower. After applying the correction, the OK Lab PM10 data seem to match the LfU PM10 reference data better for both phases. The matching can be quantified by a correlation of the OK Lab PM10 data versus the LfU PM10 reference data.

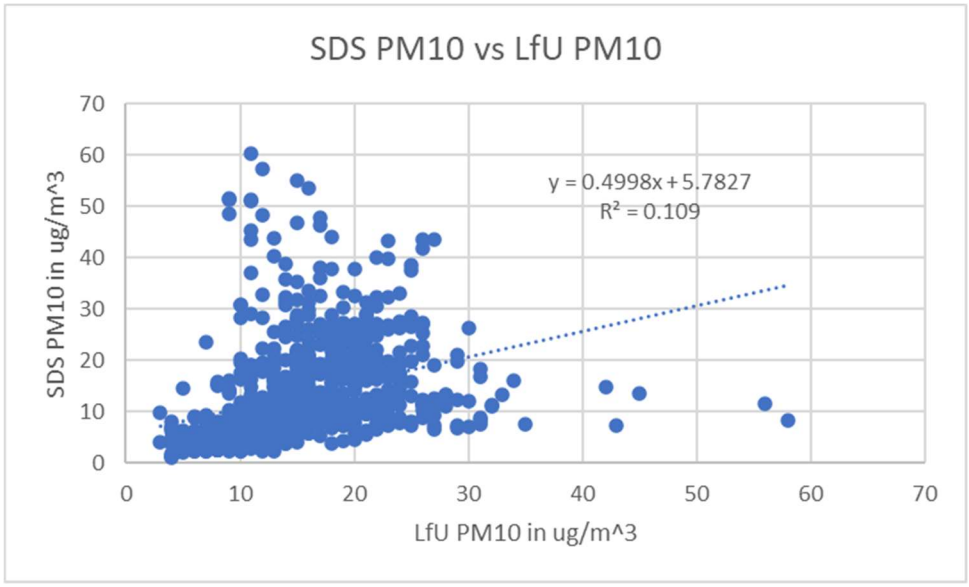

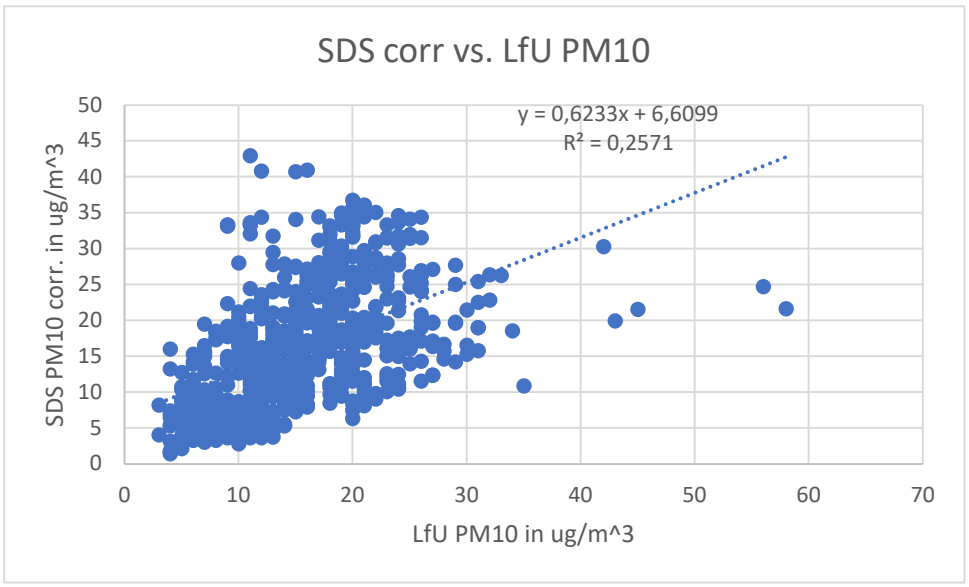

Figure 14a, b: Correlation between of the OK Lab Sensor #7687 (y-axis) and the LfU station (x-axis) before (a) and after (b) humidity correction for PM10 during November 2020

As it can be seen from Figure 14a, b the PM10 data originally are not well correlated, the coefficient of determination R^2 only amounts to 0.109. The applied humidity correction improves this value to R^2 = 0.2571 for this data set taken in November 2020.

For PM2.5, the matching of the uncorrected OK Lab sensor data and LfU reference data was already better. It is assumed that this is the case for two reasons: First, in contrast to the LfU reference station, the SDS011 is not able to detect large particles. However, the particles relevant for the mass

concentration that make up PM2.5 can be detected by the SDS011 more accurately. Second, the spatial distribution of the particles relevant for PM2.5 is more homogeneous compared to that of the particles relevant for PM10. The larger particles generated from abrasive processes near the curb side of the road (tire and brake abrasive products of vehicles) sediment very quickly whereas the small particles generated from combustion processes (car engine, heating of buildings) are suspended for a long time in the air and are mixed well by the movements of the air. Thus, they are seen by the SDS011 and by the reference station in a more stable concentration. Therefore, the compensation of the PM2.5 data gives better results (Figure 15a, b).

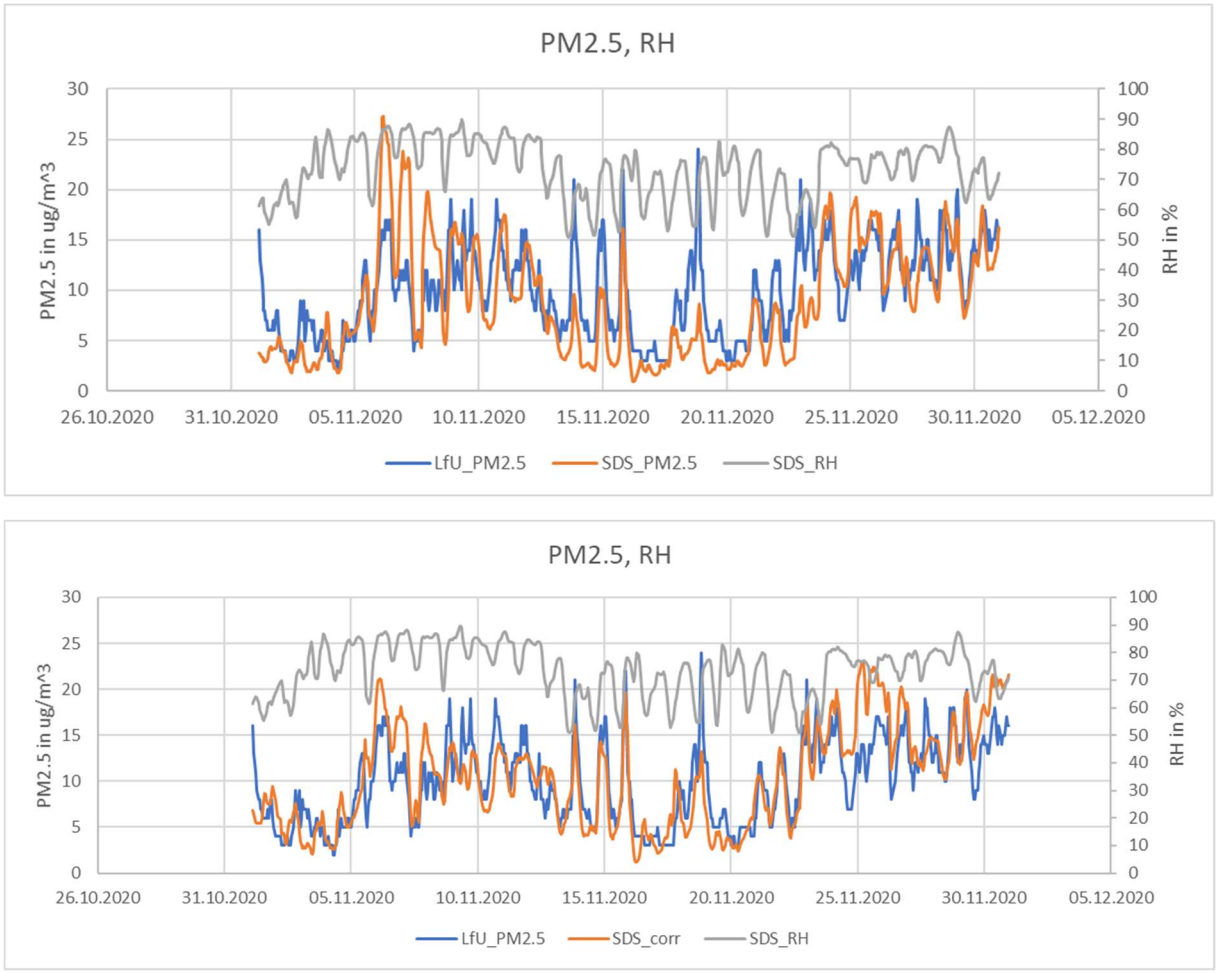

Figure 15a, b: PM2.5 and humidity data of the OK Lab Sensor #7687 (orange) and the LfU station (blue) before (a) and after (b) humidity correction during November 2020

Looking at the coefficient of determination, the better match of the PM2.5 data becomes evident from an initial value of $R^2 = 0.5166$. Applying the humidity correction to the SDS011 PM2.5 sensor data finally yields an improved value of $R^2 = 0.6531$.

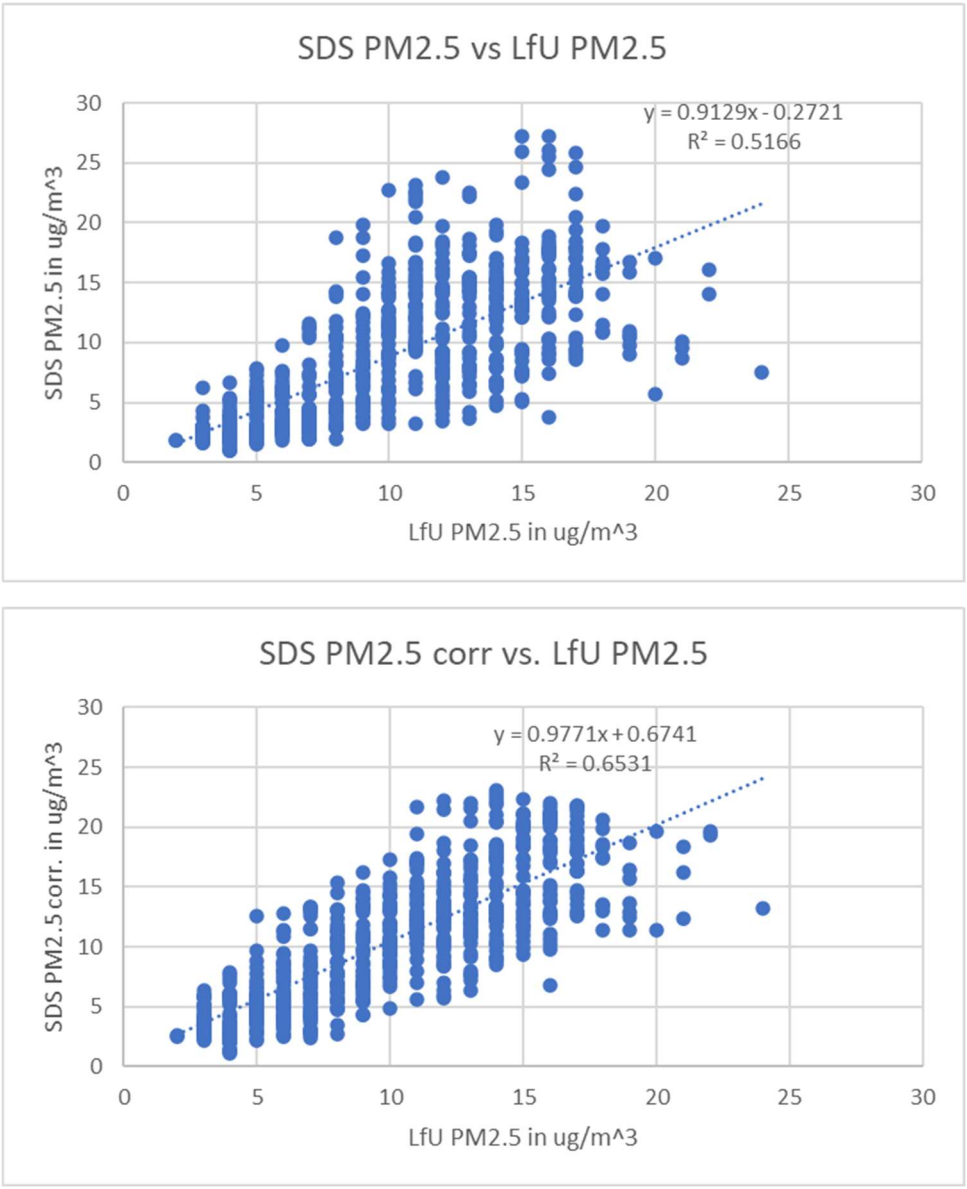

Figure 16a, b: Correlation between of the OK Lab Sensor #7687 (y-axis) and the LfU station (x-axis) before (a) and after (b) humidity correction for PM2.5 during November 2020

The humidity correction applied to PM10 and PM2.5 data is based on Hänel's hygroscopic growth model /4/. According to Hänel, the growth factor GF_d related to the particle diameter is defined by the ratio between the number concentration of grown particles under humid conditions to the number concentration under dry conditions and can be modelled by:

$$GF_d = \frac{Pd_{wet}}{Pd_{dry}} = \alpha_d \frac{1}{(1 - RH/100)^{\beta_d}}$$

Eq. 2

In this model β_d is the Hänel coefficient related to particle size determined experimentally and RH is the relative humidity in %. The additional factor α_d accounts for a growth factor that is not exactly 1 when the wet particle concentration is determined with a different sensor or method compared to the dry particle concentration.

Since the mass concentration used to calculate PM values is proportional to the 3rd power of the diameter a respective mass growth function GF_m can be defined for the particle mass in a similar way:

$$GF_m = \frac{Pm_{wet}}{Pm_{dry}} = \left(\alpha_m \frac{1}{(1 - RH/100)^{\beta_m}}\right)^3$$

Eq. 3

The mass related growth function parameters are related to the size related growth function parameters in the following way:

$$\alpha_d = \alpha_m{}^{\frac{1}{3}}, \qquad \beta_d = \frac{1}{3} \cdot \beta_m$$

Eq. 4

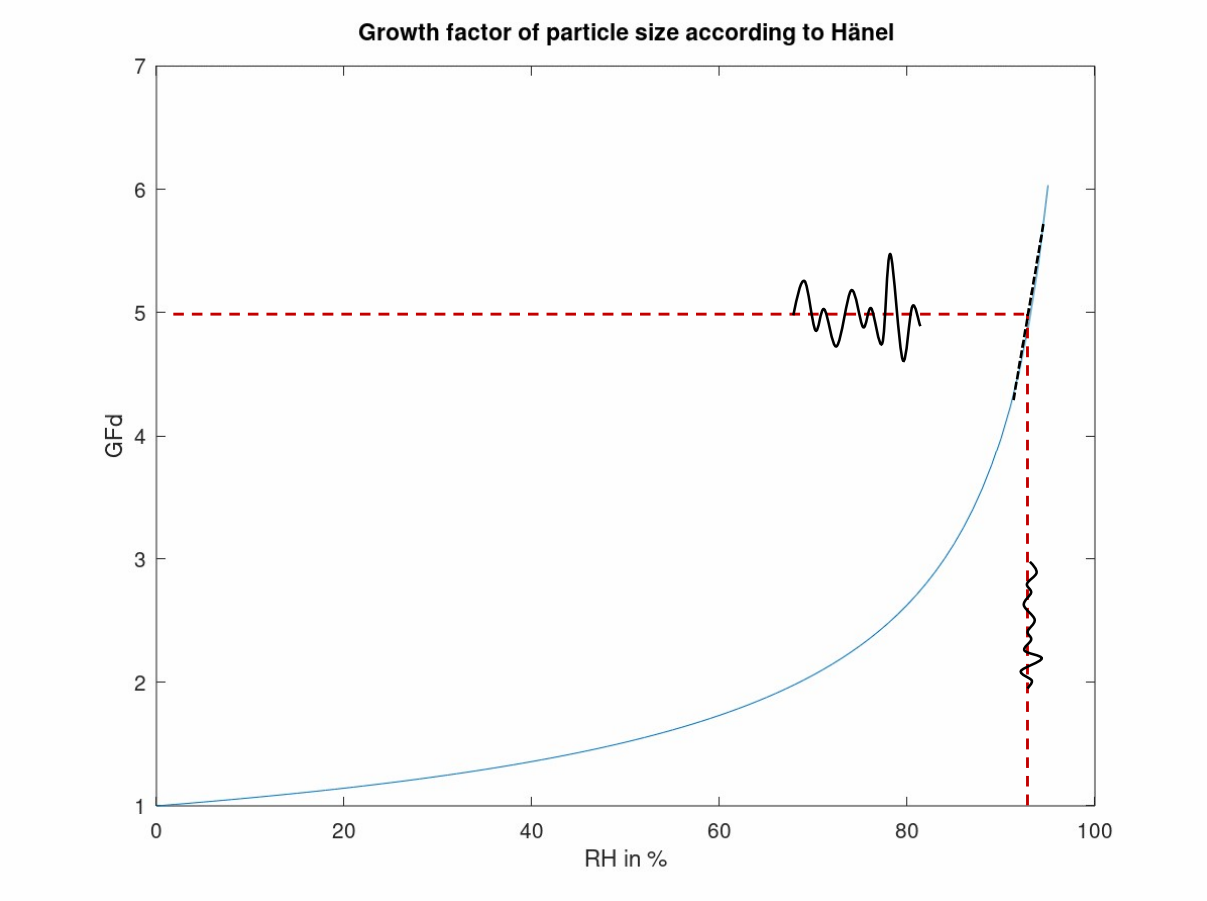

Figure 17: Example of the size growth function according to the Hänel model (α_d = 1, β_d = 0.6) and the propagation of a humidity measurement error into a growth factor error

Figure 17 shows the size related growth function GF_d for α_d = 1 and an Hänel coefficient of β_d= 0.6 . The growth factor of 5 is reached at RH = 93.14%. At this point however, the steepness of the growth function is by a factor of 24 higher compared to RH=50%. This means a small measurement error in humidity translates into a large error in the growth function value. Since the part variation and drift of the humidity sensors is also high, it is not possible to rely on just one fixed set of coefficients α_d and β_d. This effect aggravates when transitioning to the mass related growth function GF_m. In addition, the composition of the particles varies depending on time and location. As mentioned above, hygroscopicity of salts is defined by different deliquescence and efflorescence points. Different salts contained in varying quantities in the particle material, therefore the hygroscopicity and thus the growth function requires variable coefficients for a correct compensation.

Independently of either size or mass related growth function, a possible solution to this problem is the determination of the coefficients α and β from a limited set of the most recent measurement data. When we set:

$$y = \ln\left(\frac{1}{GF}\right) = \ln\left(\frac{P_{dry}}{P_{wet}}\right)$$

Eq. 5

$$x = \ln\left(1 - \frac{RH}{100}\right)$$

Eq. 6

$$a = \ln\left(\frac{1}{\alpha}\right)$$

Eq. 7

we can transform the model relationship into a linear equation for which a linear regression calculation gives the slope β and offset a of a straight line that fits into the data with a minimum error in the least mean square sense:

$$y = \beta * x + a$$

Eq. 8

In other words, the best coefficients in a least mean square sense can be determined directly from the most recent measurement data. When the above is applied to the PM2.5 data analysed in Munich, Lothstrasse, the data can be indeed linearized and a linear trendline yielding the coefficients can be fitted into the data. When the linear trendline is converted back inversely, the parametrized growth function that best fits the original data is obtained. In the example of the November 2020 data of the OK Lab sensor at Lothstrasse in Munich, the obtained values are α_m = 0.2587 and β_m = 0.8019.

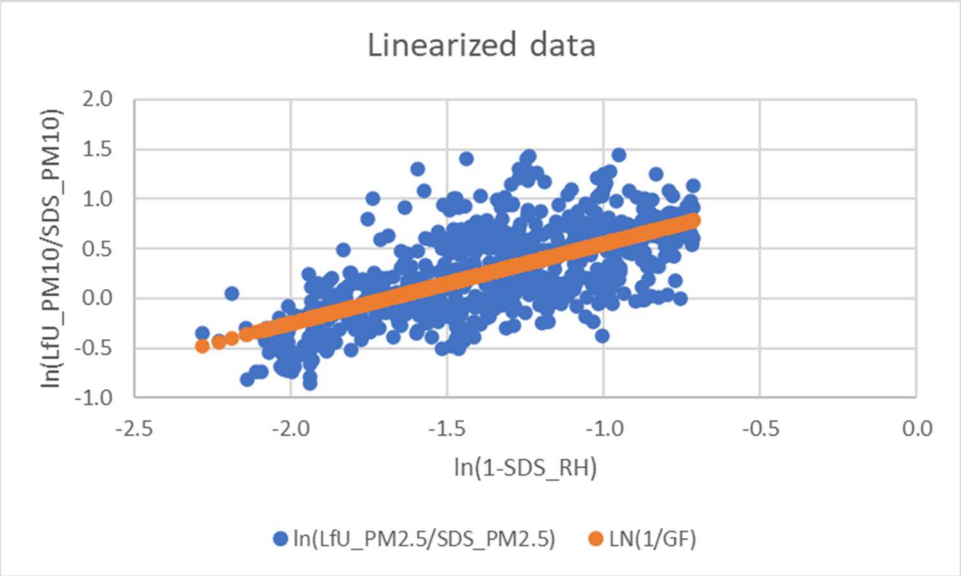

Figure 18: Linearization of the data with respect to humidity and fitting of a linear trendline

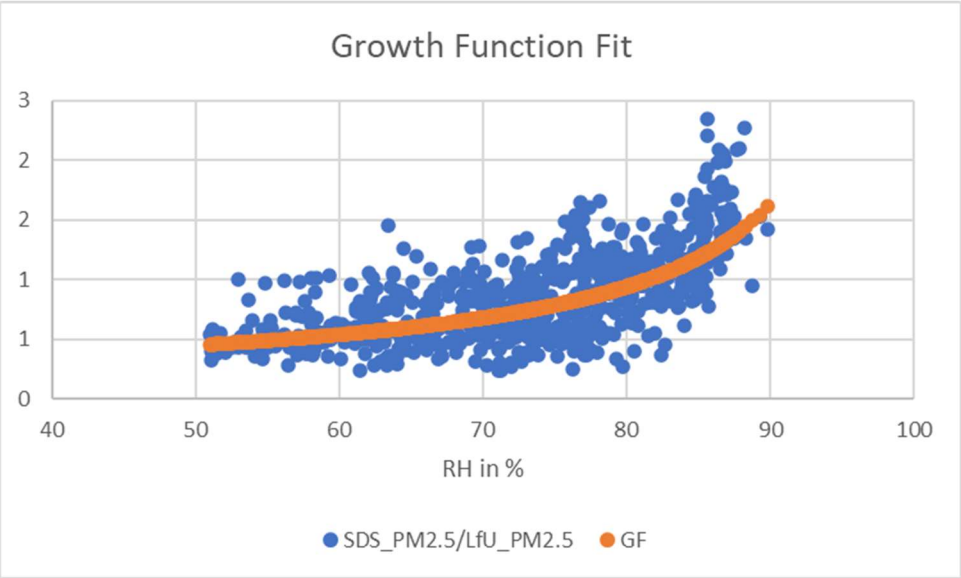

Figure 19: Conversion of the linear trendline into the growth function model

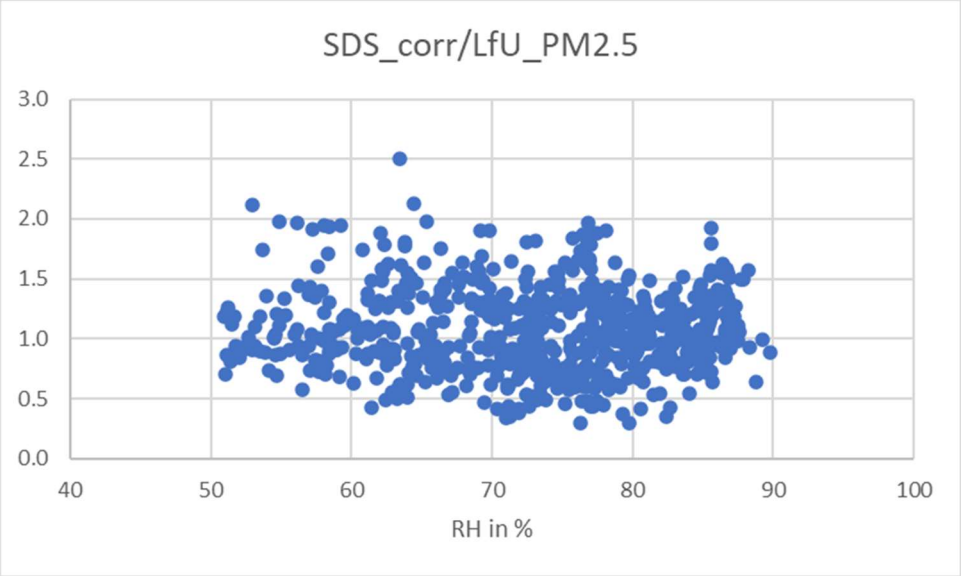

Figure 20: Correlation of the ratio between SDS011 and LfU PM2.5 data versus humidity after humidity correction in November 2020 showing values varying around a value of 1, independent of RH

When the correction is applied to the SDS011 PM2.5 data, the ratio between the corrected OK Lab PM2.5 sensor data and the LfU PM2.5 reference data indeed vary around the value of 1, as expected. Consequently, the correction can be "trained" for the best Hänel coefficient β_m and for the coefficient α_m from measurement data in conjunction with data from a reference instrument.

A key question remains however: are the coefficients from the training period also valid at a later point in time when a reference instrument is no longer available? If reference data are still available, this can be validated. For validation, the coefficients of the training phase are applied to the validation phase. In this example low-cost sensor data from December 2020 were used for validation.

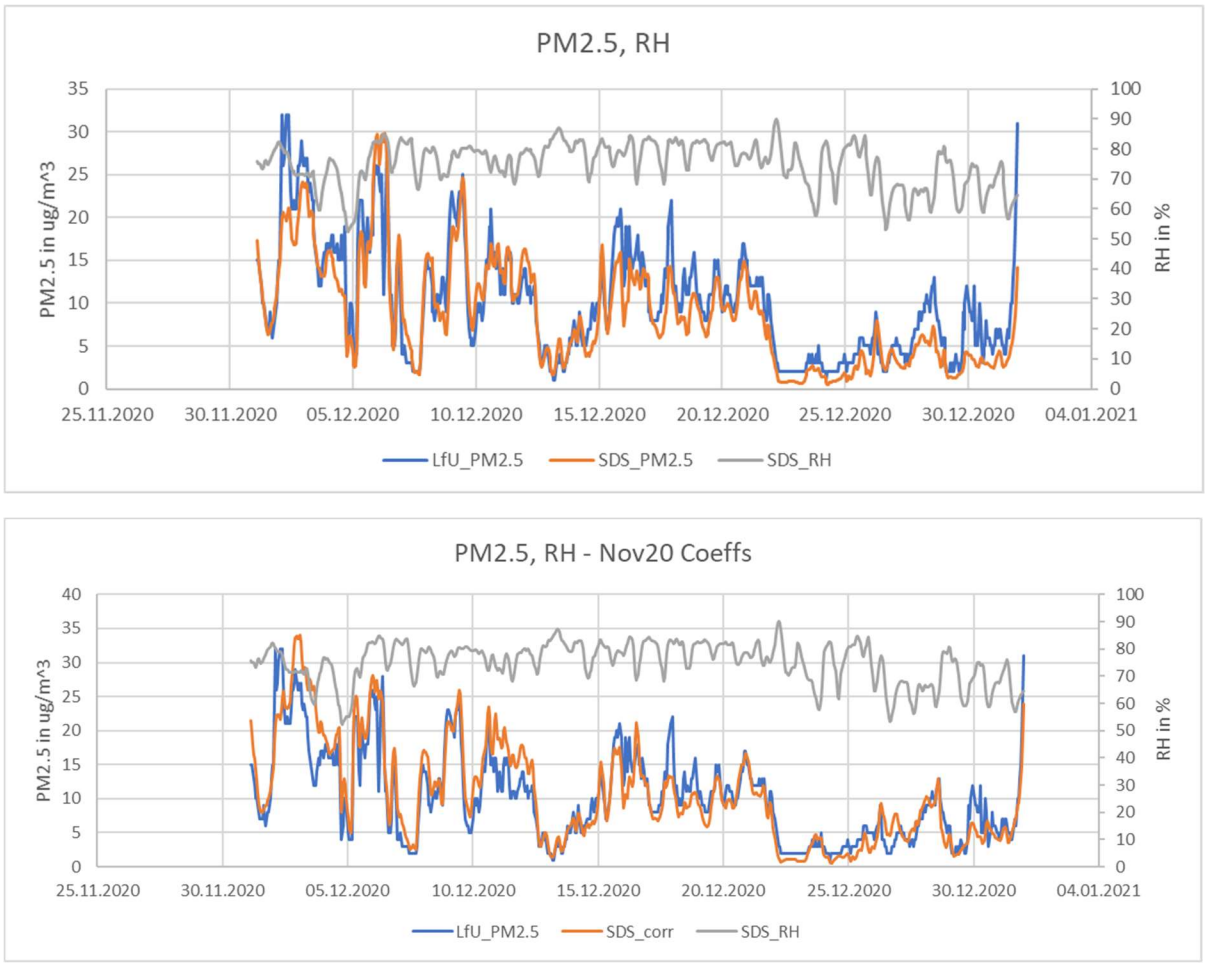

Figure 21a, b: PM2.5 and humidity data of the OK Lab Sensor and the PM2.5 data of the LfU station during validation phase in December 2020 before and after humidity correction using coefficients of the training phase in November 2020

The evaluation of the validation phase data in December 2020 using the coefficients from the training phase in November indicates, that the humidity correction still gives reasonable results one month later. In December however, no high humidity phase occurred, therefore the initial correlation of the PM2.5 data between low-cost sensor and LfU reference station is already better (R^2 = 0.8185). The humidity correction with the coefficients from the training phase in November 2020 still give a small improvement yielding a coefficient of determination of R^2 = 0.8325.

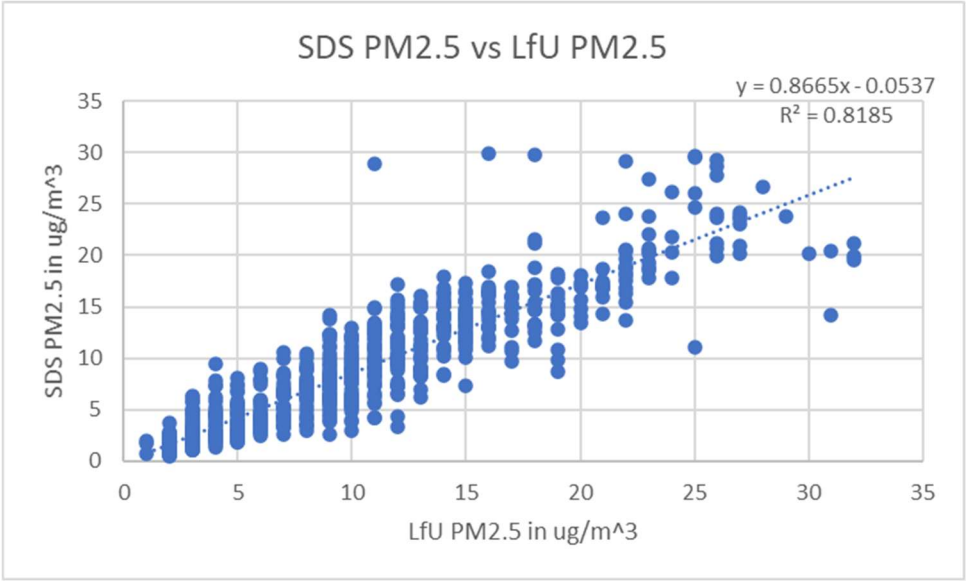

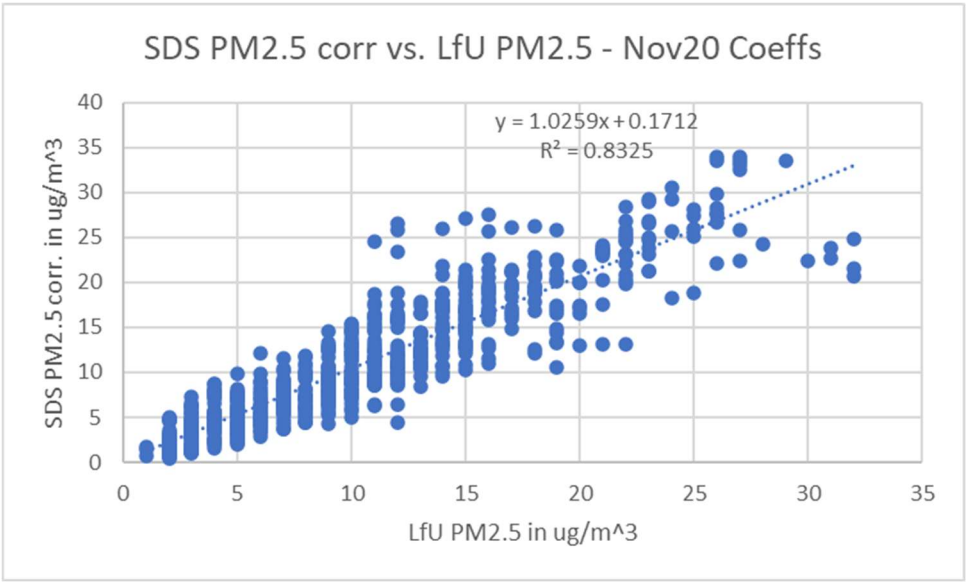

Figure 22a, b: Correlation between the OK Lab PM2.5 Sensor data and the PM2.5 data of the LfU station during validation phase in December 2020 before and after humidity correction using coefficients of the training phase in November 2020

Nevertheless, it becomes clear, that a key requirement for using coefficients from a training phase for a later measurement period (or potentially after a location change of the sensor) where no reference instrument is available anymore, are similar hygroscopic properties of the aerosol as during training. This may not be the case when the chemical composition of the aerosol changes, due to seasonal weather conditions or due to a location change of the sensor. For example, the aerosol in a city near the seacoast may contain a lot of NaCl crystals also depending on wind conditions. In contrast, the aerosol in a rural area may strongly be influenced by ammonia gas emissions from season-depending farming activities forming secondary ammonium nitrate and ammonium sulphate particles with different hygroscopic growth characteristics compared to NaCl. This again is different to an urban environment, either urban background or close to a road with varying traffic loads. Therefore, the coefficients trained with the help of a reference system at one location at one point in time may not be transferable to other locations at a different time due to the change in the hygroscopic characteristics of the particles.

An additional problem may be the occurrence of fog events. A fog event shows up with jumping changes of PM concentrations to extremely high values. This contrasts to a PM concentration increase

due to hygroscopic growth. The typical hygroscopic growth models therefore are no longer valid for data containing fog events. The detection of a fog event in measurement data for excluding these data is not always trivial, however.

Construction of a measurement box for Comparison of a SDS011 with and without a low-cost aerosol dryer

The other option to achieve a correction for any kind of humidity influences is the use of an aerosol dryer in front of the PM-sensor inlet. Such drying systems are used for professional environmental PM-measurement equipment. The aerosol dryer may help for correction of both, fog, and hygroscopic growth. Both effects result in particles being enclosed by water causing in an increase of the diameter determined by the laser scattering sensor. The aerosol dryer corrects this error by removing the water from the particles and causes recrystallization of hygroscopic salts before the laser scattering measurement. Three principles for aerosol drying systems are widely used, diffusion drying using silica gel, a membrane such as Nafion® or thermal drying.

Silica-gel dryers are cheap but require regular service to ensure a constant water absorption capability and thus are not well suited for longer term and unattended outdoor usage. Nafion®-tubes need to be long compared to a thermal dryer and do not meet the cost goals for a low-cost application. Therefore, a low-cost thermal dryer appeared to be the best solution.

Construction of the aerosol dryer

The dryer used in this work was created with a resistive wire that was wound on a brass tube with 7mm diameter and 500mm length to form a heating coil. The brass tube fits directly on the gas inlet of the SDS011 low-cost PM sensor. The resistance was dimensioned such that an electrical power of approximately 10W will be delivered to the heating coil when the supply voltage is adjusted to 8V at the DC/DC converter with 12V being supplied to its input. The coil was wound around an adhesive ceramic foil covering the tube to provide a better thermal coupling and to provide electrical isolation simultaneously. The heating-coil was wrapped with a heat tolerant fleece material for thermal isolation. To give the dryer a mechanical stability and to protect it against rain, it was enclosed by a plastic protection tube.

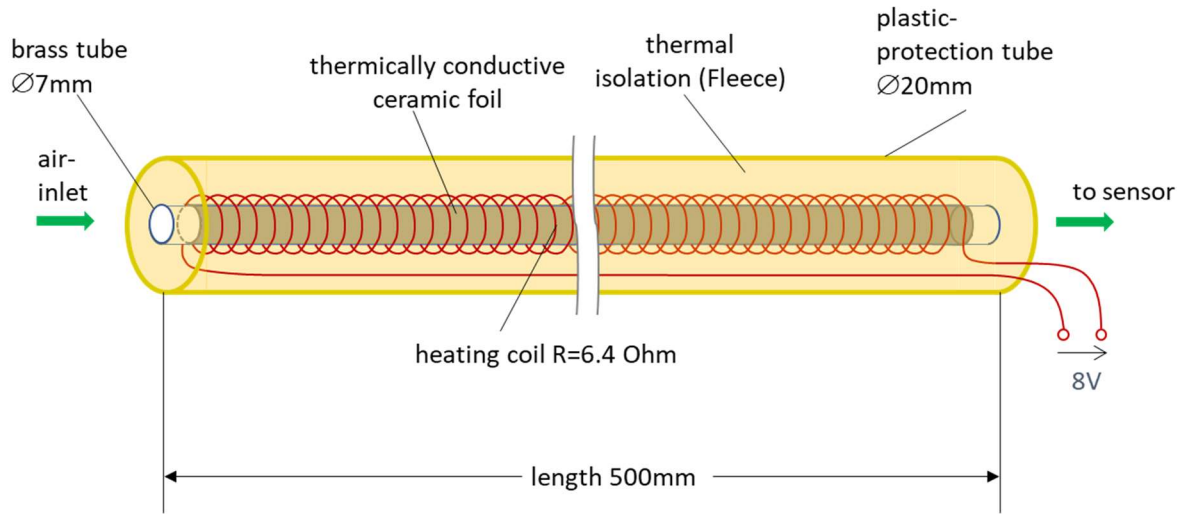

Figure 23: Construction of the low-cost thermal aerosol dryer

It quickly became apparent that it is important to also isolate the SDS011 sensor body thermally, not just the dryer, to ensure that the aerosol does not cool down in the measurement chamber of the sensor. This was achieved by enclosing the SDS011 into a 5mm polystyrene foam while providing a slot for the air exhausted by the fan.

Aerosol dryer control

The dryer control was implemented by regulating the humidity in the exhausted air to a fixed level. For this purpose, an electronic switch was constructed that gets activated by a microcontroller. The heating of the dryer is turned on when the humidity senses a relative humidity value larger than 35% inside the PM-sensor. The value of 35% was chosen by considering the efflorescence of sodium chlorate. For turning off the heating the same threshold was used, since the thermal capacitance of the brass tube causes a substantial delay in temperature increase or decrease after activation or deactivation of the heating. The microcontroller activates the heating by driving a logic high level to the gate of a power NMOS transistor that turns on the heating current supplied from the 8V output of the DC/DC converter.

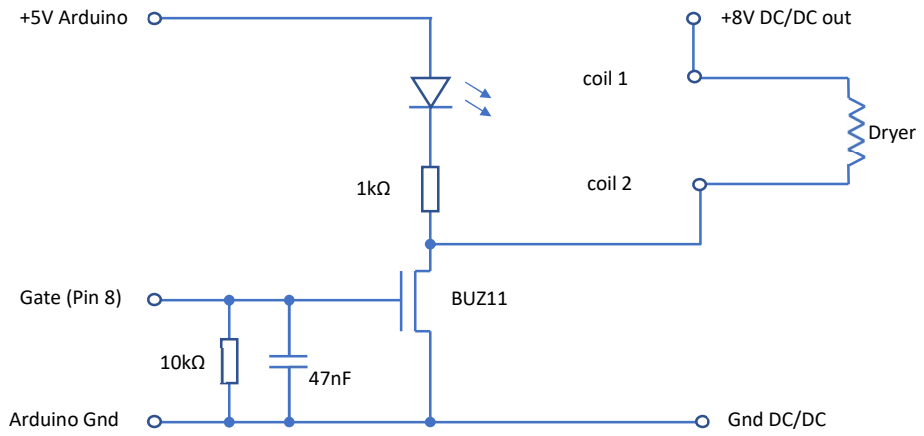

Figure 24: Circuit diagram of the control switch for the dryer implemented using a NMOS transistor

Modification of the SD011 sensor

For the humidity control of the dryer, it was required to modify the SDS011 sensor since it is not equipped with an internal humidity sensor. The SDS011 was modified to integrate the humidity sensor HYT221 from IST AG, Switzerland into the air exhaust chamber below the fan. To position the sensor such that it does not affect the aerosol flow, a worn out SDS011 sensor was opened and the construction of the gas flow was analysed prior to drilling a hole into the exhaust chamber of the SDS011 sensor used in the measurement box.

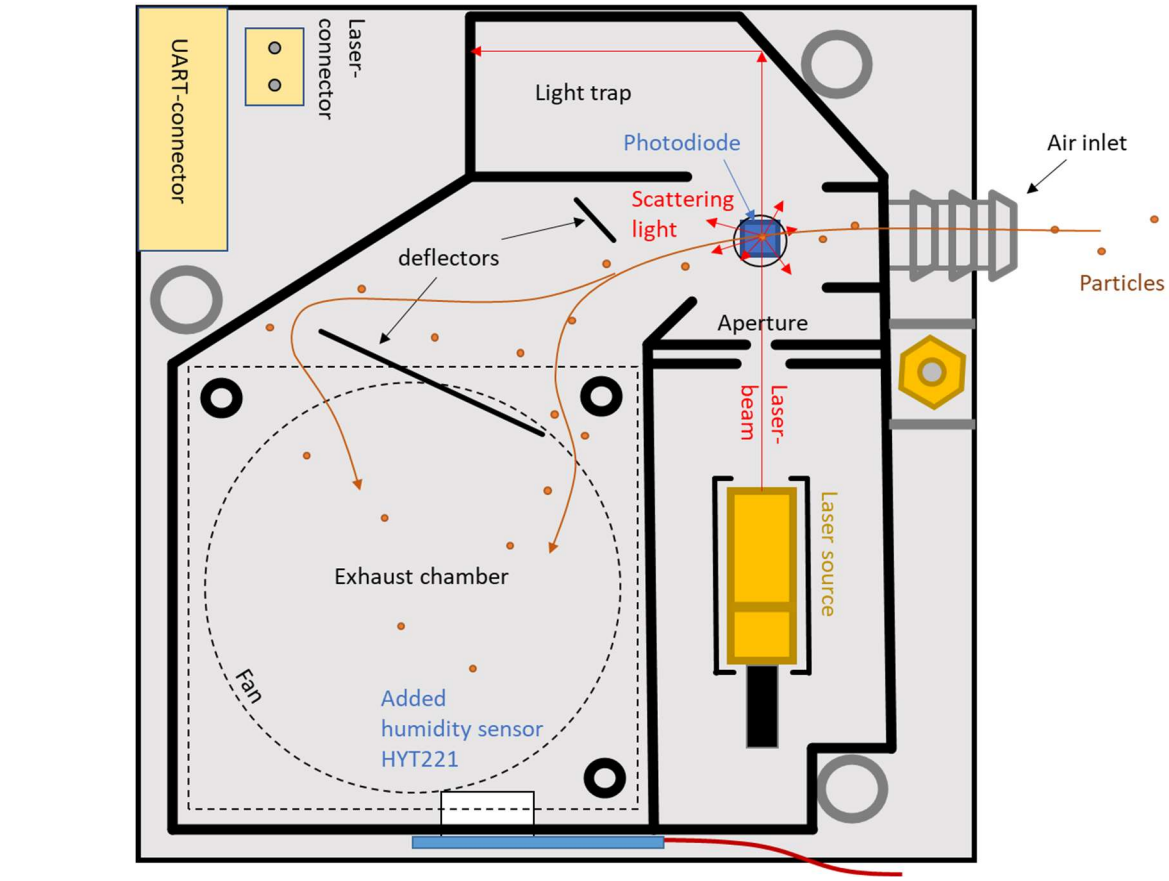

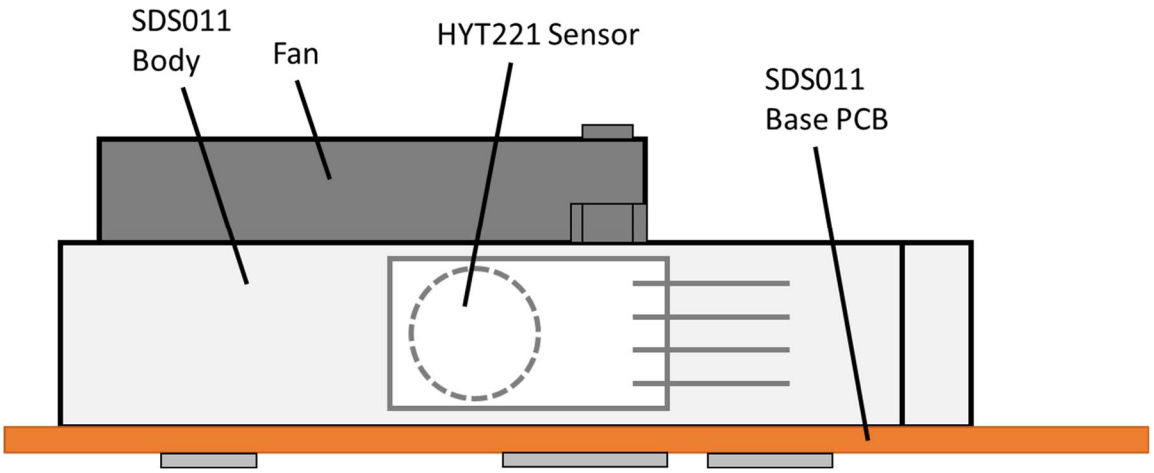

Figure 25: Internal construction of the SDS011 sensor and location of the added HYT221 sensor in the exhaust chamber, top view (a) and side view (b)

For the analysis of the efficiency of the aerosol dryer we constructed a Twin-SDS measurement box for the simultaneous operation of two SDS011 sensors. For the efficiency analysis we equipped one SDS011 with the thermal dryer as described above and the other SDS011 equipped with an identical tube but without heating coil and without thermal isolation. The measurement results of both sensors are stored on SD-card together with a timestamp from a real time clock for later analysis. For datalogging and for the real time clock (RTC) a ready-to-use datalogging shield from Adafruit.com, USA was used. This shield was stacked piggy-back on the Arduino Mega microcontroller.

An Arduino Mega microcontroller reads out the SDS011 sensors via their UART-interfaces, initiates the data-logging and performs the dryer control by reading the HYT sensor and activating the heater switch. The control circuitry of the dryer containing the NMOS switching transistor was soldered on a self-made Arduino shield plugged on top of the datalogging shield.

Figure 26 shows a block diagram of the Twin-SDS measurement box and Figure 27 and Figure 28 shows photos of the box.

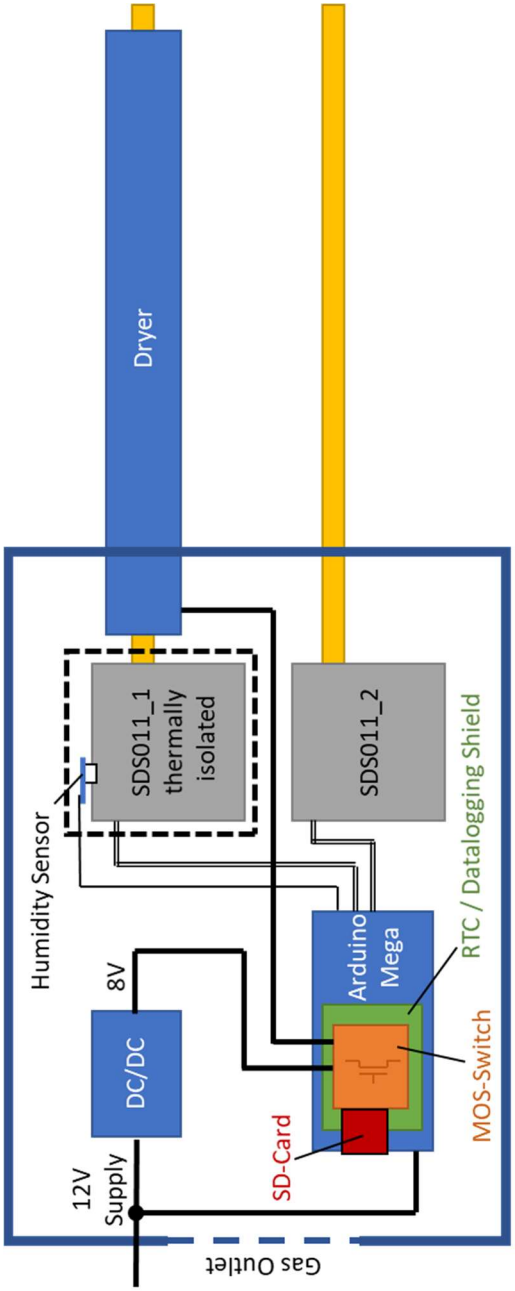

Figure 26: block diagram of the Twin-SDS measurement box for a SDS011 sensor with and without aerosol dryer

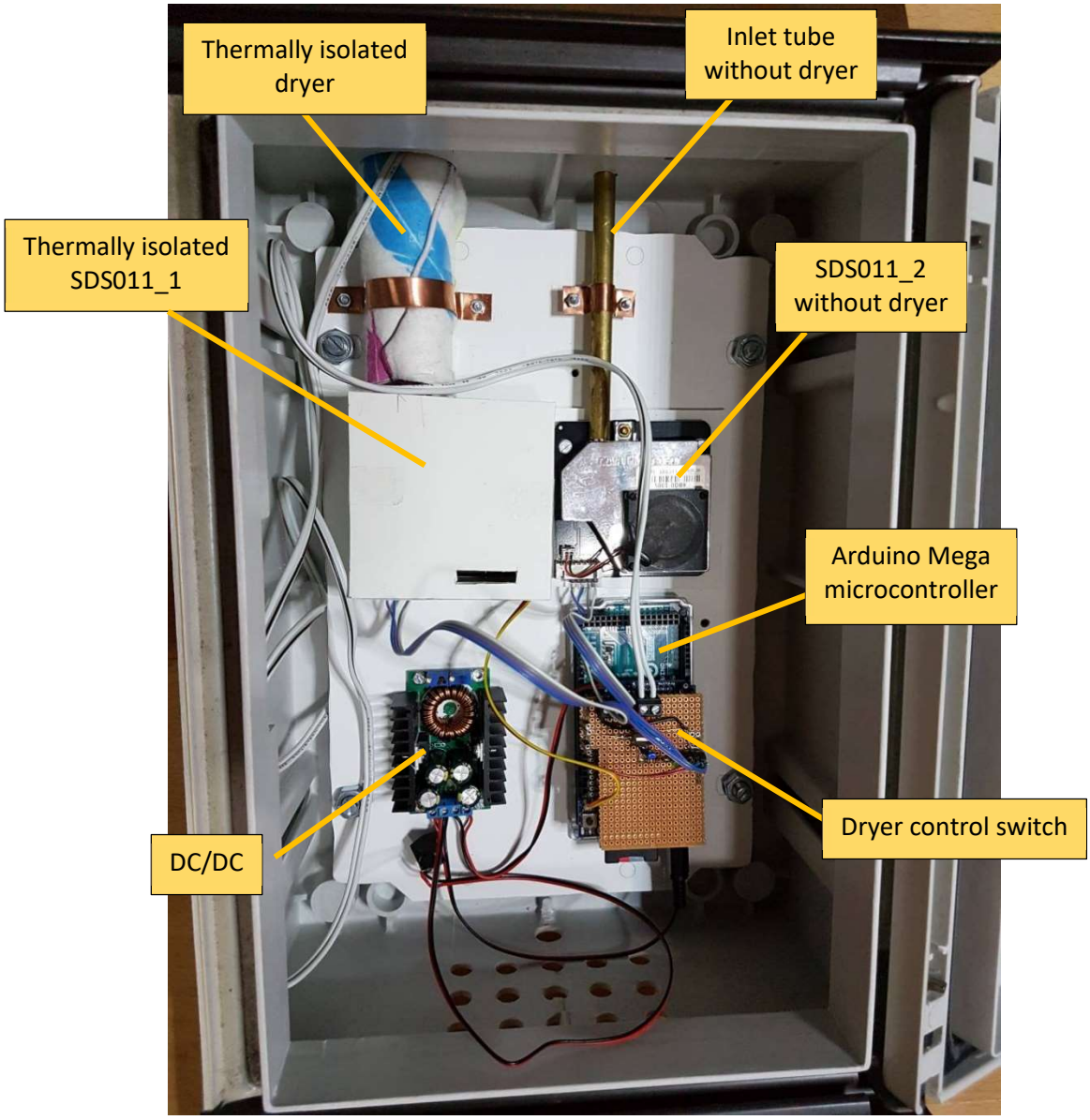

Figure 27: Interior of the Twin-SDS measurement box

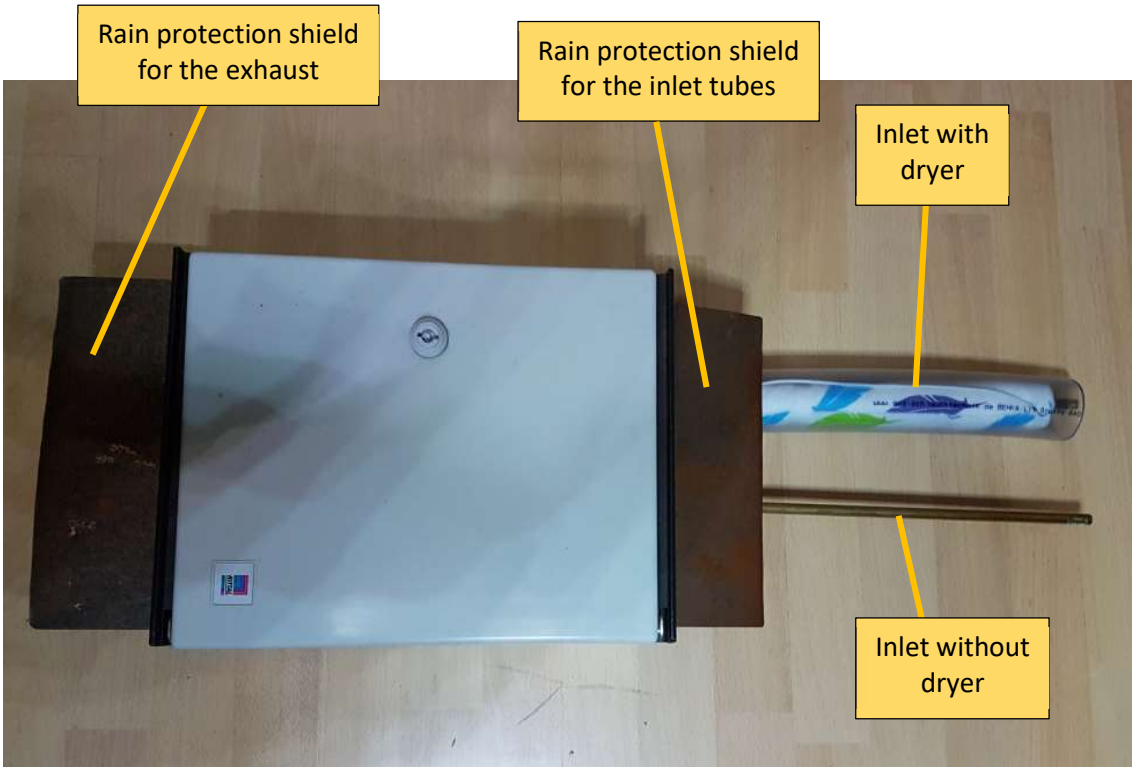

Figure 28: Exterior of the Twin-SDS measurement box

Lab measurements

Comparison of both SDS011 devices

To check the performance of both SDS011, the Twin-SDS measurement box was put into a small test room together with an ultrasonic room humidifier. Both SDS011 were operated in parallel and the dryer was kept off completely initially. When being turned on, the ultrasonic humidifier generates small fog droplets with a mass distribution below 5um. This mass distribution had been checked with an aerosol spectrometer before. In the experiment, the humidifier was activated until both devices reached PM10 values about 500ug/m^3 and then was turned off. The door of the test room was kept closed about 10 hours. During this time, the fog sedimented and the mass concentration decreased according to an exponential law.

With this measurement (see Figure 29) we could confirm that the two SDS011 devices selected from a couple of available devices show very equivalent results for both, the PM10 and the PM2.5 values. For PM2.5, the results were almost equal and for PM10 the values were such similar that we decided not to apply any particular calibration. However, it must be noted again that the SDS011 is not able to report a true PM10 value, it rather estimates it from the distribution of smaller diameters as it was shown in previous research.

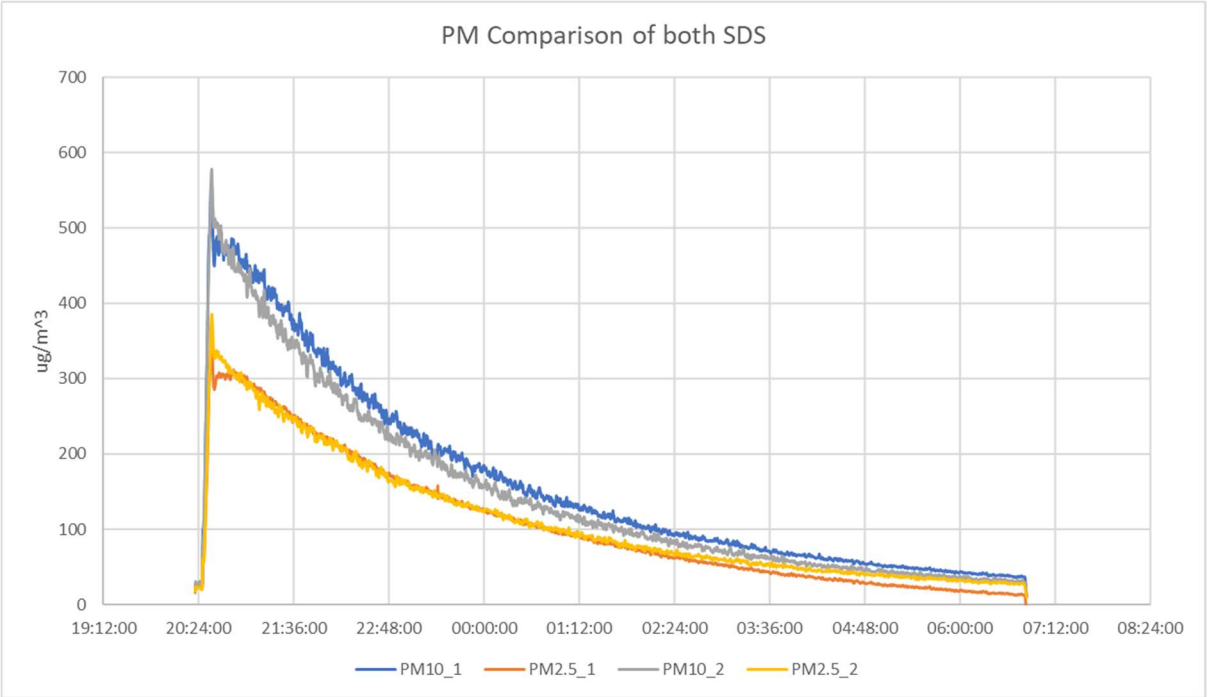

Figure 29: PM10 and PM2.5 results from both SDS011 sensors and the dryer completely deactivated as a response to fog generated from an ultrasonic room humidifier in the lab

Dryer Efficiency in the lab

To validate the functionality of the aerosol dryer and to analyse its efficiency, the above experiment with the ultrasonic humidifier was repeated, and the dryer was turned on for only one hour after the mass concentration had dropped from about 500ug/m^3 to 300ug/m^3. As it can be seen clearly, the dryer significantly reduces the reported PM10 mass concentration of the fog droplets by a factor of about 2 when the electrical energy supplied to the heating coil is adjusted to about 10W. The same efficiency was obtained with respect to the PM2.5 values.

From this experiment we concluded that the thermal energy applied is sufficient to reach even higher efficiencies in outdoor ambient air where mass concentrations are smaller particularly during hygroscopic growth events.

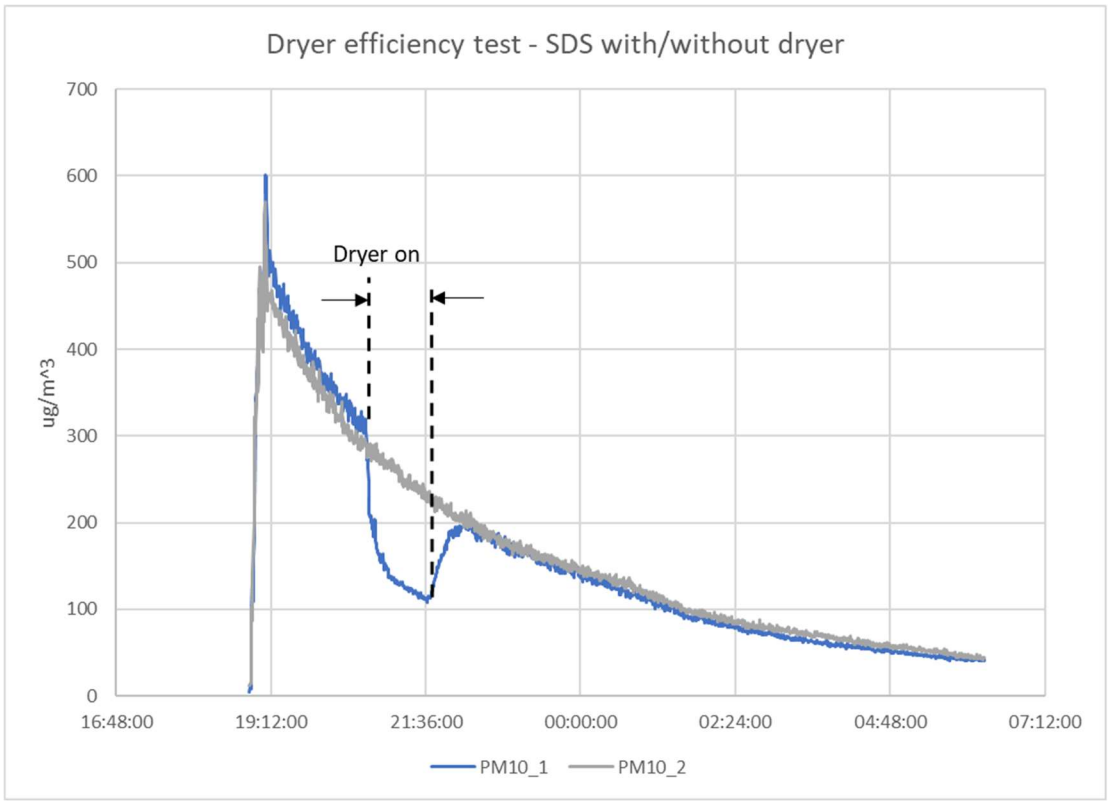

Figure 30: Effect of the aerosol dryer on PM10 readings in the lab for fog generated with an ultrasonic room humidifier, the dryer attached to the SDS011_1 turned on for one hour

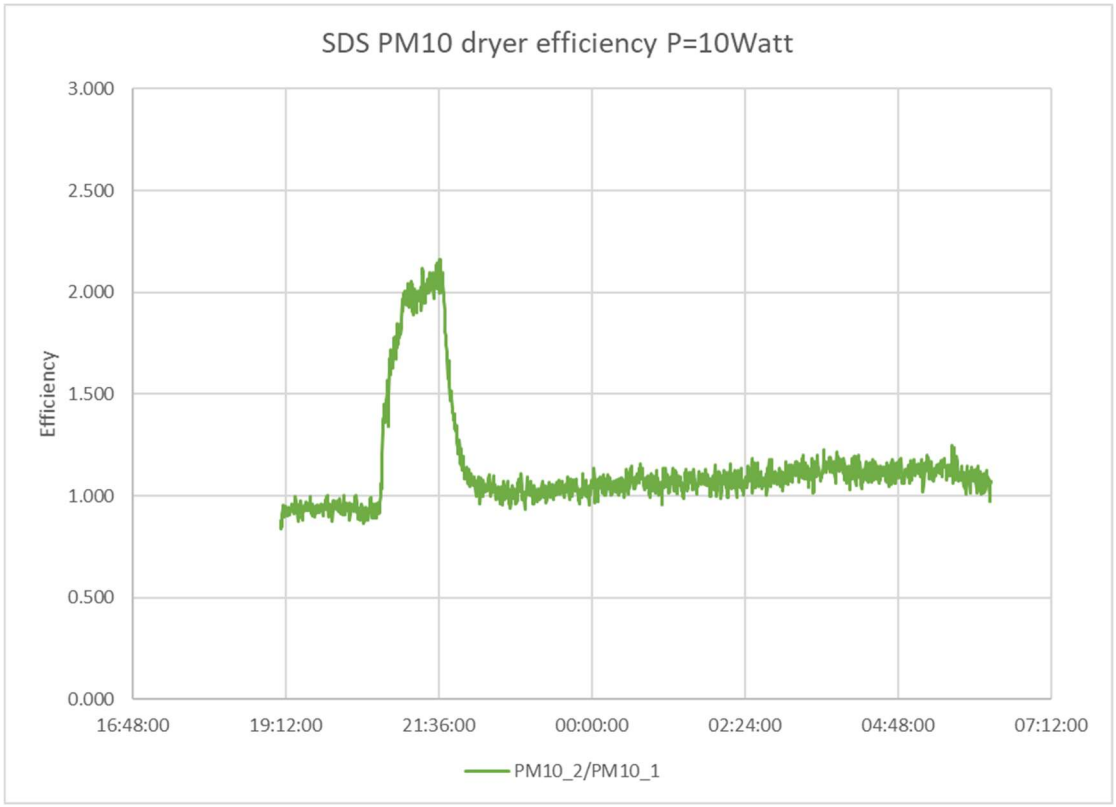

Figure 31: Efficiency of the aerosol dryer in the lab for fog generated with the ultrasonic room humidifier, the dryer attached to the SDS011_1 turned on for one hour

Tests of the dryer control loop in outdoor air

The operation of the dryer in the outdoor ambient air was tested and adjusted during an episode with high humidity. The threshold for the dryer control was set to 35% to safely stay below the efflorescence of most hygroscopic salts contained in urban aerosols and to ensure simultaneously that the aerosol is not overheated. Figure 32 shows the result of the reported PM10 values of both SDS devices and Figure 33 shows the humidity (orange) and the temperature values (blue) measured by the HYT221 sensor integrated into the SDS011 as well as the control signal to the electronic switch (grey).

When the time resolution is sufficiently high and the averaging time is less than 1 minute, it can be observed that the oscillation of the electrical power caused by the switching of the heating coil maps into a similar oscillation of the measured PM10 mass concentration of SDS_1 with the attached dryer whereas the SDS_2 device without dryer just shows regular noise. Obviously, the particle mass reacts very quickly on the change of the thermal energy. The oscillation gets filtered out when the averaging time is increased to more than 30 minutes and therefore has no longer an impact when comparing for example to hourly values of a reference instrument. On the other hand, the oscillations in high resolution data seem to be a valuable monitoring information because it indicates the efficiency of the dryer during operation.

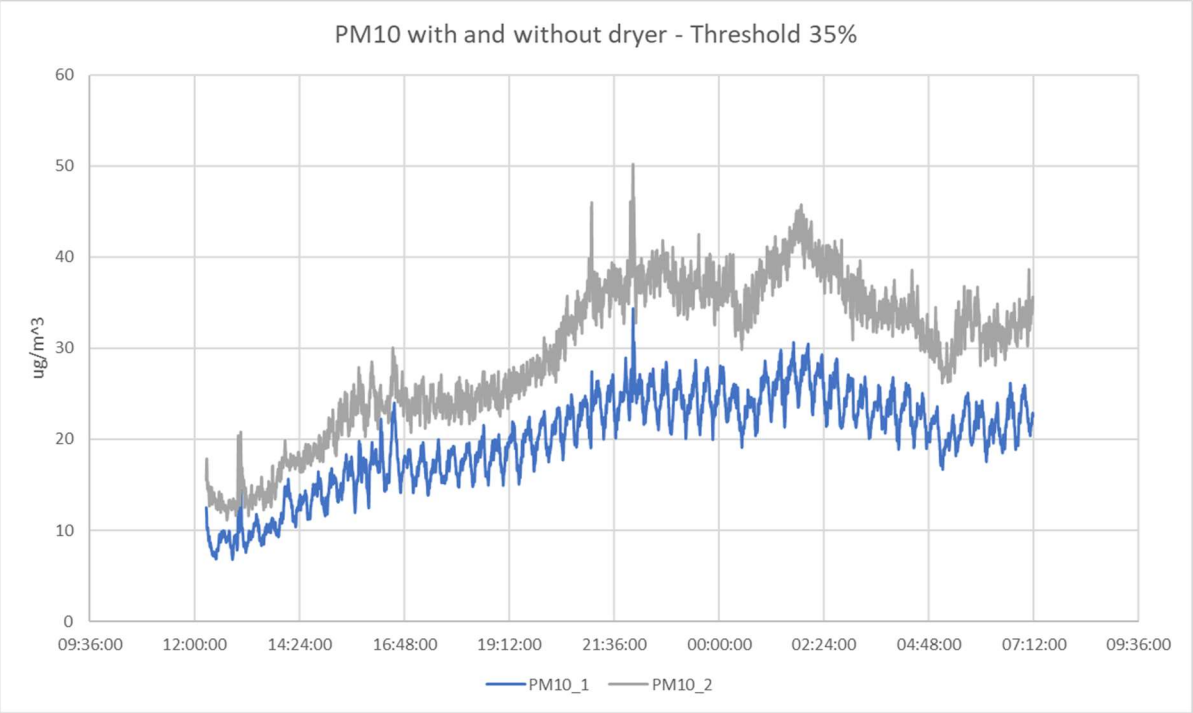

Figure 32: PM10 values of SDS011 sensor with (blue) and without dryer (grey) during an episode of high humidity

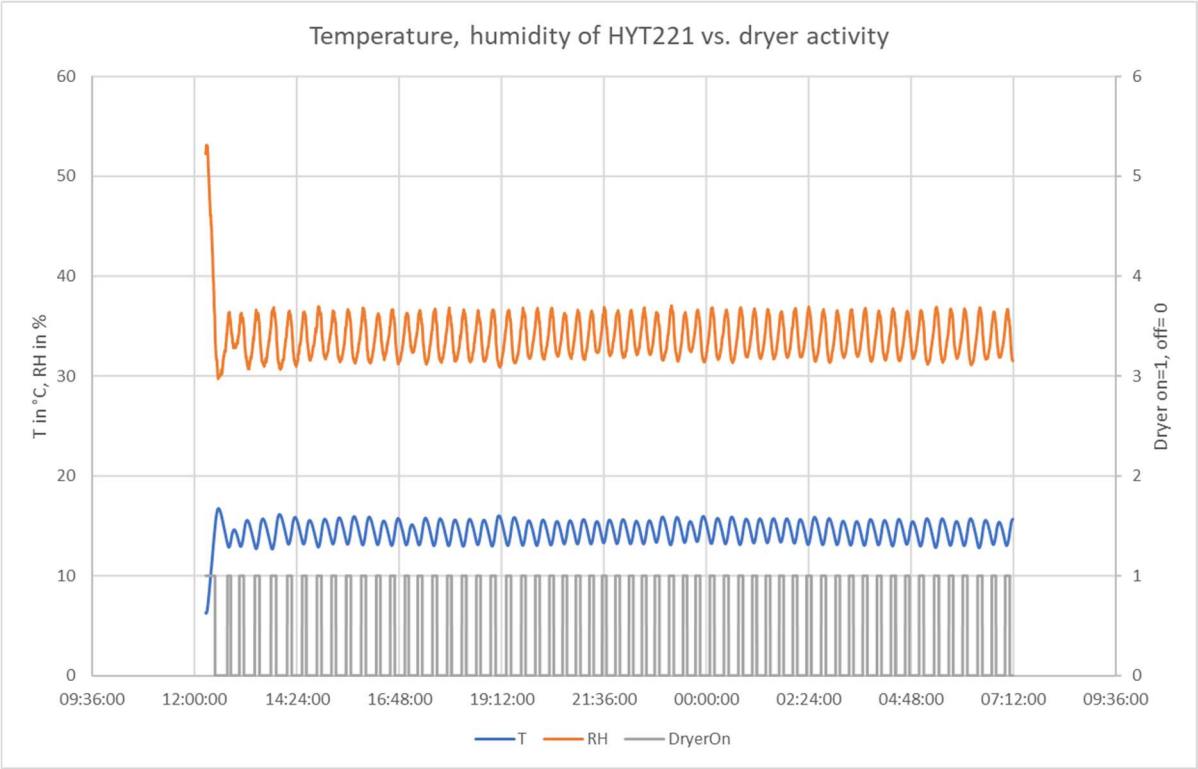

Figure 33: Temperature (blue), relative humidity (orange) as detected in the exhaust chamber by the added HYT21 sensor during an episode of high humidity, the grey signal shows the control signal to the dryer switch

As it can be seen in Figure 33, the control loop keeps the humidity close to 35% with some oscillations because of the inertial behaviour of the thermal energy transferred to the air and sensed in the exhaust chamber. These oscillations of temperature in turn map into small oscillations in the PM concentration due to particle growth that gets modulated by temperature.

Field measurements

Measurements Jan 10 – Jan 31, 2021 in Stuttgart

A first field experiment with the Twin-SDS measurement box was carried out from January 10 to January 31, 2021 in a suburb of Stuttgart with the purpose to capture a typical fog and hygroscopic growth event. In parallel to the box an external temperature/humidity sensor (HYT221) was operated to record the outside ambient air parameters at a small distance. The sensor was not built into the box to avoid heat transfer influencing the humidity measurements. A first evaluation of the data was performed by calculating 10-minute average values to decimate the raw data.

The recorded data indicated a hygroscopic growth event between the 16th and 18th of January where mainly PM10 of sensor 1 with dryer (blue) shows significantly smaller concentrations compared to sensor 2 without dryer (grey) for several hours. In contrast, at the end of the measurement period, on the 30th of January at around 23:30h, a sharp spike (clipped at 40ug/m^3 in the graph) is visible for the sensor 2 without dryer (grey), which is not visible in the data of the sensor 1 with dryer (blue). This was the result of a strong fog event. In between, there are periods where both sensors reported similar values.

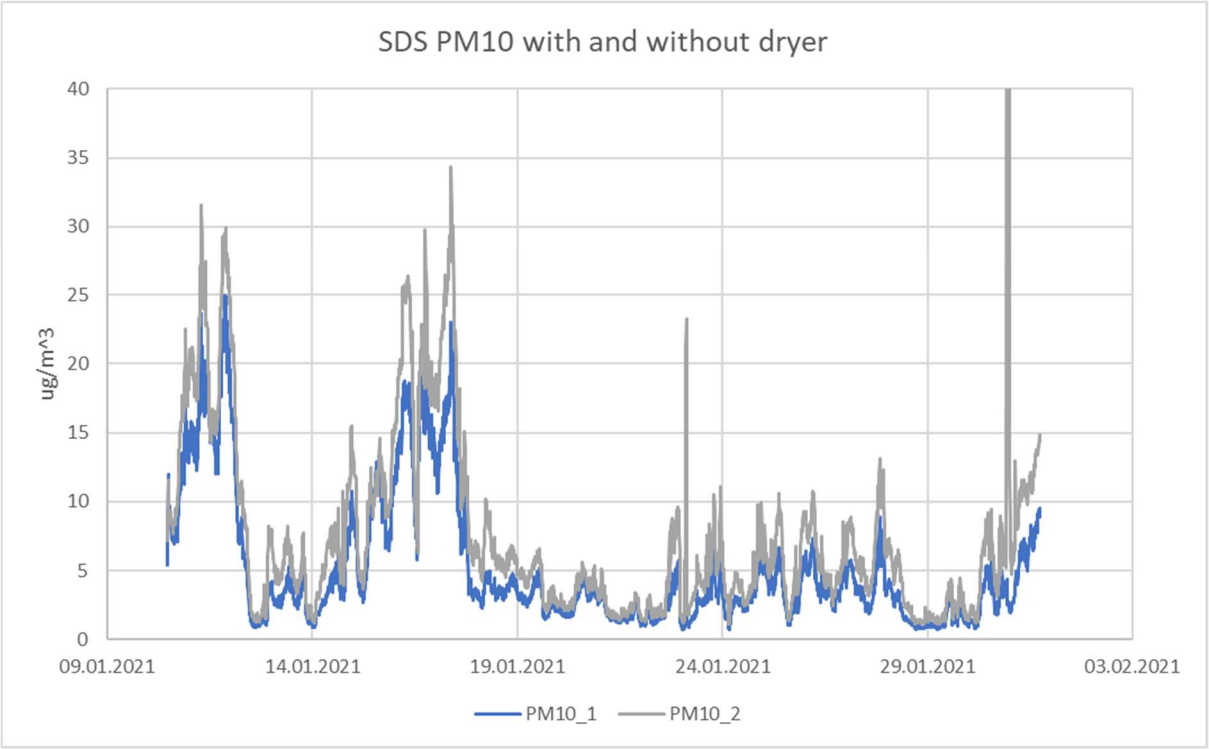

Figure 34: PM10 data from the field experiment in January 2020 showing a hygroscopic growth event during January 16th-18th and a fog event on January 30th, PM10_1 with dryer(blue) and PM10_2 without dryer(grey), 10min averages

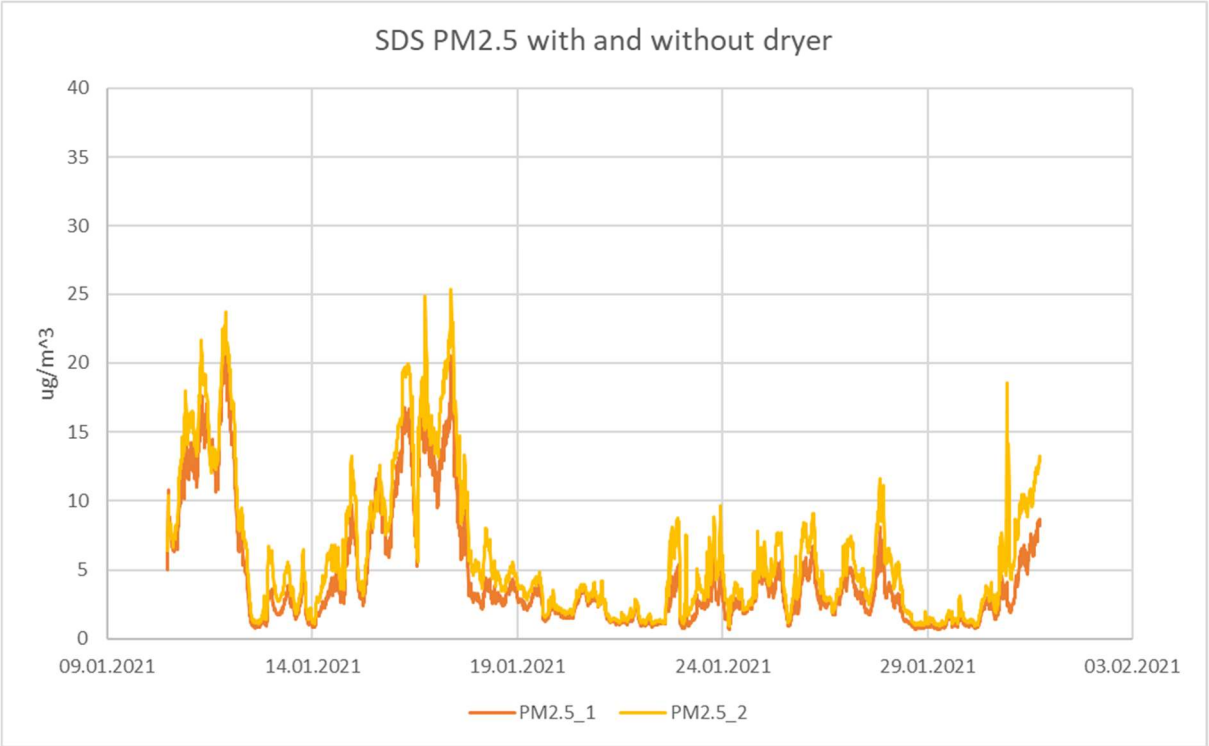

Figure 35: PM2.5 data from the field experiment in January 2020 showing a hygroscopic growth event during January 16th-18th and a fog event on January 30th, PM2.5_1 with dryer (orange) and PM2.5_2 without dryer (yellow), 10min averages

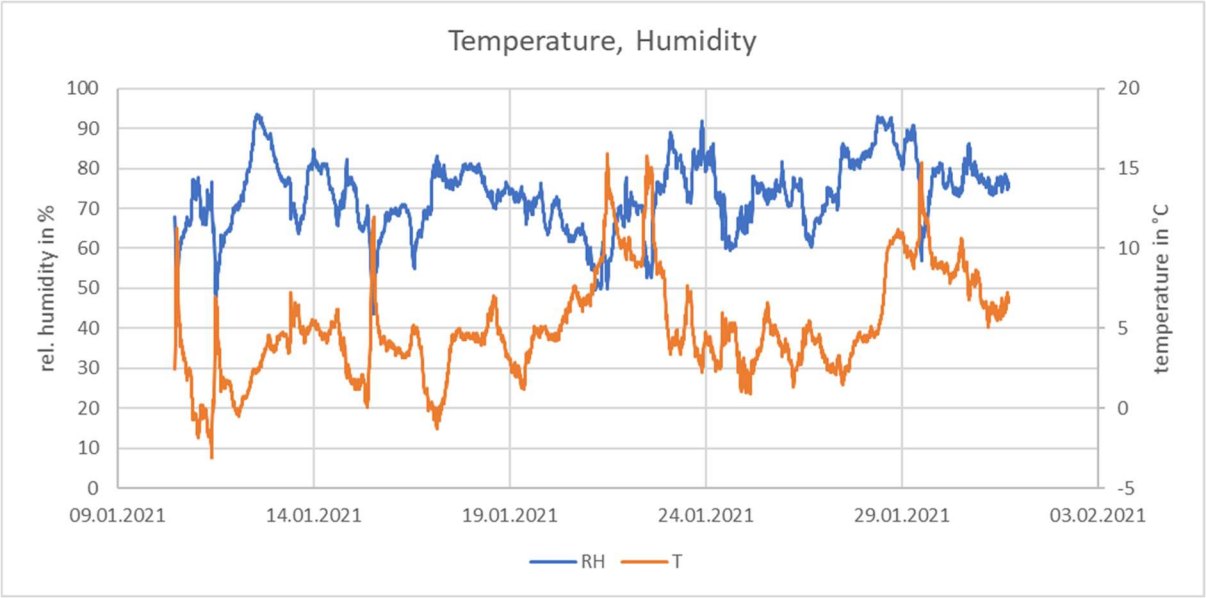

Figure 36: Humidity data (blue) and temperature data (orange) of the outside ambient air during the field experiment in January 2020 showing a hygroscopic growth event during January 16th-18th and a fog event at January 30th, 10min averages

The recorded humidity data showed high values during both events, but they cannot be clearly assigned to extremely high or even maximum values. During the fog event the humidity sensor recorded about between 76 and 78% relative humidity. The influence of humidity was stronger on PM10 values reported from the sensor compared to PM2.5.

When the data of sensor 2 without dryer are plotted against the data of sensor 1 with dryer the points do not match the anticipated behaviour of a consistent growth function with humidity according to a typical growth model. Instead, at two humidity regions the sensor 2 without dryer shows excessive values for PM2.5 (Figure 37).

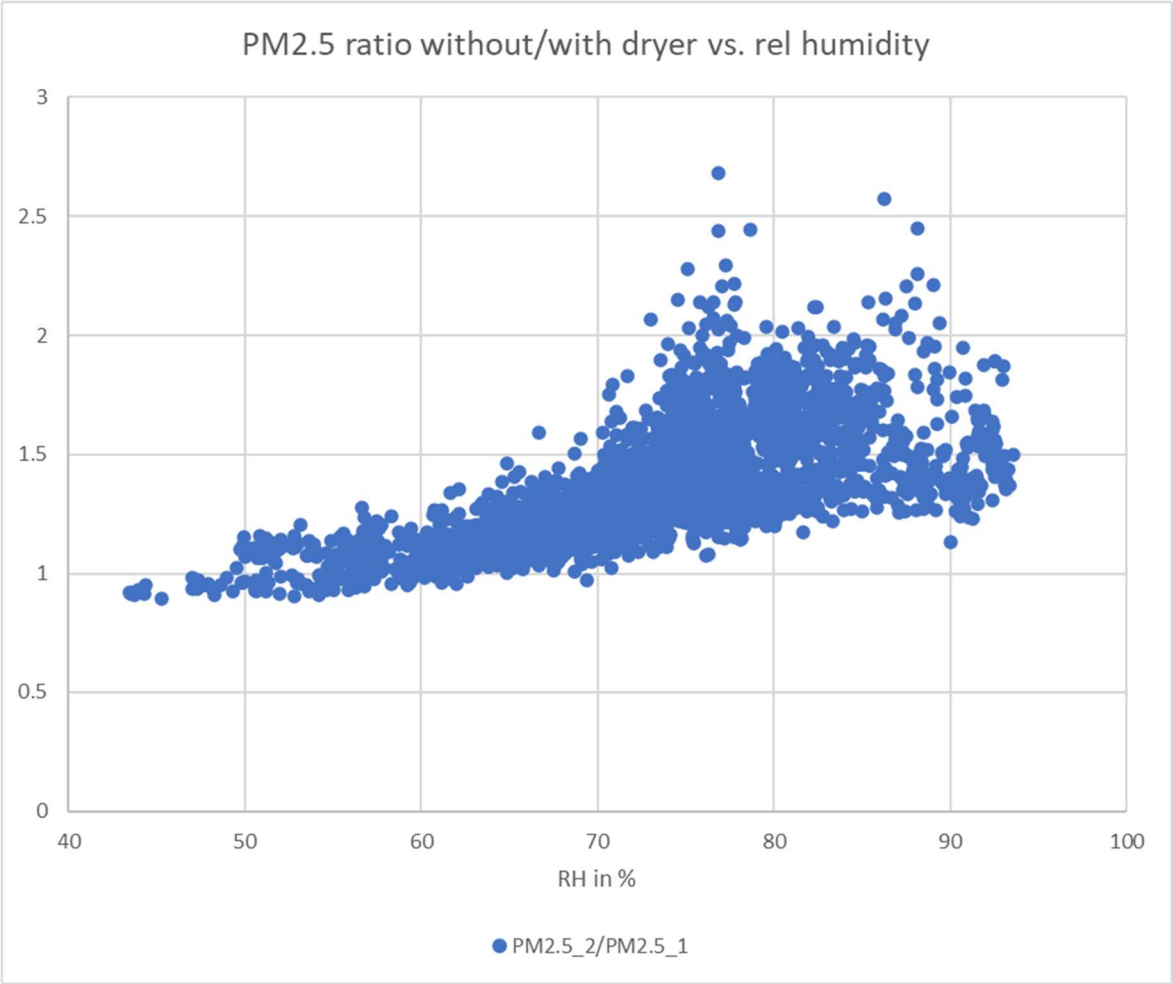

Figure 37: PM2.5 ratio of wet and dry particles plotted vs. humidity for the whole measurement period of January 2020, high values occur at two levels of humidity (around 77% RH and around 87% RH)

For further analysis, the data were averaged to 1-minute intervals to obtain high resolution data with a zoom into the region of anticipated hygroscopic growth and into the fog event. The fog event manifests as a sudden jumping to remarkably high values in PM10 of the sensor 2 without dryer, an order of magnitude higher than the values measured shortly before. During the event, the values show high variation as well. The sensor 1 with dryer does not show any impact at all. It appears that the dryer was able to completely suppress the fog event. For PM2.5, a jump to high values occurs too for sensor 2 without dryer but the jump is smaller and does no longer require a logarithmic scale to display the dynamics of the jump. Again, the dryer on sensor 1 completely suppresses the fog impact on the PM2.5 results.

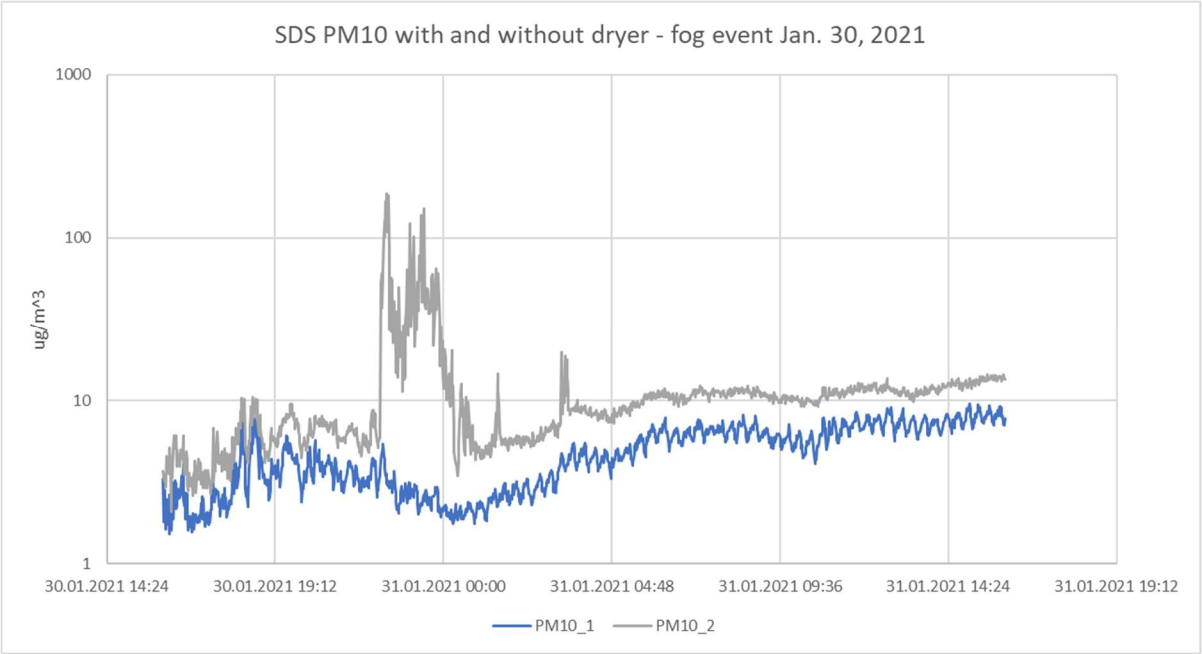

Figure 38: PM10 on a log scale during the fog event on January 30th with dryer (blue) and without dryer (grey), 1-min averages

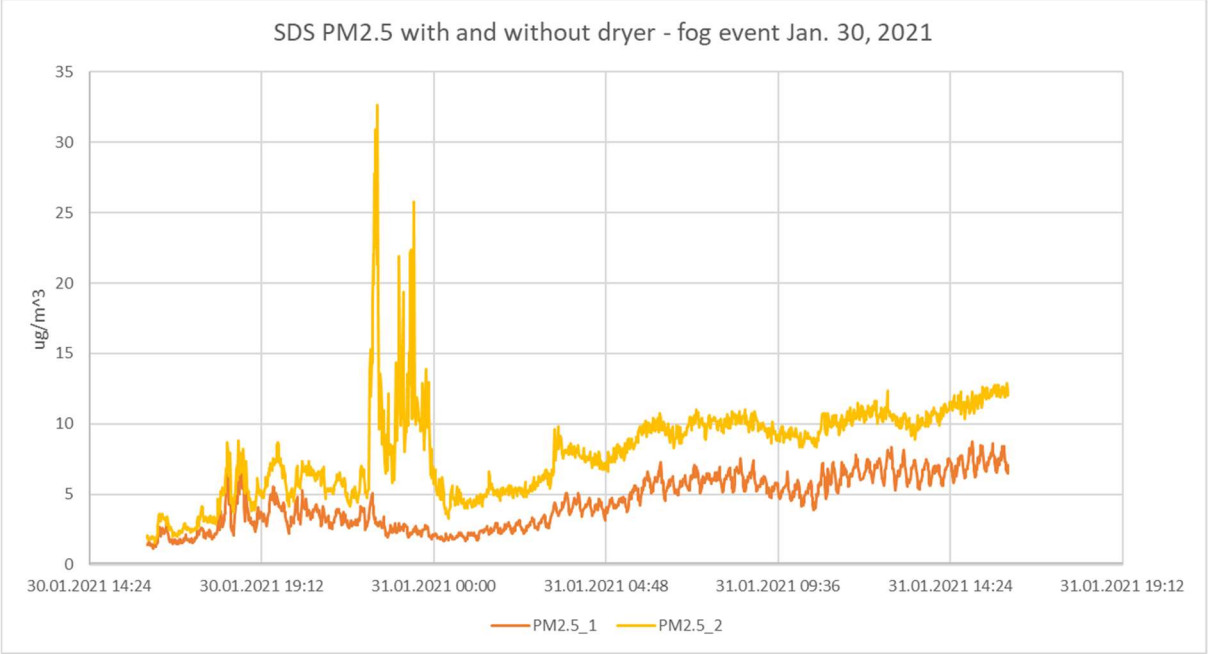

Figure 39: PM2.5 on a linear scale during the fog event on January 30th with dryer (blue) and without dryer (grey), 1-min averages

Similarly, the data constrained to the hygroscopic growth event from January 15th-18th were analysed with high temporal resolution of 1 minute. It can be observed that the PM10 result of the sensor is more affected by the growth than the PM2.5 result.

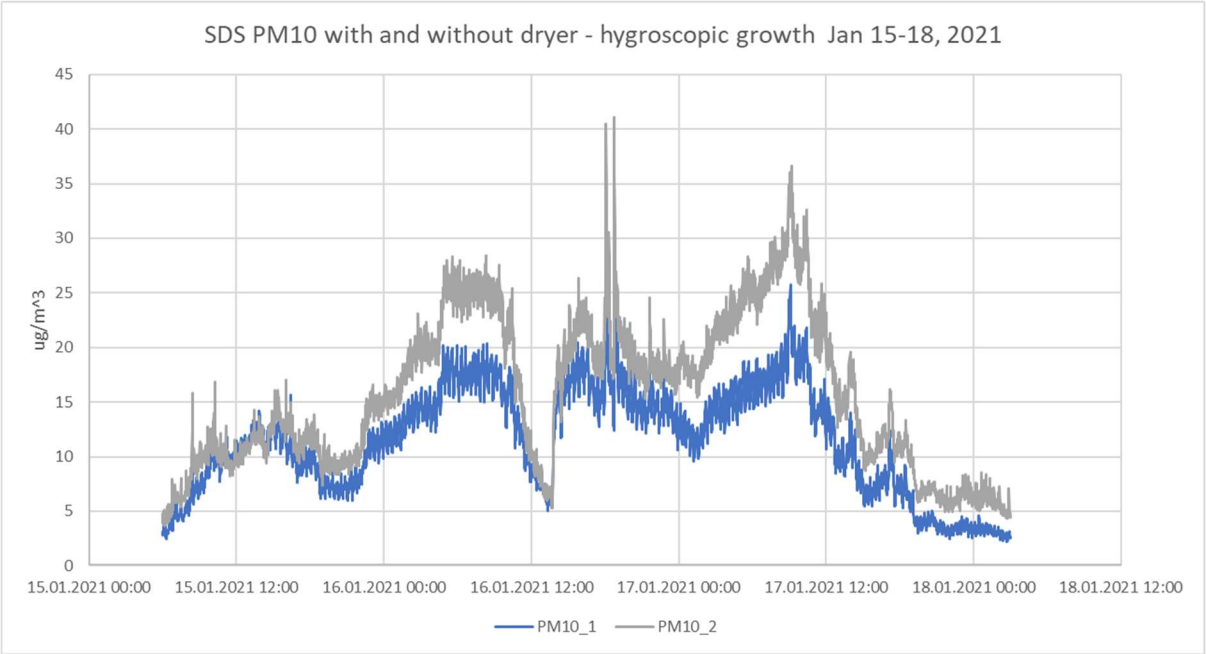

Figure 40: PM10 during the hygroscopic growth event on January 16th – 18th with dryer (blue) and without dryer (grey), 1-min averages

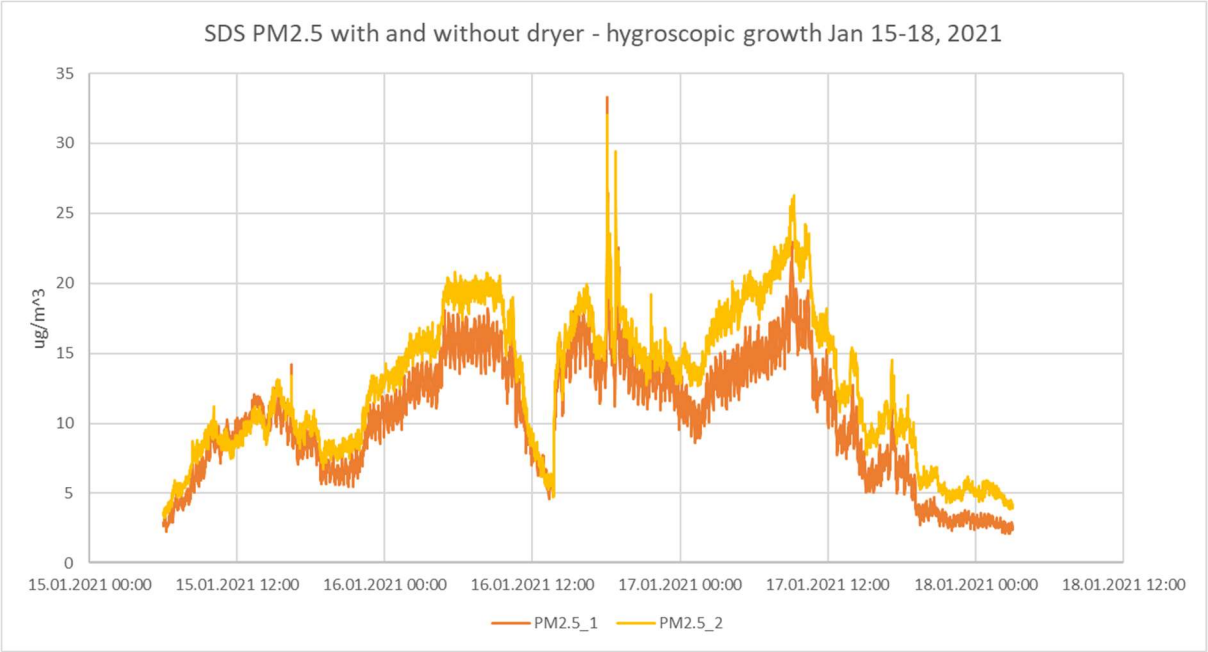

Figure 41: PM2.5 during the hygroscopic growth event on January 16th – 18th with dryer (orange) and without dryer (yellow), 1-min averages

A remarkably interesting outcome is, that the measurement data constrained to the fog and the hygroscopic growth event show completely different growth function results when plotting data versus the humidity. Whereas the fog event does not yield a growth function that can be modelled with a continuous function, the constraint to the hygroscopic growth event indeed yields a growth function that can be matched well to a continuous growth model such as the one described by Hänel. This is the case for both the PM10 and the PM2.5 data. For PM10, the maximum growth yields a factor of about 1.7 at 80% relative humidity whereas for PM2.5 it yields a factor of 1.6 at 80% relative

humidity. The Hänel coefficients with respect to mass growth are $\beta_m = 0.54$ for PM10 and $\beta_m = 0.49$ for PM2.5. These results appear to be plausible for a hygroscopic growth event even though the Hänel coefficients are only half of what was obtained when comparing the OK Lab sensor # 7687 to the LfU reference station ($\beta_m = 0.8019$ for PM2.5).

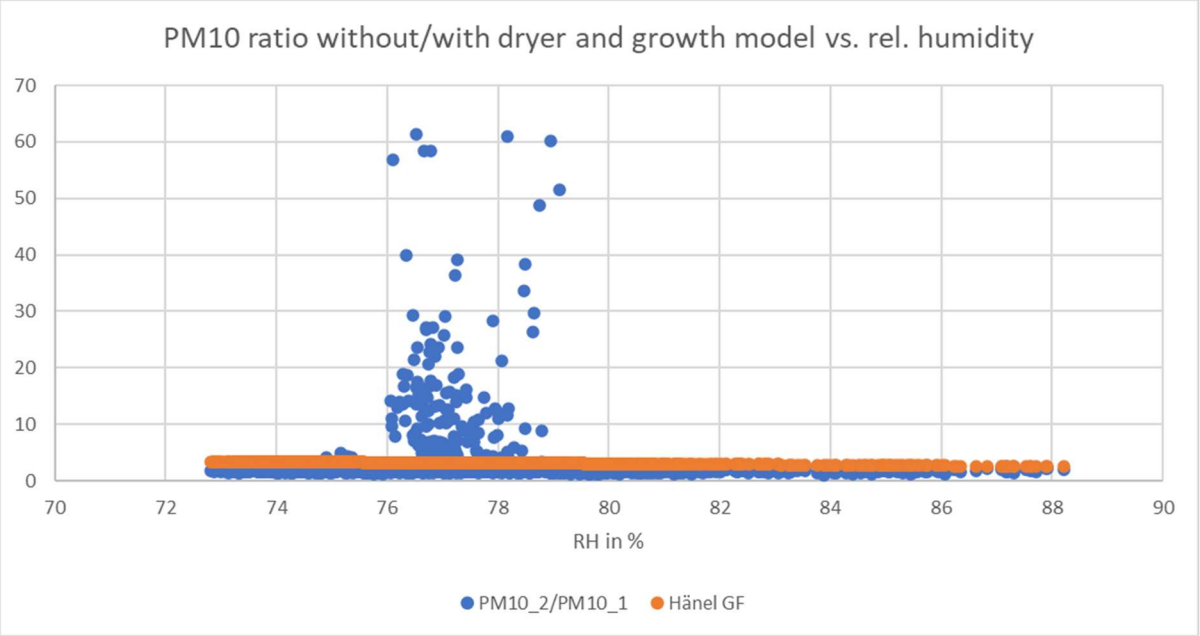

Figure 42: PM10 ratio of wet and dry particles plotted vs. humidity for the fog event on January 30th (blue) and fitting of a growth model according to Hänel (orange), high values occur at a humidity level of 77% RH

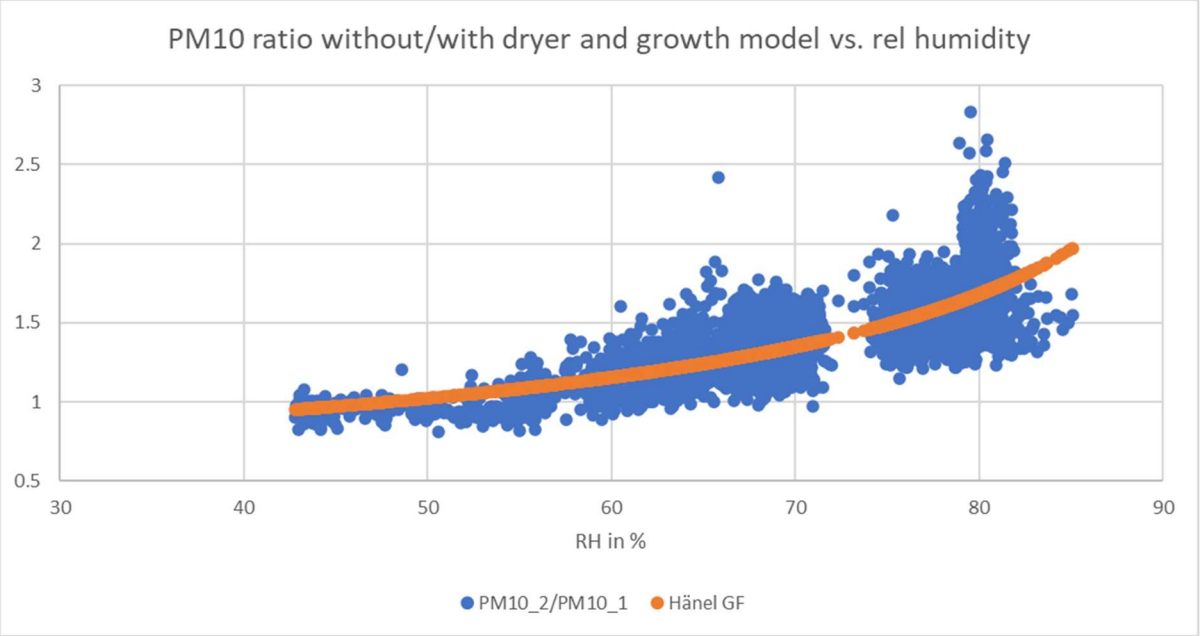

Figure 43: PM10 ratio of wet and dry particles plotted vs. humidity for the hygroscopic growth event January 16th -18th (blue) and fitting of a growth model according to Hänel (orange)

When plotting the ratio of PM values of wet and dry particles, which means the data from the sensor without dryer divided by those with dryer for the fog and the hygroscopic growth events and an individual zoom into these timeframes is applied, a significant difference pops up (Figure 42 and Figure 43, Figure 44 and Figure 45). The fog event shows a singular increase at around 77% RH and an extremely poor model fit for a growth function according to the Hänel model. In contrast, the

measured data during the hygroscopic growth event show a typical growth behaviour and the model fit for a growth function according to Hänel is possible for PM10 and PM2.5 with a relatively good quality of fit.

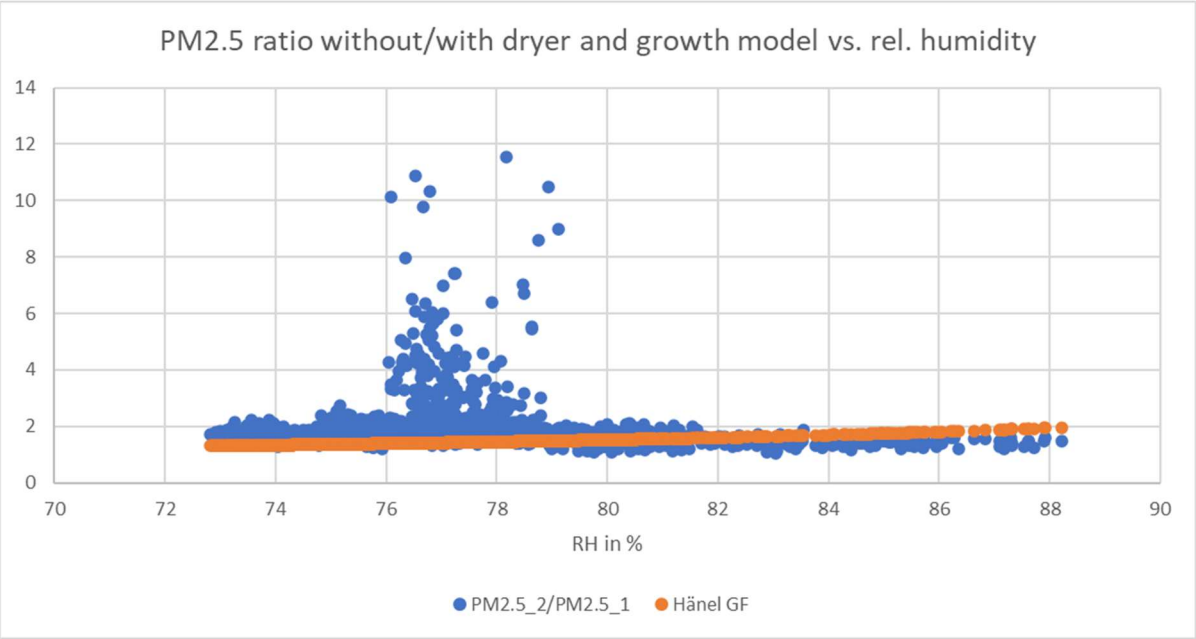

Figure 44: PM2.5 ratio of wet and dry particles plotted vs. humidity for the fog event on January 30th (blue) and fitting of a growth model according to Hänel (orange), high values occur at a humidity level of 77% RH

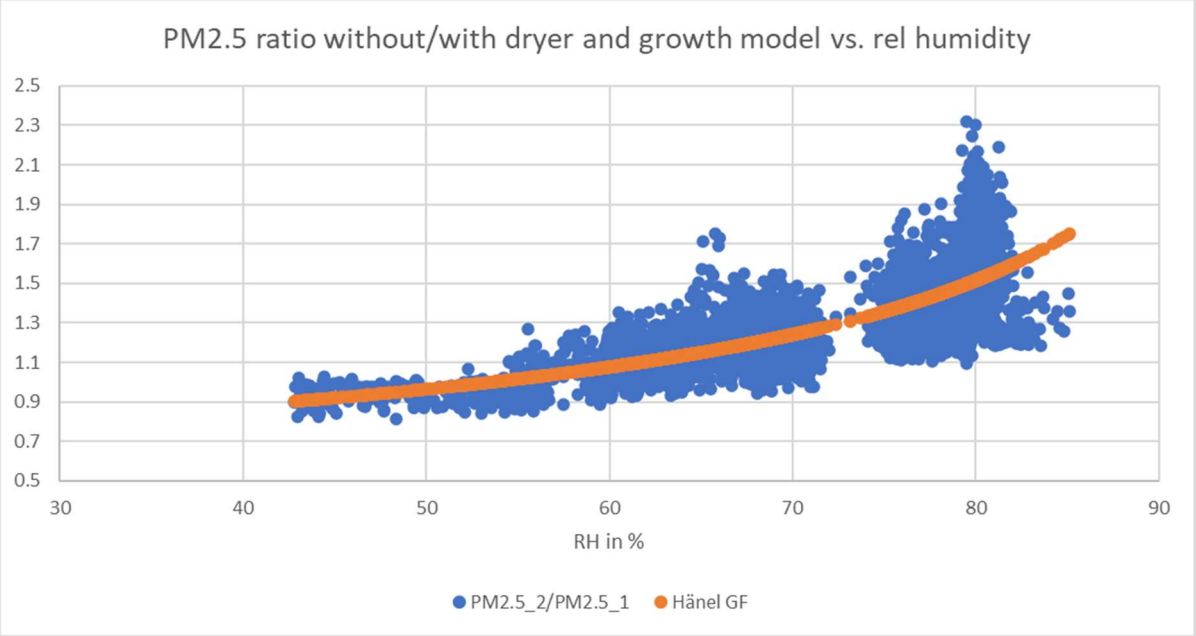

Figure 45: PM2.5 ratio of wet and dry particles plotted vs. humidity for the hygroscopic growth event January 16th-18th (blue) and fitting of a growth model according to Hänel (orange)

This finding seems to be important to understand a major difference between typical fog events and hygroscopic growth. The occurrence of fog events in a data set can obviously jeopardize the modelling and visualization of hygroscopic growth over the whole measurement period.

A key element for understanding such particle phenomenon is the size distribution. Since the particle mass is related to the volume of the particles, not only the distribution of the number of particles versus their diameter is important but also their volume or mass distribution with respect to their

diameter. Since the volume and thus the mass is proportional to the third power of the diameter d (the size), a mass distribution typically has a completely different shape than a number distribution. PM refers to a mass concentration and therefore is calculated by summing up the product of the number bins times d^3, times the collection efficiency of the respective PM filter (implemented by software by the low-cost sensor). Consequently, it is important to understand what size bins contributed most to a PM value.

To better understand this dependency, another particle sensor (Alphasense OPC-N3) was operated in parallel to the Twin-SDS measurement box that has the capability to spectrally resolve the particle number concentration with respect to their size. Using the volume of a sphere and assuming the density of water, the values in the number bins were converted into mass values and the mass distribution was determined. Since the Alphasense OPC-N3 is a small sensor made of plastic, it allows to much better analyse the humidity influence compared to a professional instrument with a high thermal mass that is also generating a lot of heat internally.

During the fog event at 30th of January the OPC-N3 data were used to calculate the mass spectrum versus size of the aerosol. As it can be seen clearly from Figure 47a and b, the fog droplets generated an extremely high peak in mass concentration around 10um, also extending to sizes smaller than 5um and to sizes larger than 15um. Since the OPC can really measure a true PM10 value from all particle sizes relevant for PM10, it shows a much higher PM10 peak value compared to the SDS011 (Figure 46). The fact that the fog droplet distribution ranged down to less than 5um however, caused the SDS011 to detect a fraction of the droplets and to react with high values in the PM10 output. In contrast, fog droplets larger than 5um are no longer detected by the SDS011 and therefore the PM10 values are smaller than that of the OPC.

Since fog may show up with various droplet size distributions depending on meteorological conditions, it may happen that the SDS011 is not able to detect a fog event with droplet sizes significantly larger than 5um (heavy, wet fog). A requirement for a fog event to be detected by the SDS011 is therefore that the droplet size extends to the smaller sizes below 5um (dry and very cold fog, haze, and mist).

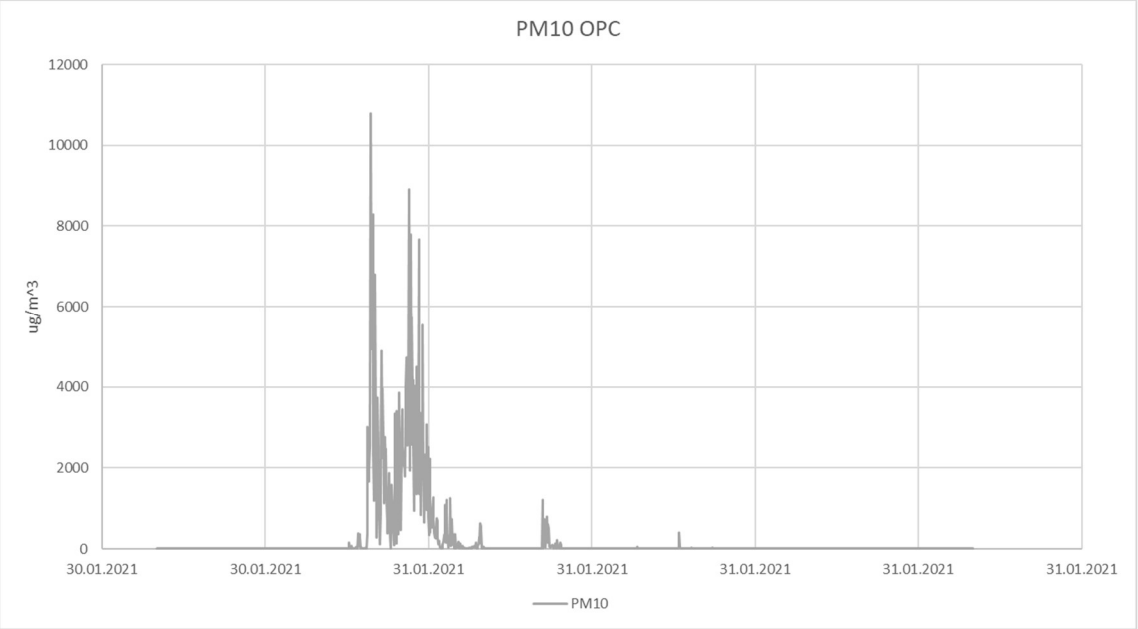

Figure 46: PM10 concentration as measured by the Alphasense OPC-Nr sensor during the fog event on January 30th, 2021

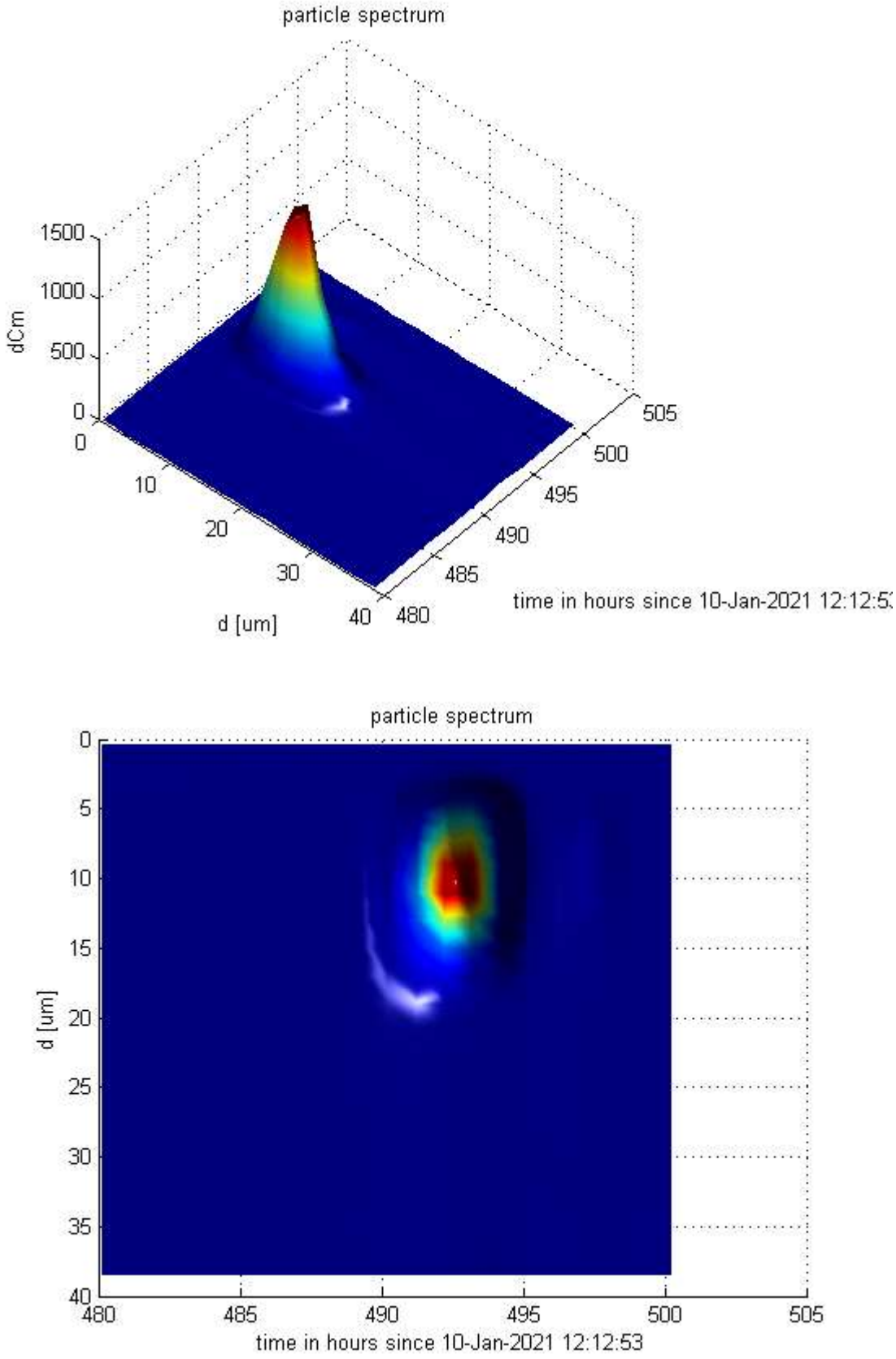

Figure 47a, b: Different views of the mass concentration as measured by the Alphasense OPC-Nr sensor during the fog event in January 30th2021, clearly its centre can be identified at 10um

Sahara Dust Event on Feb 6, 2021

Between February 3rd and 8th, a field experiment was carried out during weather conditions that caused a moderate hygroscopic growth phase with a relative humidity around 80%. On February 6th however, a strong Sahara dust event occurred and was captured by the sensors. Since an Alphasense OPC-N3 was running in parallel to the SDS011 sensors, it was possible to identify the mass spectrum and to better understand the behaviour of the SDS011 low-cost sensor.

During the 6th of February, the SKIRON Atmospheric Modelling and Weather Forecasting Group of University of Athens predicted a large dust cloud from Sahara to reach Germany.

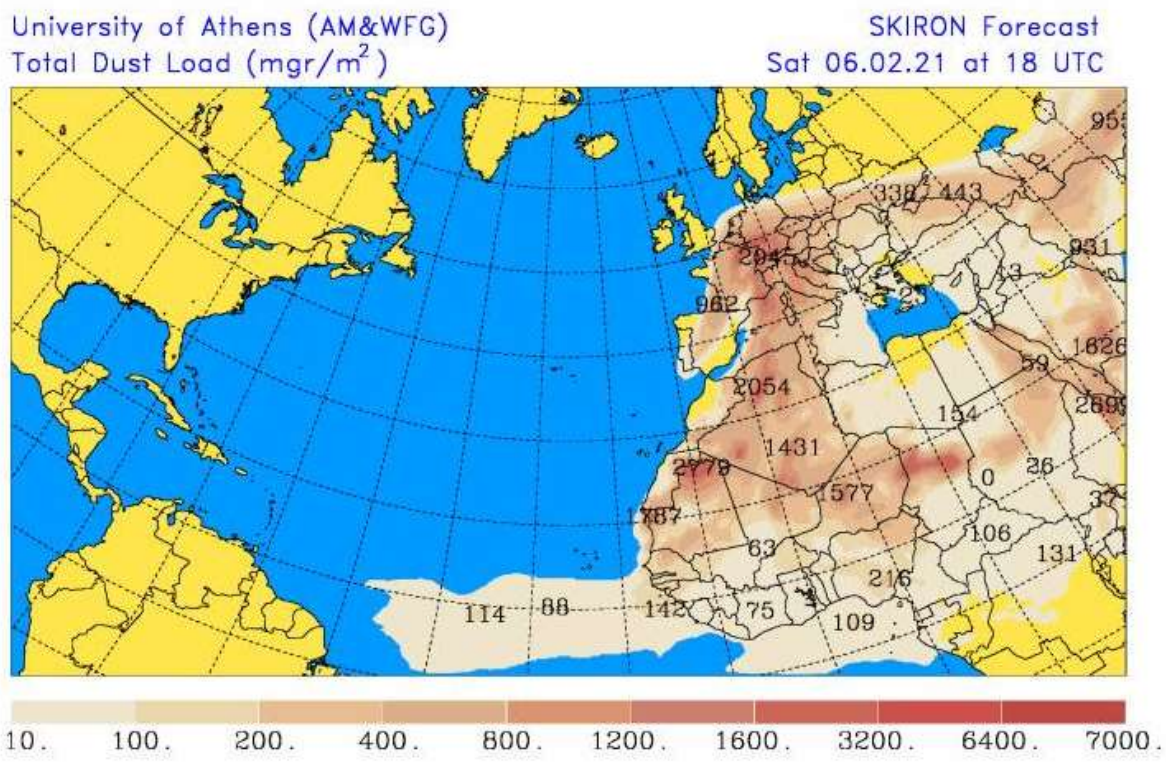

Figure 48: Forecast of the Sahara dust event from AM&WFG group, University of Athens (source: https://forecast.uoa.gr/en/forecast-maps/dust/europe)

In pictures of the Meteosat satellites a huge dust cloud moving from the North of Africa over Spain towards Central Europe was visible. At Feb. 6th at noon the air mass reached Germany and at 18:00h it covered Germany completely. The red-brown dust cloud caused very impressive light effects. A portion of the dust sedimented and also acted as condensation nuclei in the humid air.

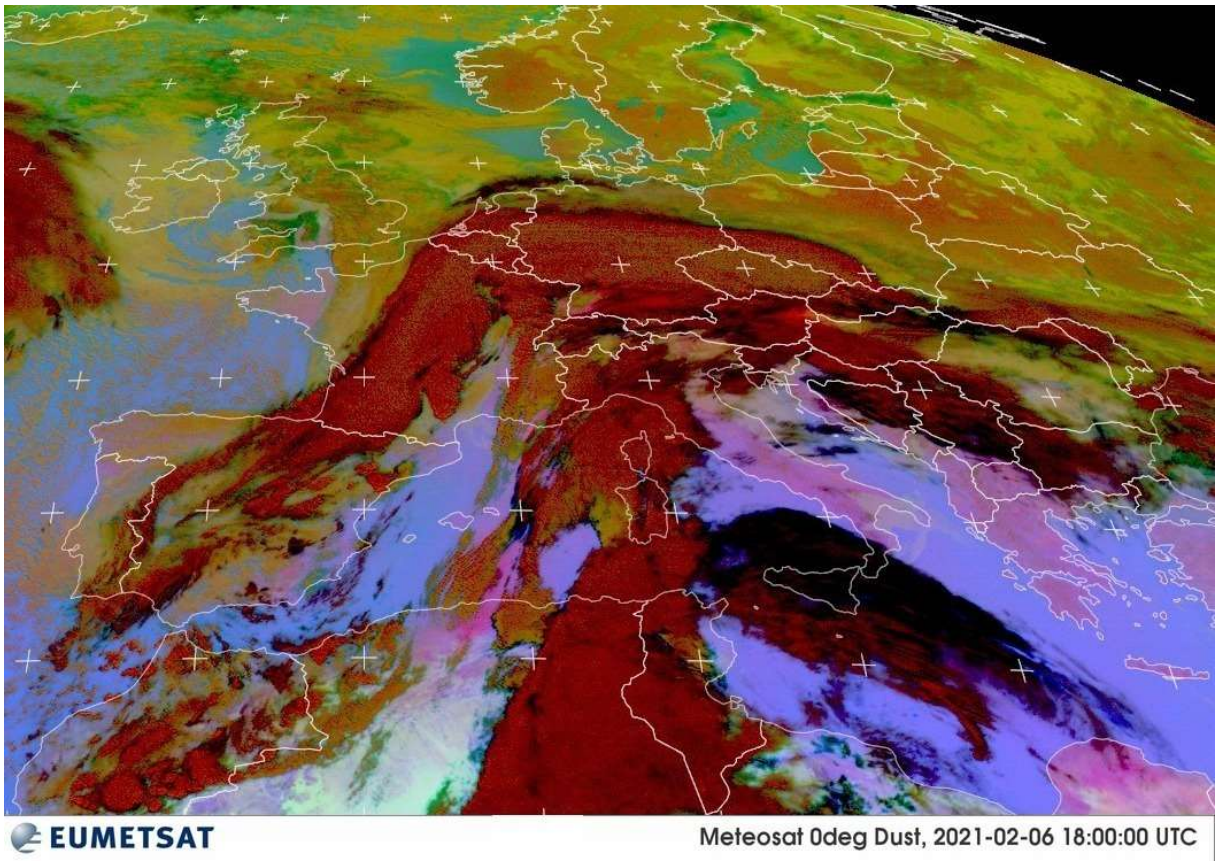

Figure 49: The Sahara dust event as seen by the Meteosat Satellites of Eumetsat group (source: https://eumetview.eumetsat.int/static-images/MSG/RGB/DUST/CENTRALEUROPE/index.htm)

Figure 50: View of the city of Stuttgart at noon of February 6th, red-orange dust clouds caused a strange illumination of the city

Figure 51: In the morning of February 7th, cars were covered with red-brown dust contained in condensing water

The OPC clearly mapped the hygroscopic growth event starting on Feb. 3rd into both PM2.5 and PM10. It ended with heavy rain beginning of Feb. 8th. The Sahara dust event occurring on Feb. 6th was superimposed on top requiring a logarithmic scale to fully show the mass concentration dynamics. Whereas PM2.5 reacted moderate, PM10 values show extremely high values of several milligram per cubic meter of mass concentration.

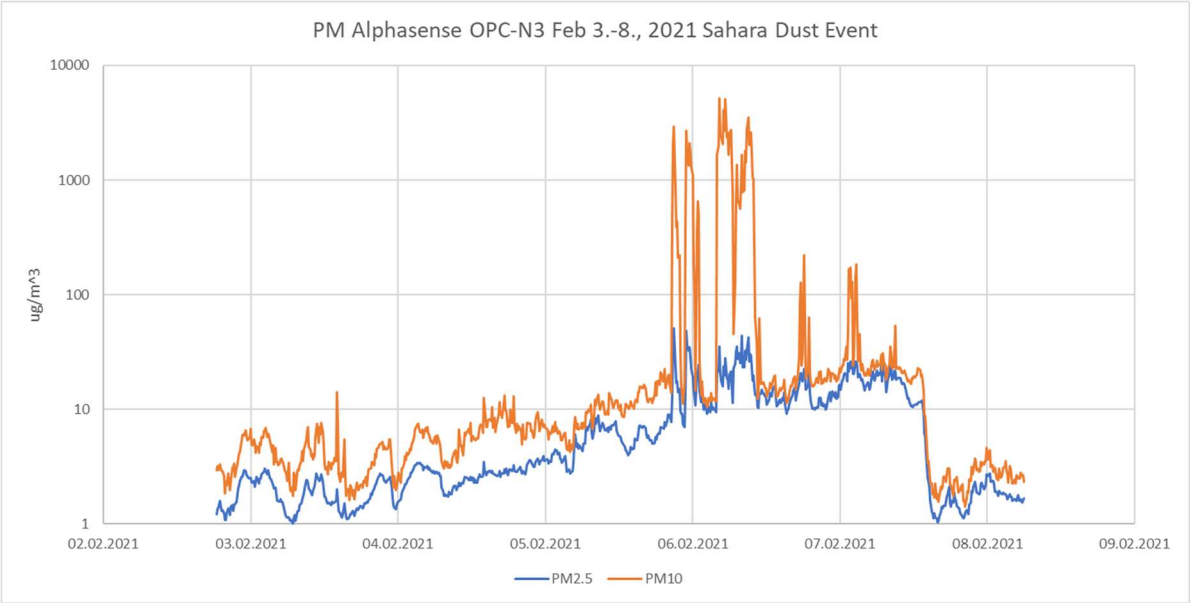

Figure 52: PM2.5 and PM10 values measured with an Alphasense OPC-N3 sensor during the Sahara dust event showing milligrams per cubic meter of mass concentration in PM10

The spectral analysis of mass concentration with respect to particle size clearly shows the centre mass concentration around 25um. That means most of the particle mass was located outside of the PM10 filter efficiency specification. However, it also becomes evident that the mass distribution was wide enough to reach the 10um still with sufficiently high mass concentration values and to have PM10 showing large peaks (Figure 53).

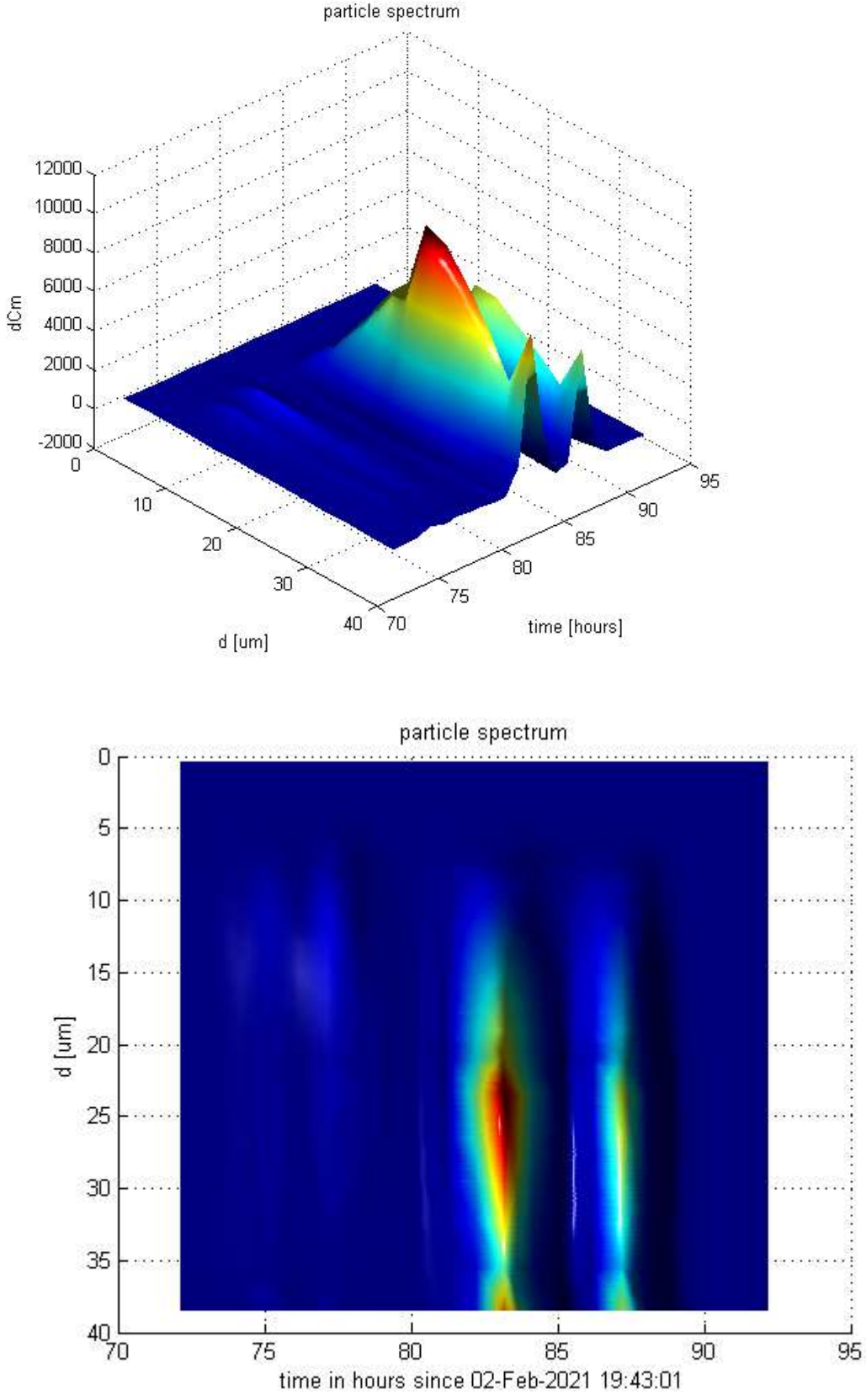

Figure 53: Different views of the mass concentration as measured by the Alphasense OPC-N3 sensor during the Sahara dust event on Feb 6th 2021, clearly its centre can be identified at 25um

A remarkably interesting finding was, that the OK Lab network indeed reported elevated values mainly in the morning of Feb. 7th. However, this was mainly due to the growth effect of small particles in the morning haze. The Twin-SDS measurement box reported moderately high PM values starting from Feb. 3rd on with a peaking value of 35ug/m^3 for PM10 on Feb. 7th. On Feb 6th only small but sharp spikes reaching only about 30ug/m^3 for PM10 are visible for the SDS011 without dryer and about 20ug/m^3 for the SDS with dryer. This is a clear indication that the Sahara dust event was almost invisible to the SDS011 due to its detection limit of smaller than 5um for the size of the particles. However, the hygroscopic growth that occurs at much smaller particle sizes is clearly visible to the SDS011 in the PM10 and PM2.5 value outputs.

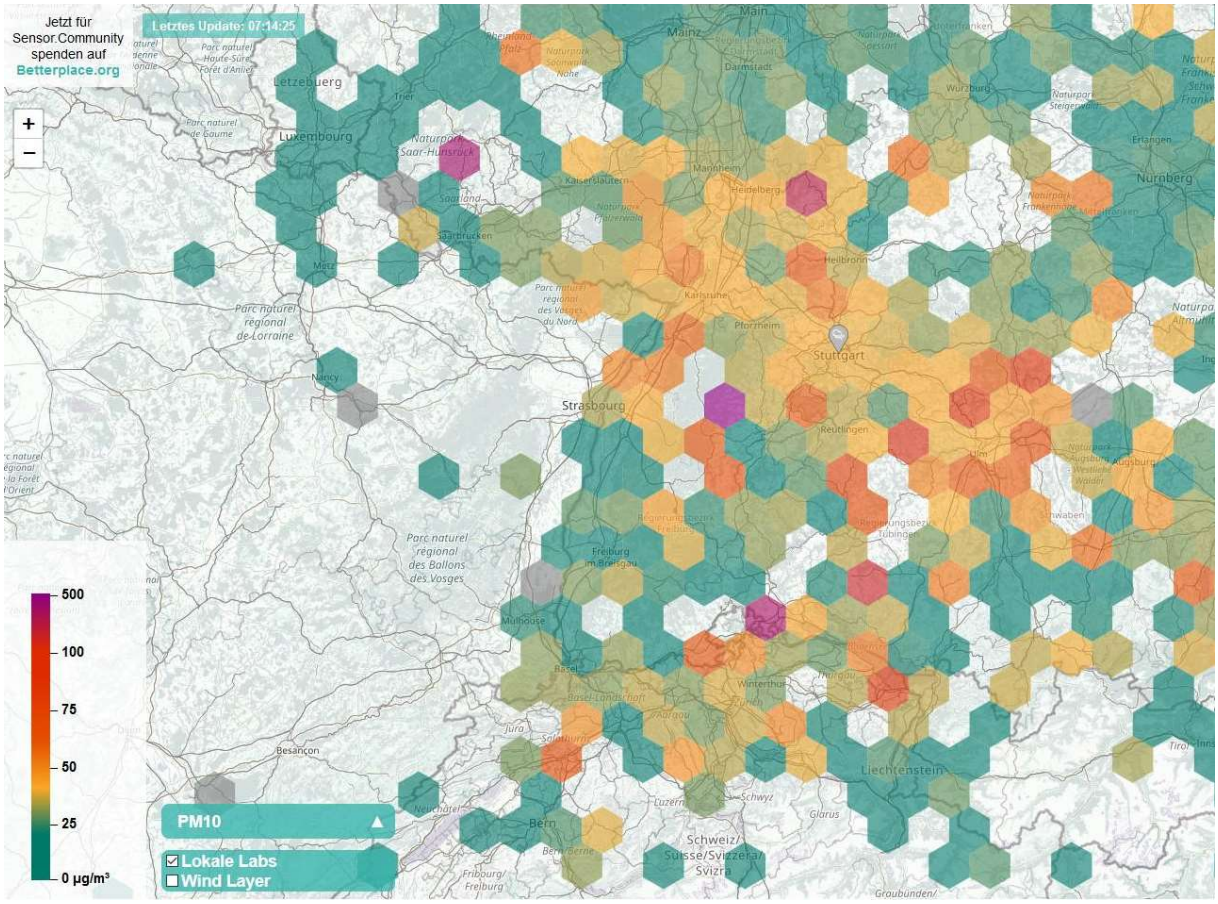

Figure 54: OK Lab sensor network map (luftdaten.info) in the morning of February 7th

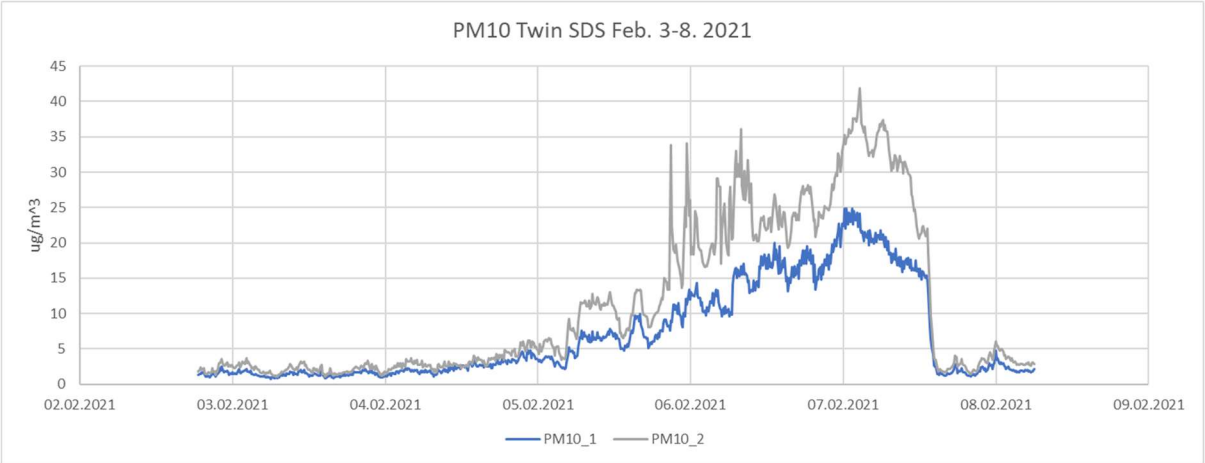

Figure 55: PM10 as seen by the SDS011_1 with dryer (blue) and by the SDS011_2 without dryer (grey) during the Sahara dust event February 3rd -8th, 2021, the dust event becomes visible only from small, short steep spikes on February 6th

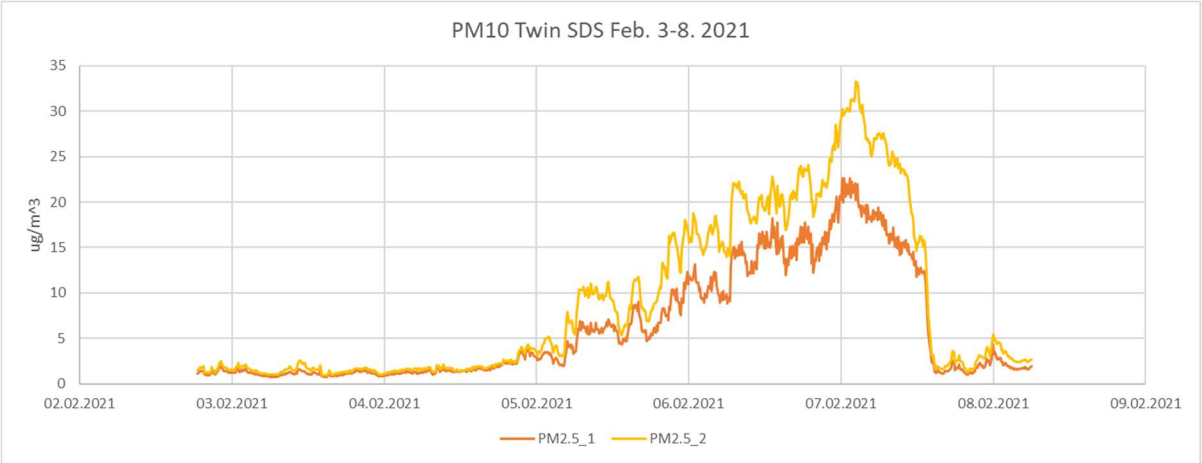

Figure 56: PM2.5 as seen by the SDS011_1 with dryer (blue) and by the SDS011_2 without dryer (grey) during the Sahara dust event February 3rd-8th, 2021

Again, the hygroscopic growth suggests fitting a model like the one of Hänel into the ratio of wet/dry particles obtained from the ratio of the PM2.5 data from the SDS011 without dryer divided by the PM2.5 data from the SDS011 with dryer. This indeed worked well with an α_m = 1.026 and a Hänel-coefficient β_m = 0.1861 related to the mass growth GF_m. The variation of the samples around the model function is large but it can be observed that the model fit is good.

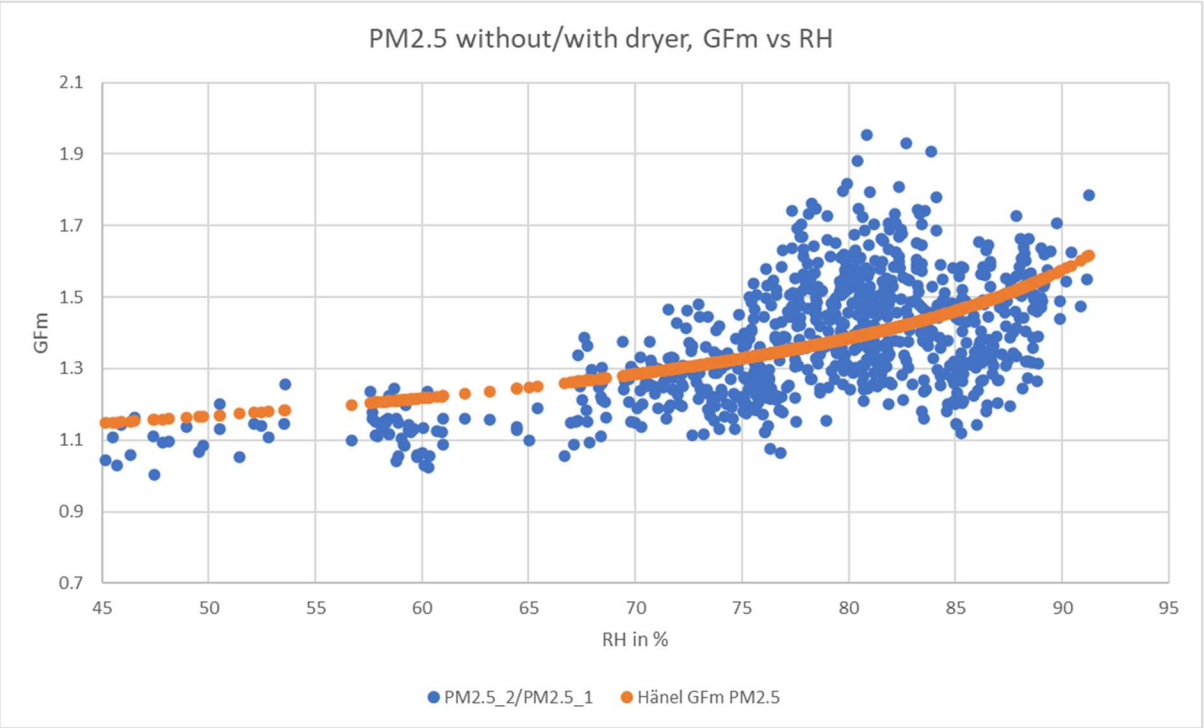

Figure 57: GF_m obtained from the ratio of the PM2.5 data from the SDS011 without dryer and the PM2.5 data from the SDS011 with dryer versus a fit of the Hänel model

Interestingly, the growth function GF_m obtained this way can be used to correct the data from the SDS011 without the dryer. When the data are corrected by $1/GF_m$ then we get a good match to the SDS011_1 data with dryer. This can be expressed in the formula:

$$PM2.5_{with\ dryer} = \frac{1}{GF_m} PM2.5_{witho\quad dryer}$$

Eq. 9

And

$$GF_m = \alpha_m \cdot \frac{1}{(1 - RH)^{\beta_m}}$$

Eq. 10

From a correlation plot between the corrected PM2.5 data from the SDS011 without dryer and the data from the SDS011 with dryer during this restricted time period, we can see an excellent correlation with a coefficient of determination $R^2 = 0.9907$.

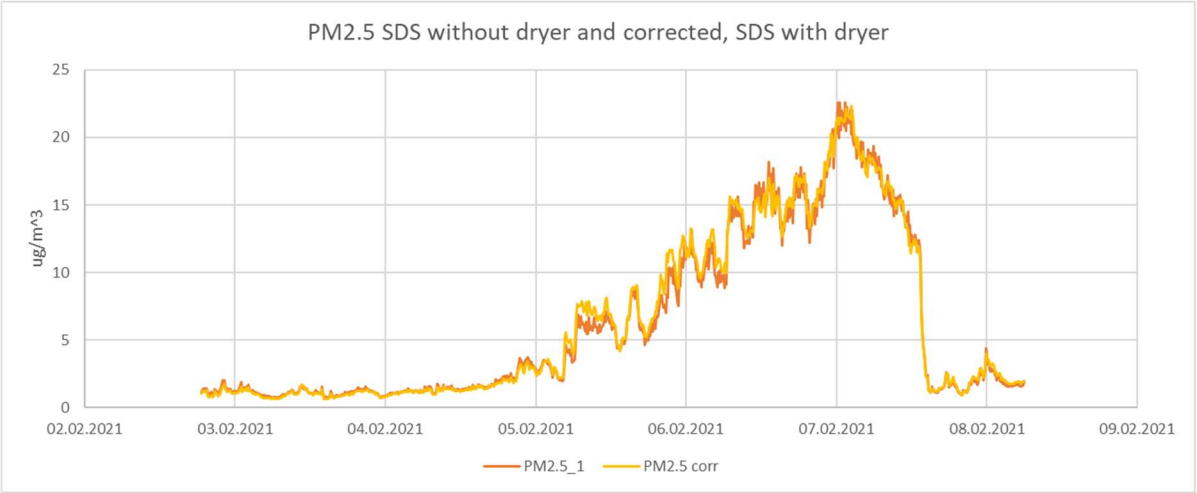

Figure 58: Corrected PM2.5 data from the SDS011_2 without dryer (yellow) and data from the SDS011_1 with dryer (orange), a particularly good matching is achieved

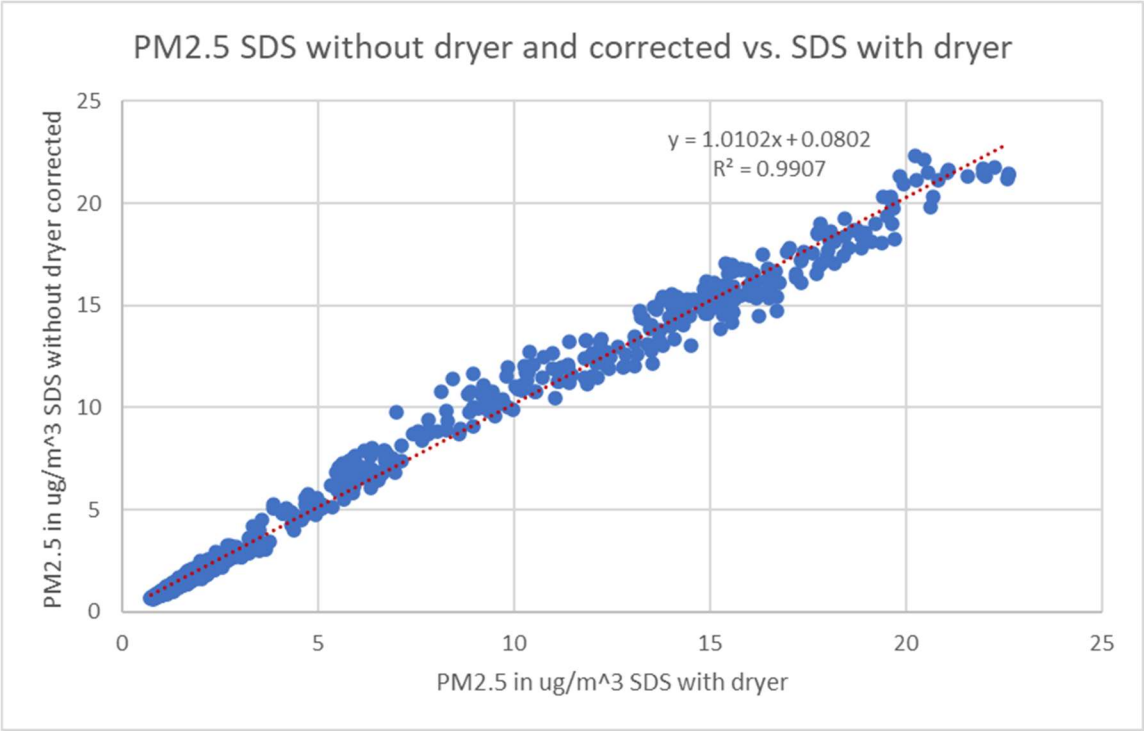

Figure 59: Correlation of corrected PM2.5 data from the SDS011_2 without dryer and PM2.5 data from the SDS011_1 with dryer, a good coefficient of determination is achieved

When we do the same data processing for PM10, GF_m obtained from the ratio of the PM10 data from the SDS011 without dryer divided by the PM10 data from the SDS011 with dryer, outliers can be observed for a relative humidity of 83%. These outliers occur because of the Sahara event for which the fitted Hänel model seems to be no longer valid. This behaviour during the Sahara dust event looks remarkably like that of a strong fog event.

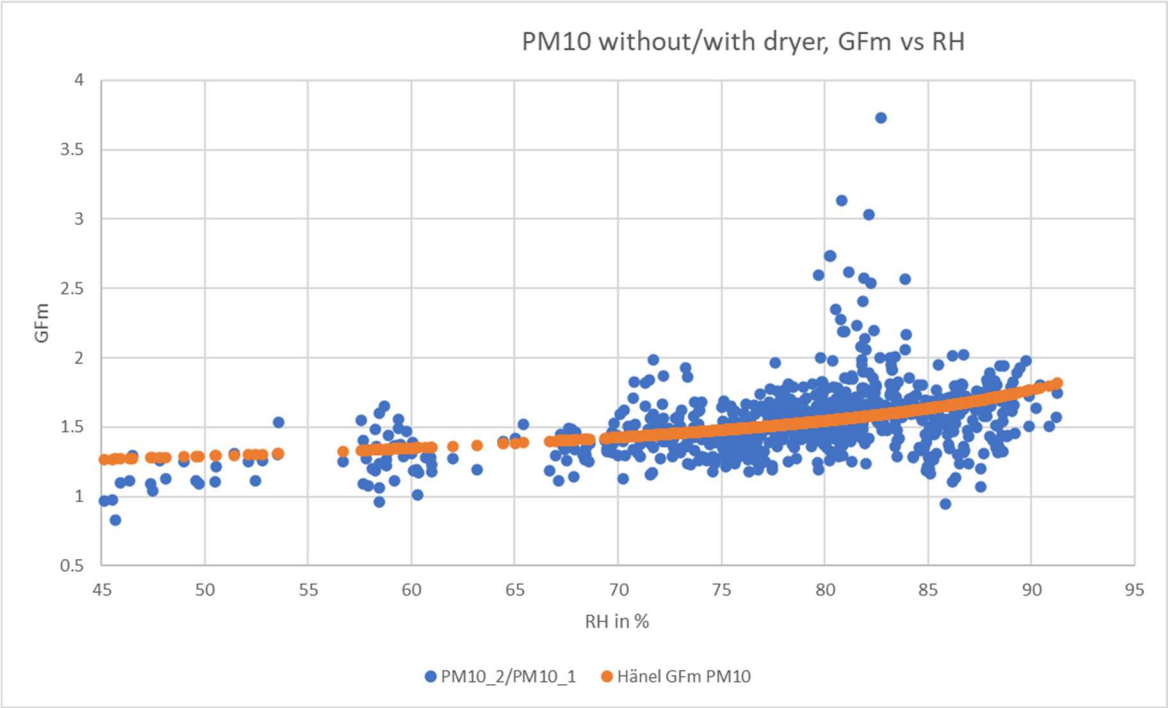

Figure 60: GF_m obtained from the ratio of the PM10 data from the SDS011 without dryer and the PM2.5 data from the SDS011 with dryer versus a fit of the Hänel model

Co-location measurement at Munich Maker Lab Feb 17- Mar 3, 2021

For the quantitative validation of PM results, a co-location field experiment was executed at the Munich Maker Lab e.V. located at Dachauer Strasse 112h, about 550m away from the governmental measurement station located in Munich Lothstrasse (N48.15455° E11.55466°). For this purpose, a second Twin-SDS measurement box containing an SDS011 with dryer and a SDS011 without dryer was constructed. It was installed on a building opposite to the Munich Maker Lab e.V. (N48.15861° E11.55045°) to avoid direct sunlight irradiation (see Figure 11, Figure 61 and Figure 62). In Figure 61, the LfU station at Lothstrasse close to the tall building of the Hochschule Munich is marked with a green arrow and the location of the Twin-SDS measurement box is marked with a green circle. The decision to locate the measurement box close to Maker Lab was mainly due to the fear of theft and vandalism but also to ease service and support with the help of the Munich Maker Lab. Since it was already understood that a low-cost PM sensor like the SDS011 is not able to measure PM10 correctly, the idea was to concentrate on PM2.5 for quantitative comparison. Due to the much smaller mass of the particles, a correlation of the PM2.5 mass concentration across this distance of 550m, the given topography and building development was assumed to be given.

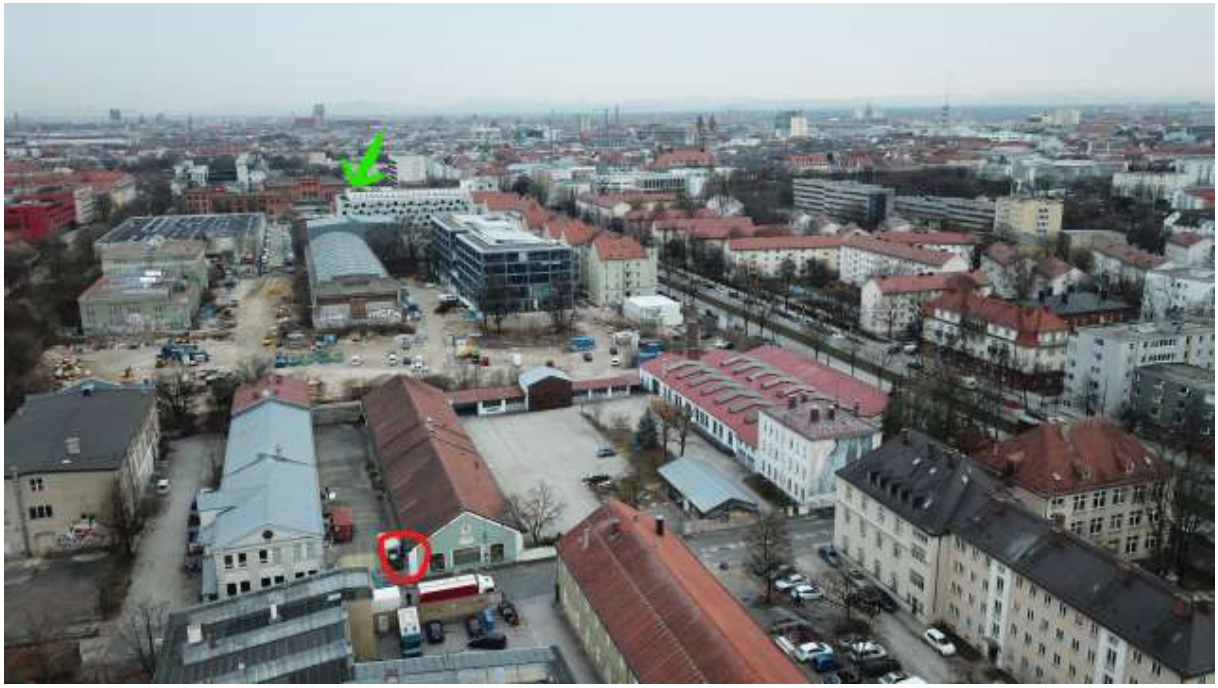

Figure 61: Position of the Twin-SDS measurement box at Maker Lab Munich (red circle) with respect to the LfU reference station in Munich Lothstrasse (green arrow)

Figure 62: Position of the Twin-SDS measurement box used for the co-location measurement at the wall of a building opposite to Munich Maker Lab e.V.

The co-location measurement period lasted from February 17th to March 3rd and contained a major fog event in the night of 21st to 22nd of March, a strong Sahara dust event lasting from February 23rd to February 27th and a phase of hygroscopic growth from February 27th to March 3rd. These three major events are clearly visible in Figure 63, Figure 64, Figure 65 and Figure 66.

Figure 63 shows the PM10 and PM2.5 results of the governmental measurement station operated by LfU and considered as a reference station. The massive increase of PM10 in relation to PM2.5 indicates the coarse particles typically contained in Sahara dust.

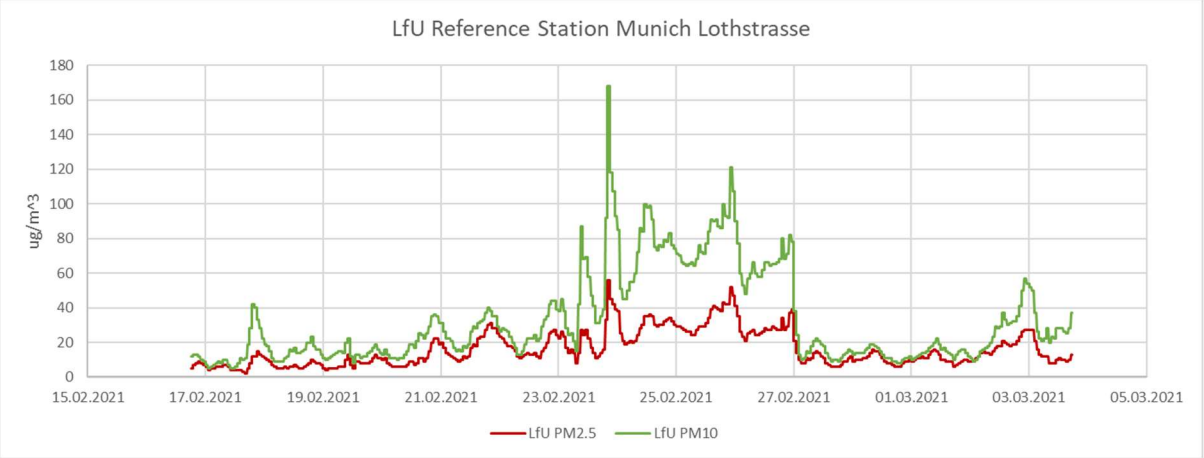

Figure 63: PM2.5(red) and PM10 (green) results of the LfU reference station at Munich Lothstrasse (1h averages) during the co-location measurement February 17th – March 3rd, 2021

Figure 64 shows the comparison of the raw data from the LfU PM2.5 reference (red curve) to the results of the Twin-SDS box containing the SDS1 with dryer and the SDS2 without dryer for time intervals of 1h. The sharp peak in the PM10 values of the SDS011 without dryer (SDS2_PM10) compared to SDS1_PM10 of the SDS011 with dryer (grey curve) on February 22nd indicates the fog event.

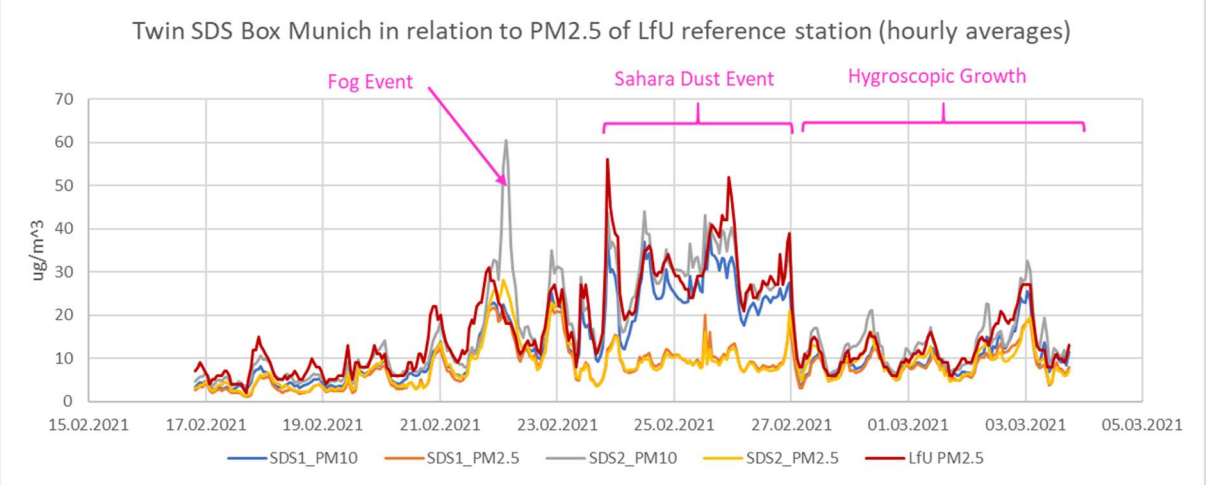

Figure 64: Results of the Twin SDS measurement box for SDS1 with dryer and SDS without dryer (1h averages) in relation to PM2.5 of the LfU reference station during the co-location measurement February 17th – March 3rd, 2021

Figure 65 shows the result of the Twin-SDS measurement box in time intervals of 10min. There, the abrupt increase of PM10 during the fog event appears even more pronounced, whereas the hygroscopic growth phase starting at February 27th can still hardly be recognised.

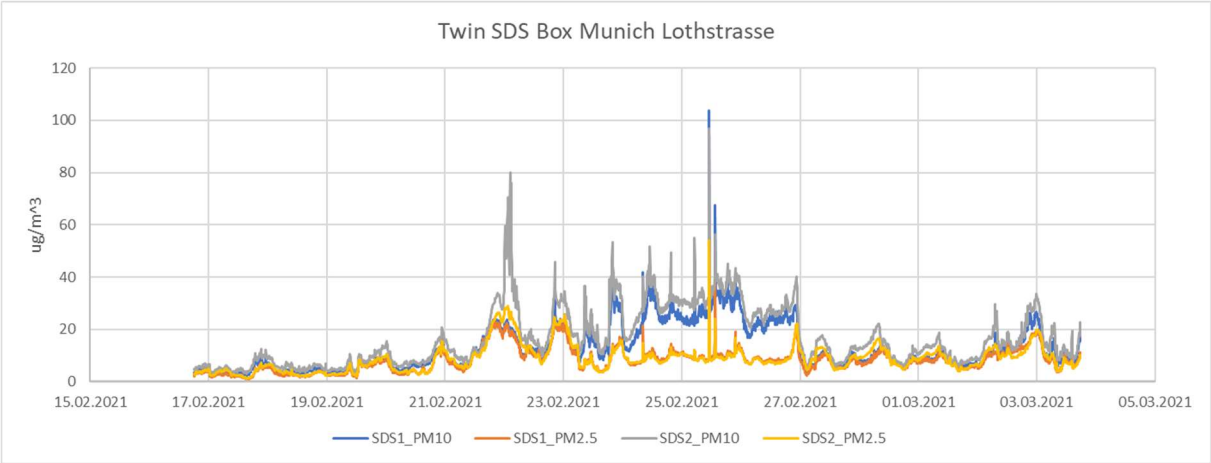

Figure 65:Results of the Twin SDS measurement box for SDS1 with dryer and SDS2 without dryer (10min averages)

However, when plotting the ratio between SDS2 without dryer and SDS1 with dryer for the PM10 or PM2.5 results jointly with relative humidity as in Figure 65 and Figure 66, the fog event as well as the growth phase become clearly visible. The hygroscopic growths occurred in 5 soft waves during the nights of February 27th – to March 3rd. This is visible from the oscillating relative humidity with high peaks up to 70% relative humidity that is correlated to the oscillating ratio between wet and dry mass of particles as measured by the SDS without and with dryer.

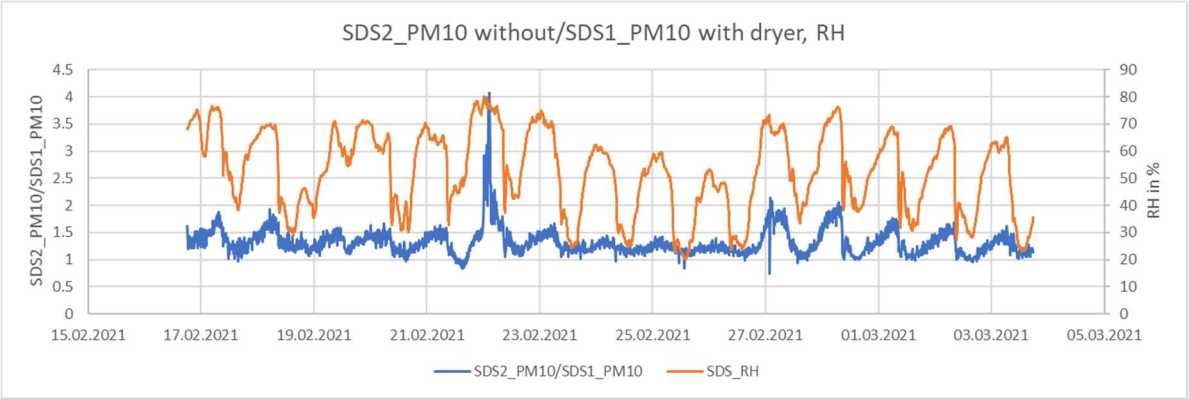

Figure 66: Ratio of PM10 for SDS without / with dryer and relative humidity during the co-location experiment

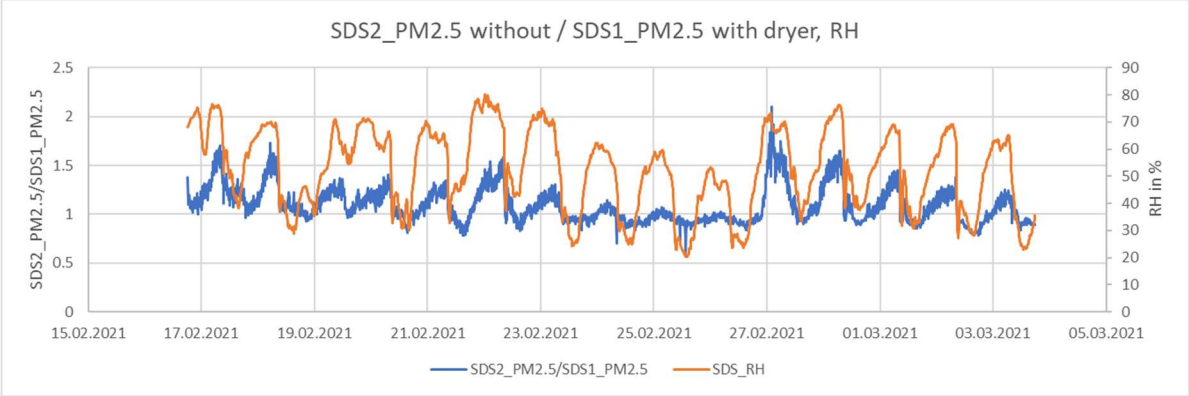

Figure 67: Ratio of PM2.5 for SDS without / with dryer and relative humidity during the co-location experiment

When the overall measurement period of the co-location experiment is observed based on hourly averages, the correlation plots of the SDS011 with dryer (SDS_1) and without dryer (SDS_2) versus PM2.5 of the LfU reference station clearly shows an improvement in the coefficient of determination

R^2 for the SDS011 equipped with the dryer (see Figure 68 to Figure 71). Whereas the coefficient of determination improves from R^2 = 0.2635 to R^2 = 0.4262 for PM2.5 when using the dryer, it is a surprising and exceptional result that the correlation of PM10 of the SDS011 versus PM2.5 of the reference station improves from R^2 = 0.7826 to R^2 = 0.911 when using the dryer. This means, that the PM10 output of the SDS011 with dryer matches extremely well the PM2.5 results of the LfU reference station. Furthermore, the PM10 results of the SDS011 with dryer matches the PM2.5 results of the LfU reference station much better that the PM2.5 results of the SDS011 with dryer.

When observing the SDS011 results versus time in Figure 64, a major reason for this behaviour becomes apparent: During the Sahara dust event, the PM2.5 results of the SDS011 do almost not react on the change of the particle distribution compared to the reference station, whereas the PM10 results do show a clear reaction. This behaviour indicates that the SDS011 implements a collection efficiency for particles contributing to PM2.5 that ends too early with respect to diameter. A further indication for this behaviour can be taken from Figure 78. This graph shows the mass distribution of the Sahara dust when the dust cloud crossed the Alps. It shows a distribution with high values starting at about 1.5µm ranging to beyond 9µm. Obviously, the fraction starting at 1.5µm is not mapped adequately into PM2.5 but into PM10 for both SDS011 operated in the measurement box. Since on the other hand the collection efficiency for PM10 is known to also end much earlier than at a diameter of 10um, this left-shift of collection efficiency curves in the SDS011-internal processing may be the reason why PM10 of the SDS011 with dryer almost perfectly correlates to PM2.5 of the LfU reference station.

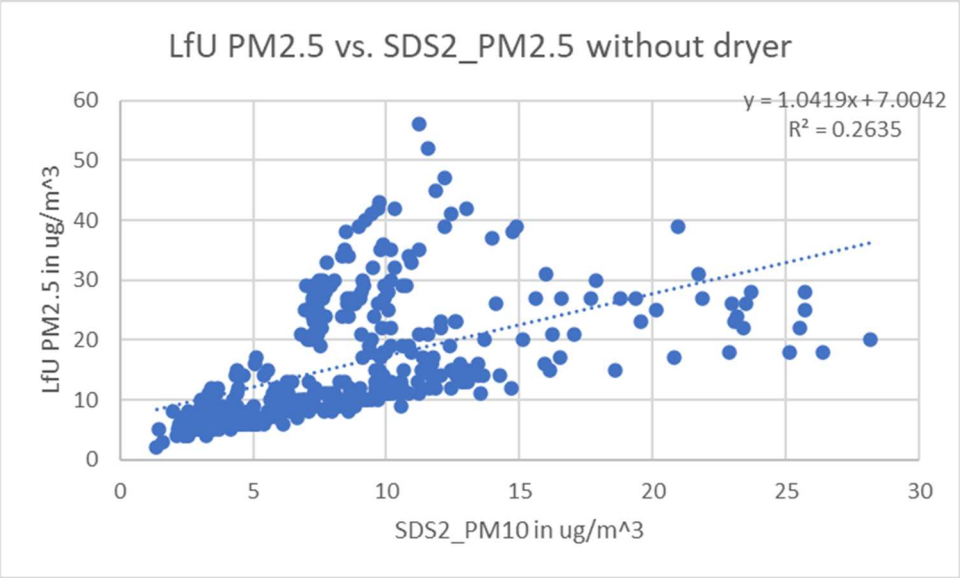

Figure 68: Correlation of LfU_PM2.5 versus SDS2_PM2.5 without dryer (hourly averages)

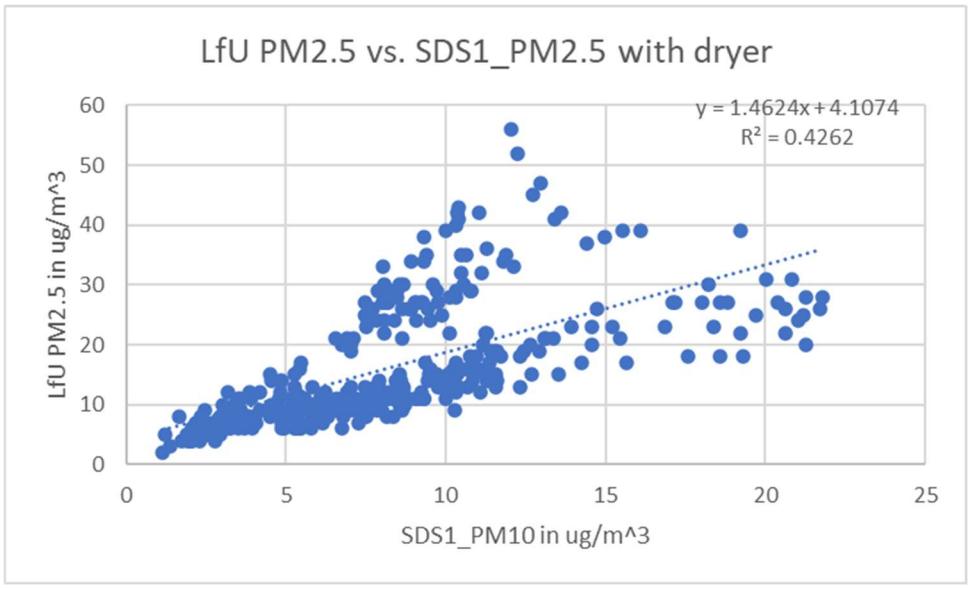

Figure 69: Correlation of LfU_PM2.5 versus SDS1_PM2.5 with dryer (hourly averages)

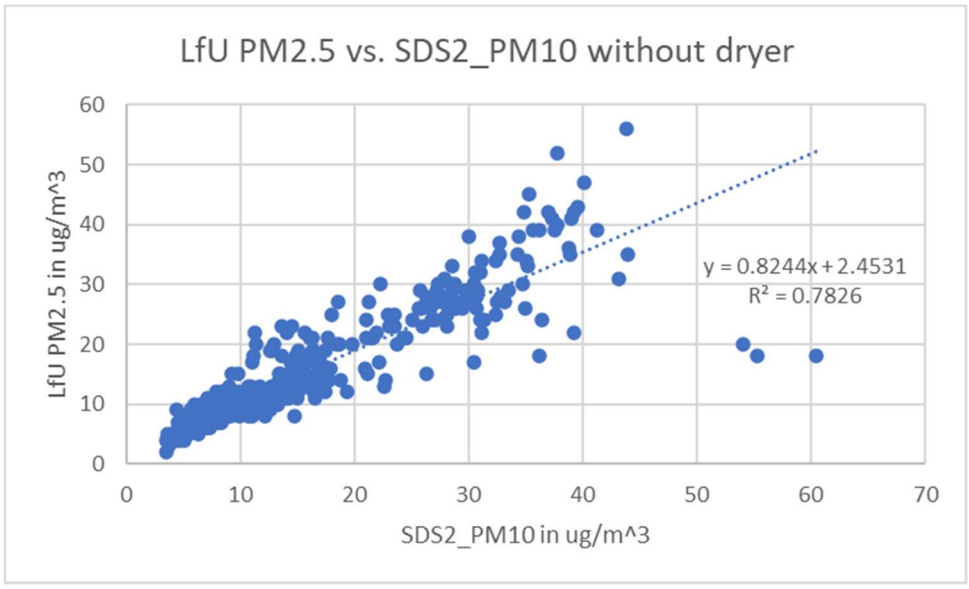

Figure 70: Correlation of LfU_PM2.5 versus SDS2_PM10 without dryer (hourly averages)

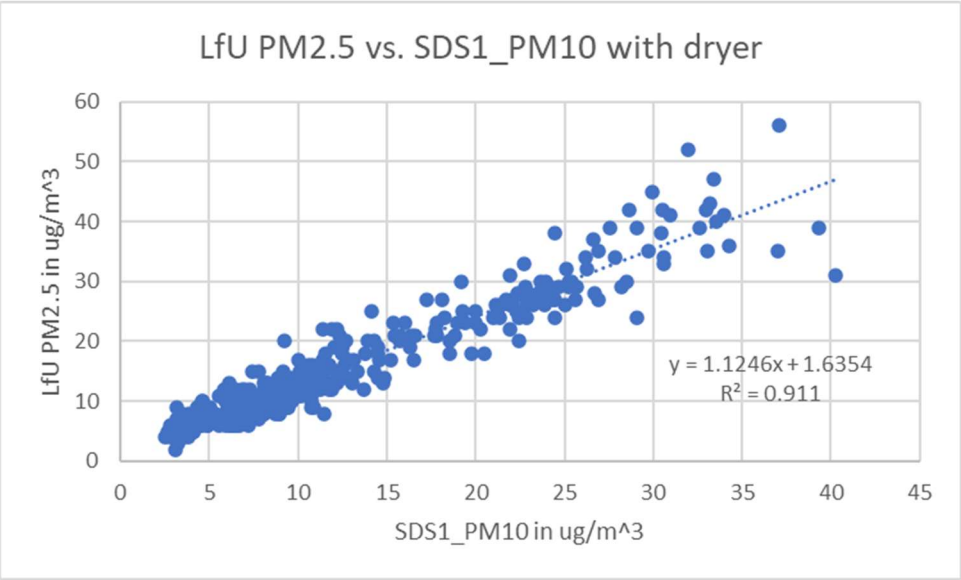

Figure 71: Correlation of LfU_PM2.5 versus SDS1_PM10 with dryer (hourly averages) showing an unexpectedly high coefficient of determination

When the coefficients of the linear regression extracted from the correlation are used to calibrate the SDS011 with dryer to the LfU reference station, the above results get confirmed. Whereas the PM2.5 signal of the SDS011 with dryer still visibly deviates from the PM2.5 values of LfU reference station, the PM10 signal of the SDS011 with dryer matches the PM2.5 values of LfU reference station extremely well (Figure 72 and Figure 73).

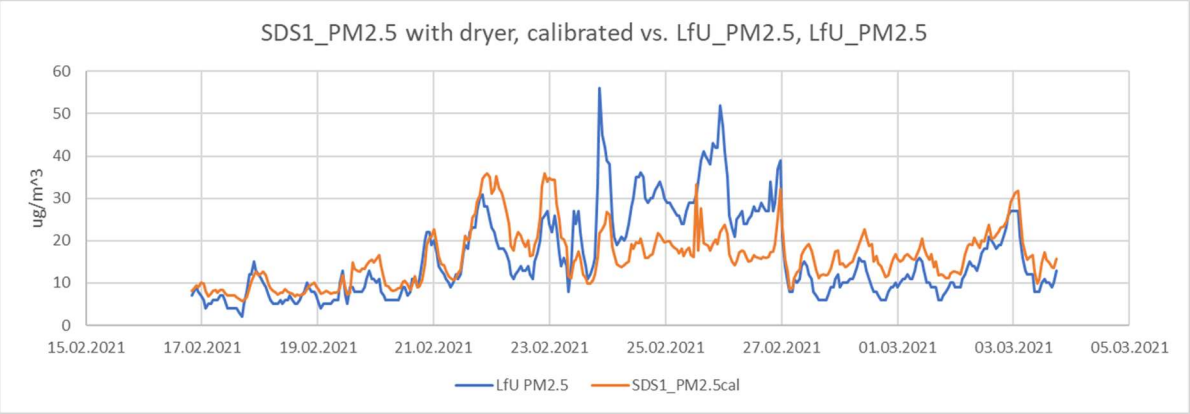

Figure 72: SDS1_PM2.5 with dryer, calibrated with respect to LfU_PM2.5 over the period of the co-location experiment (hourly averages)

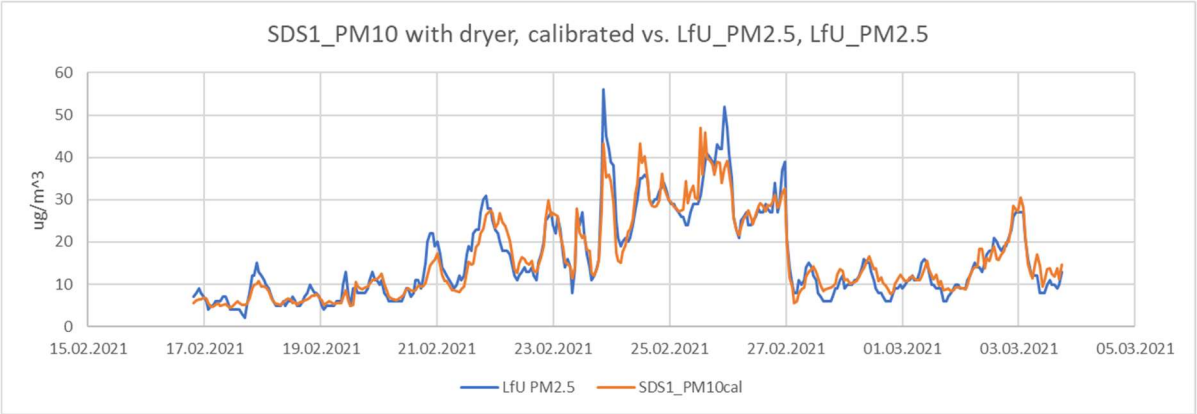

Figure 73: SDS1_PM10 with dryer, calibrated with respect to LfU_PM2.5 over the period of the co-location experiment (hourly averages) showing extremely good matching

Table 1 summarizes the results for the performance numbers RMSE (root mean square error) and coefficient of determination R^2 that express the quality of matching for the targeted PM2.5 values of the LfU reference station with respect to the PM2.5 and PM10 signals of the SDS_2 without dryer and SDS_1 with dryer over the whole measurement period based on hourly averages. The attribute calibrated refers to applying a correction based on the regression trendline.

Summary of RMSE and R^2 of PM2.5 LfU station data with respect to SDS signals		
Signal	RMSE in ug/m^3	R^2
PM2.5 SDS2 without dryer	11.40	0.264
PM2.5 SDS1 with dryer	11.21	0.426
PM2.5 SDS1 with dryer, calibrated	7.67	0.426
PM10 SDS2 without dryer	5.11	0.783
PM10 SDS1 with dryer	4.56	0.911
PM10 SDS1 with dryer, calibrated	3.02	0.911

Table 1: Summary of the results when comparing the PM2.5 data of LfU reference station with respect to the various signals generated by the Twin-SDS measurement box based on hourly averages

Figure 74 shows a close-up into the timeframe when the strong fog event occurred. During this event, the efficiency of the dryer can be observed very well. Both, the PM2.5 and PM10 signals (orange and blue curves) of the SDS1 with dryer show an almost equal mass concentration, meaning there are no large particles detected in the dry aerosol. However, the small oscillations remaining in the signals averaged across intervals of 10 minutes indicate that the dryer is working efficiently. In contrary, the SDS2 without dryer reacts extremely strong on the wet aerosol starting at midnight 21st/22nd of February mainly with the PM10 signal (grey curve) and only slightly with PM2.5 signal (yellow curve).

In parallel a high humidity was recorded by an additional HYT221 humidity sensor added to the measurement box before installation in Munich. The high humidity phase ranged from February 21st at 19:00h to February 22nd at 8:30h and reached a peak value of 80% of relative humidity. In this respect it should be mentioned that the humidity sensor mounted into a hole of the wall of the measurement box most likely detected slightly smaller values of humidity than really existed between the buildings since it gets warmed up slightly from the backside by the heat dissipated by the electronics inside the box and also by the walls of the building.

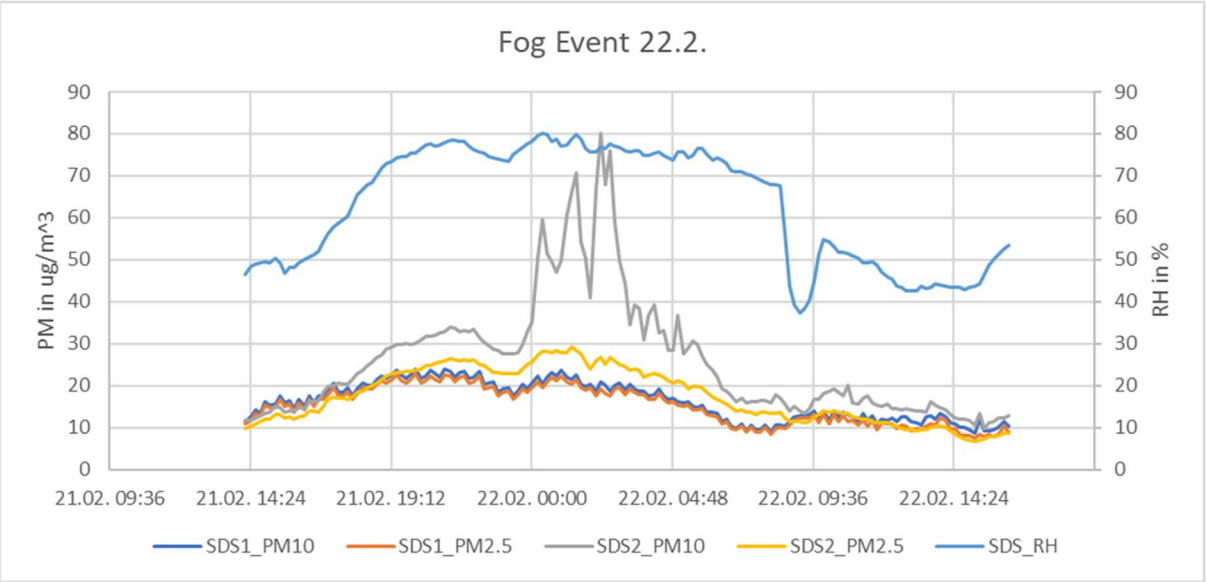

Figure 74: Results of the Twin-SDS measurement during the fog event on February 20th

As a proof that a fog event really occurred, archived photos of a web camera on a tall building in Munich Freimann were analysed. The camera is positioned such that its view is across the city of Munich towards the Alps visible at the horizon (see Figure 75, the reference picture on February 21st in the morning). Figure 76 shows an excerpt of the photo-gallery of the archived photos starting at February 21st 16:40h (lower right corner) until February 22nd at 12:10h in 10-minute intervals. It becomes very evident that the fog appeared in the view of the camera starting at February 21st at 20:00h and the view cleared up at 22nd at 9:00h. This finding matches the results of the PM measurements.

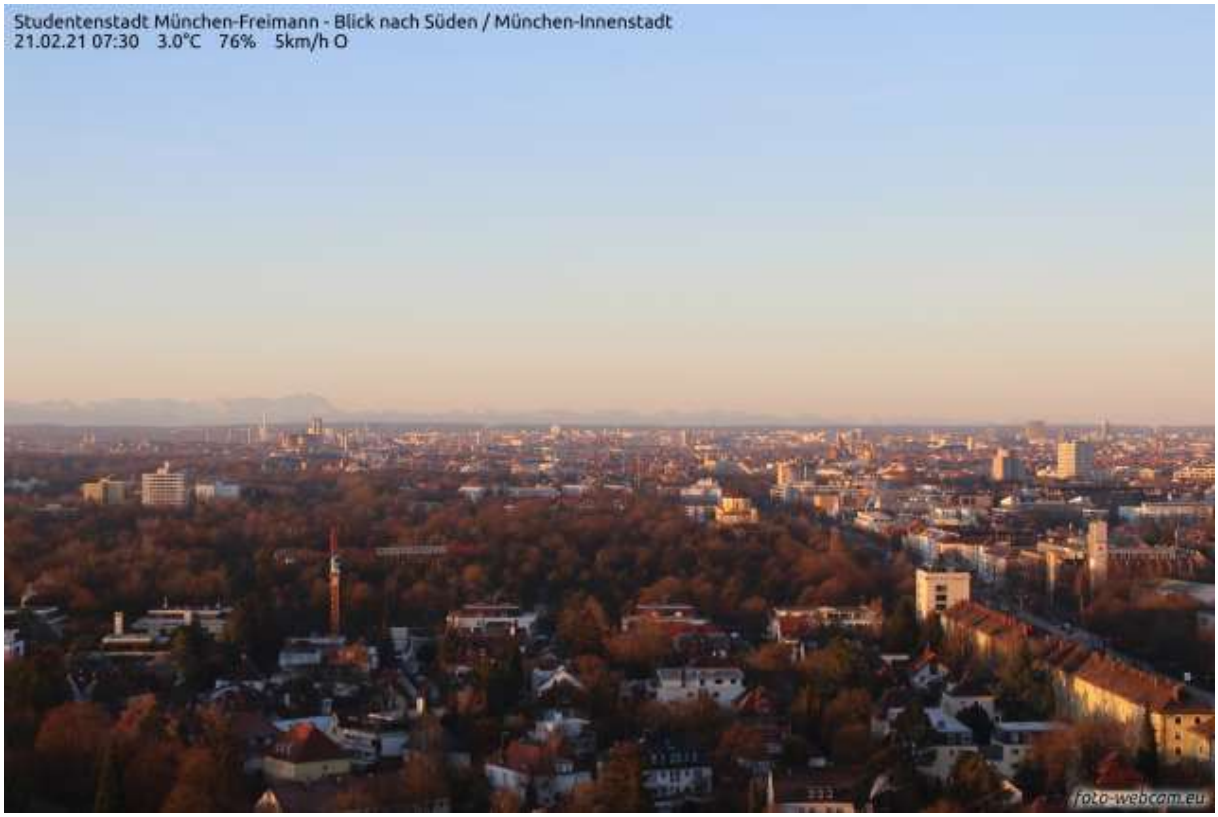

Figure 75: Reference picture of the webcam located in Munich Freimann showing the view over the ancient city of Munich to the alps (source: www.foto-webcam.eu)

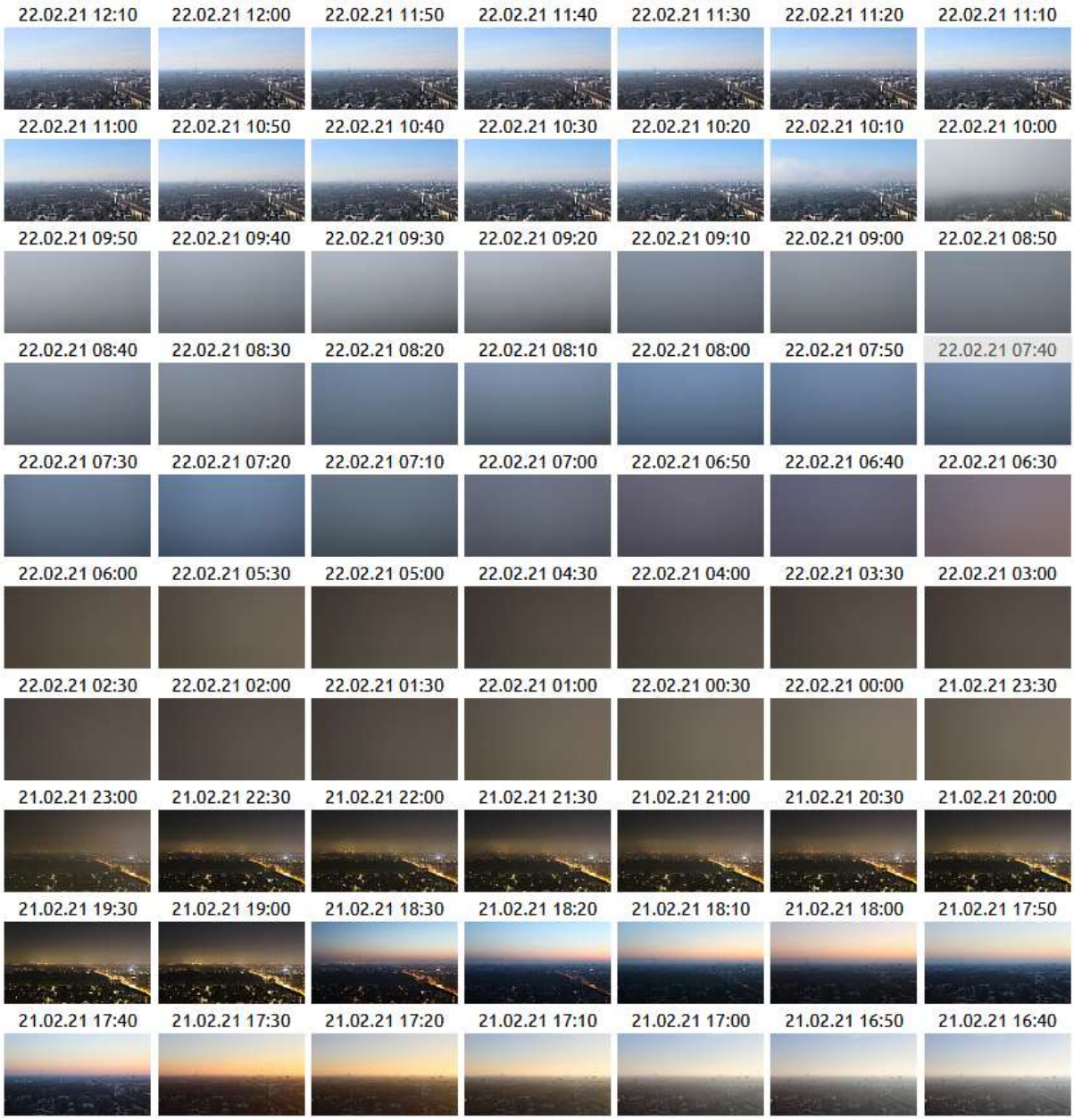

Figure 76: Picture sequence picture of the webcam located in Munich Freimann clearly showing the appearance and disappearance of fog in the night of February 22nd/23rd (source: www.foto-webcam.eu)

The Sahara dust event starting at February 23rd was already forecasted a few days before by several research platforms and professional weather forecast services such as the one provided by Zentralanstalt für Meteorologie und Geodynamik in Vienna (ZAMG). In addition, the aerosol measurement equipment of the Paul-Scherrer institute located at Jungfraujoch, Switzerland that continuously analyses the dust in the upper atmosphere announced a strong change in the aerosol spectrum particularly of the mass distribution versus the particle diameter (Figure 78). According to this forecast and the model calculations, the dust cloud covered Germany completely on February 23rd. Since the meteorological conditions indicated high pressure, low wind speeds, cold nights and an inversion layer above ground, the expected PM10 concentrations were high for the following days.

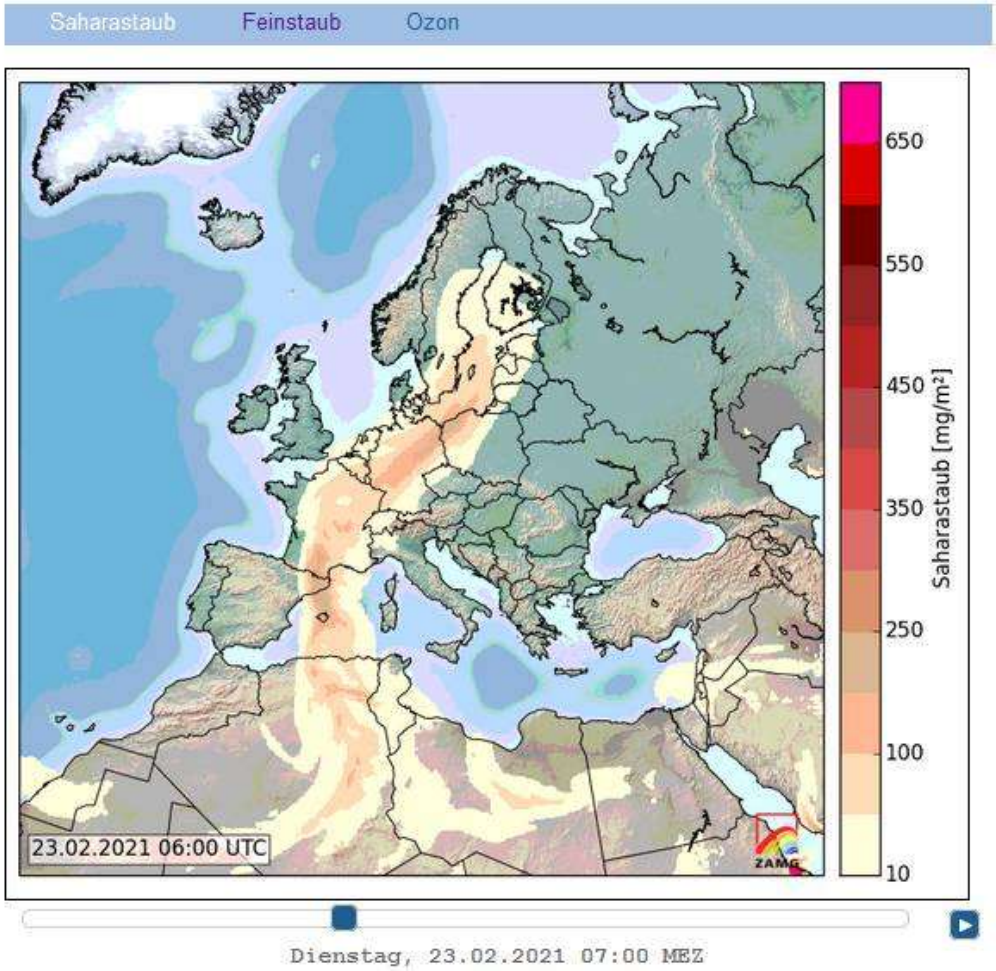

Figure 77: Forecast of Sahara dust spreading over central Europe by Zentralanstalt für Meteorologie und Geodynamik (ZAMG), Vienna for Ferubary 23rd (source: www.zamg.ac.at)

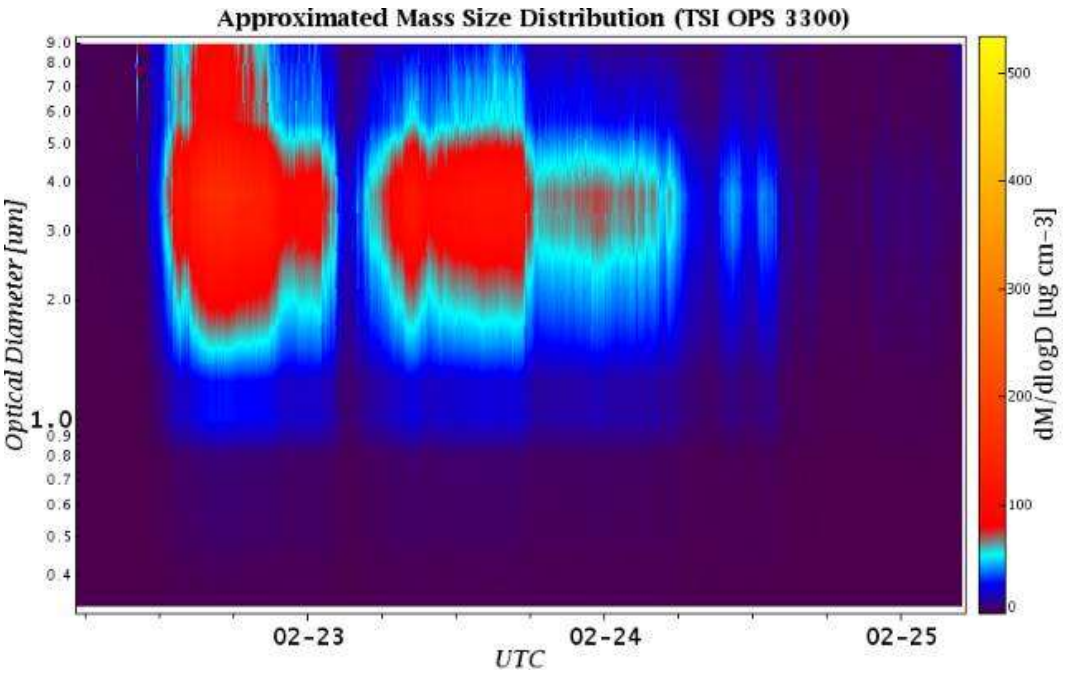

Figure 78: Aerosol data from Jungfraujoch as the Sahara dust cloud crossed the alps, recorded by LAC - Laboratory of Atmospheric Chemistry, Paul Scherrer Institute, Switzerland (source: www.psi.ch/en/lac)

However, the PM10 signals of both SDS011, with and without dryer did not react comparably to PM10 of the LfU reference station (Figure 79). This can be explained by the inability of the SDS011 to detect large particles as dominantly contained in Sahara dust.

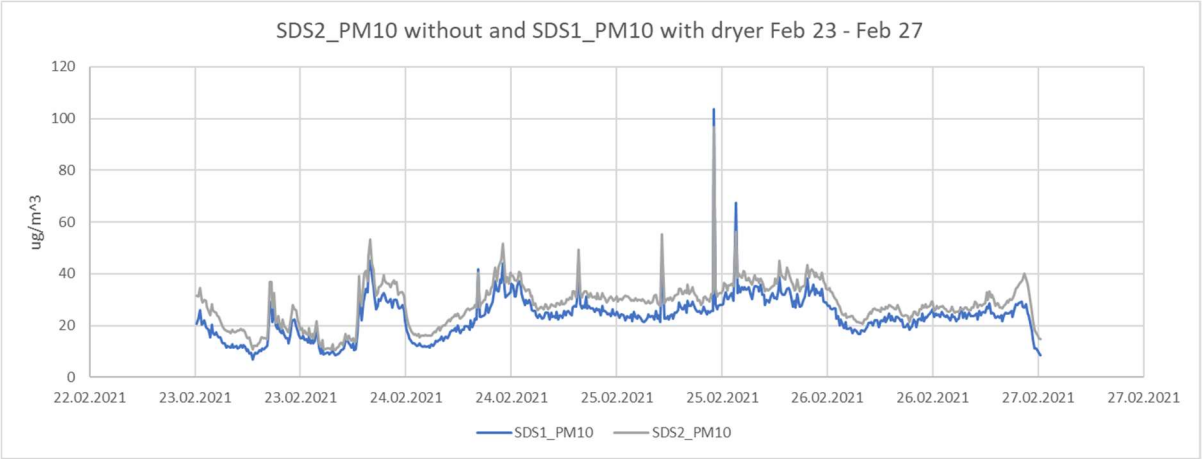

Figure 79: PM10 for SDS011_1 with and SDS011_2 without dryer during the Sahara event February 23rd - 27th

What also becomes evident during the Sahara dust event is the fact, that since the diurnal humidity variation did not exceed 60% relative humidity almost no growth occurred (Figure 80). This may also be accompanied by the fact that Sahara dust particles are not hygroscopic. When the ratio of PM10 between the SDS without dryer and the SDS with dryer, showing the ratio of the wet and the dry aerosol, is correlated to relative humidity, it only shows a minimal increase versus humidity. When a Hänel model is fitted into the data, the offset is $\alpha_m = 1.055$ and the Hänel coefficient is $\beta_m = 0.24$ during February 23rd and 27th also indicating only a small growth (Figure 81).

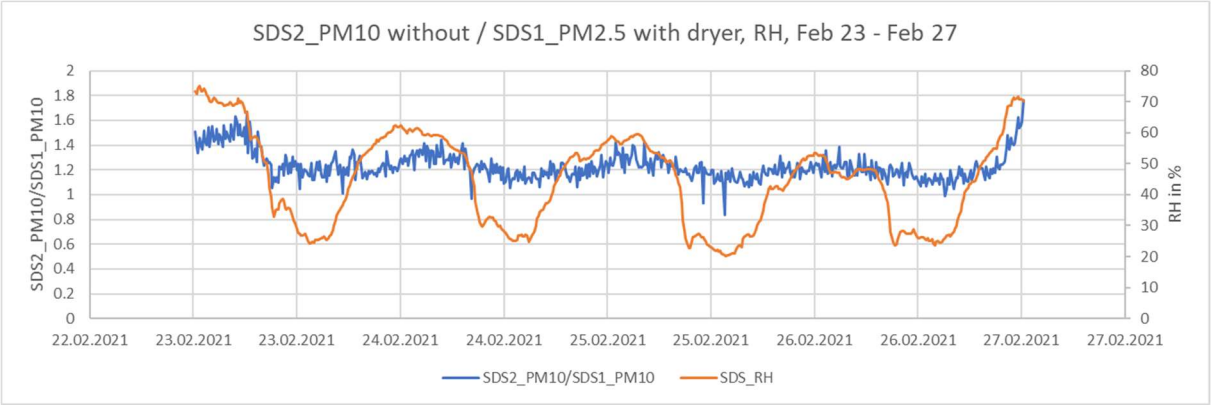

Figure 80: Ratio between PM10 for SDS2 without and SDS1 with dryer with respect to RH during the Sahara event February 23rd-27th

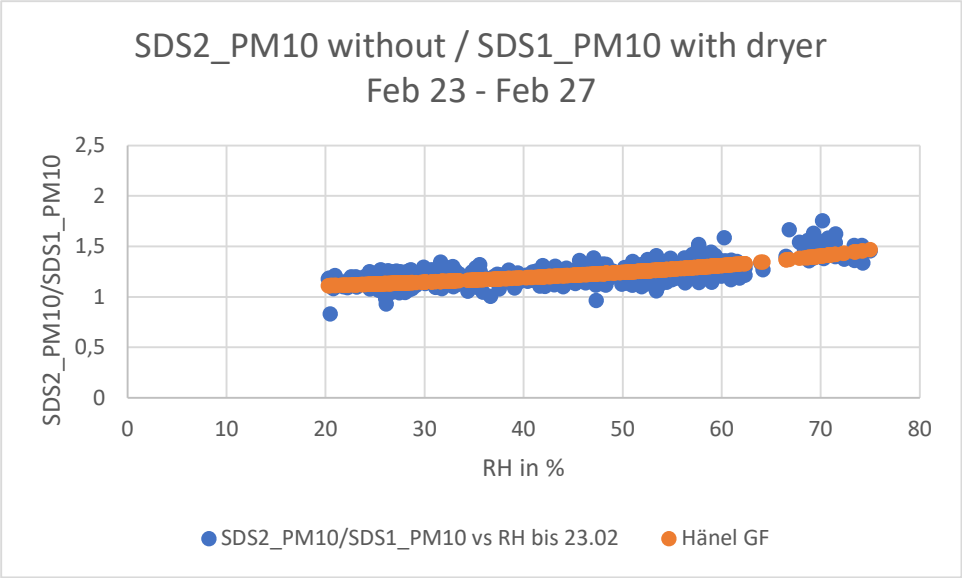

Figure 81: Correlation of the ratio between SDS2_PM10 without and SDS1_PM10 with dryer together with a fitted Hänel growth model during the Sahara event February 23rd-27th

In contrast, in the days following the Sahara dust event, a significant hygroscopic growth becomes visible. In the night of February 2nd rain occurred and cleared the air from dust. The following days were sunny, but the nights were cold (0°C) and showed high humidity. A close-up to this phase of the co-location experiment clearly shows higher PM10 values of the SDS without dryer (SDS2_PM10) compared to the SDS with dryer (SDS1_PM10). This becomes more pronounced when the ratio between the wet aerosol values and the dry aerosols is calculated from the SDS without and with the dryer. As it can be seen from Figure 83, this ratio shows an oscillating behaviour that correlates well with the diurnal variation of relative humidity. On all 5 days from February 27th until March 3rd humidity increases in the evening and reaches a maximum in the morning of the following day to drop rapidly with the upcoming sun until noon.

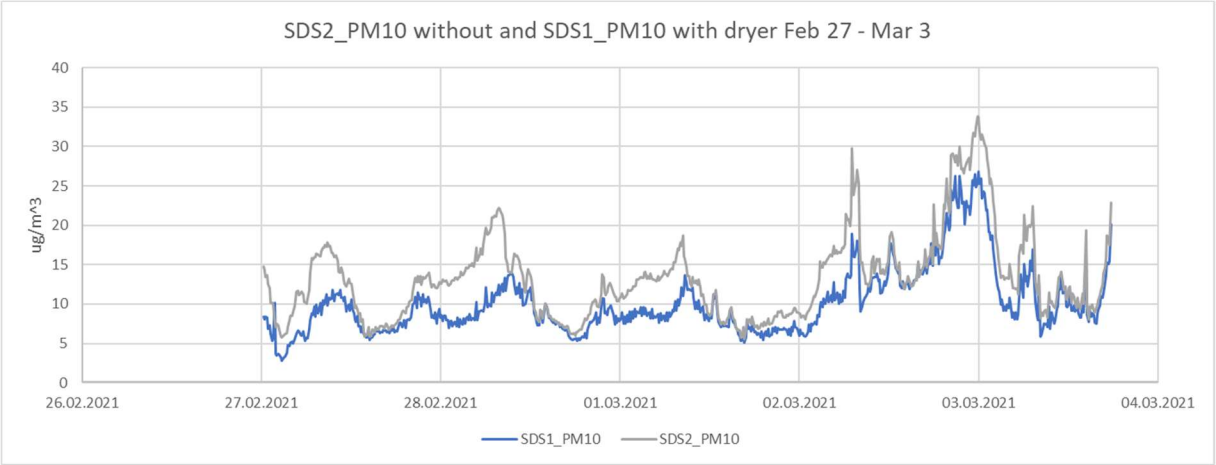

Figure 82: PM10 for SDS1 with, and SDS2 without dryer during the hygroscopic growth phase February 27th – March 3rd

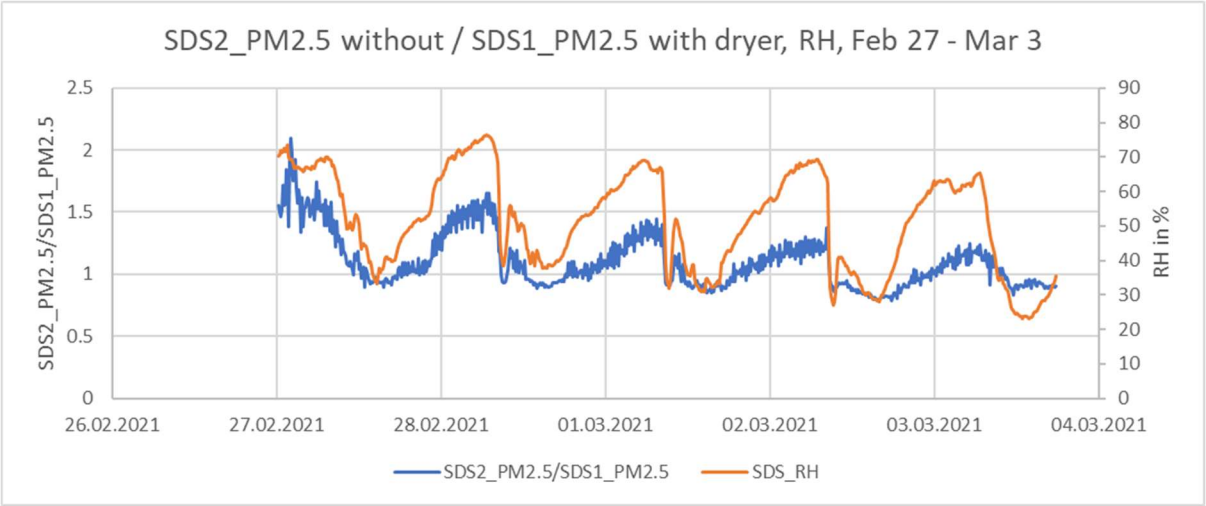

Figure 83: Ratio between PM10 for SDS2 without and SDS1 with dryer with respect to RH during the hygroscopic growth phase February 27th – March 3rd

When a correlation of the ratio between wet and dry aerosol calculated from PM10 without/with dryer is plotted versus humidity, a pronounced hygroscopic growth effect becomes visible (Figure 84). Into this data, restricted to the hygroscopic growth phase, a growth function according to the Hänel model was fitted. For this model, the offset is $\alpha_m = 0.843$ and the Hänel coefficient is $\beta_m = 0.57$. This means that in contrast to the phase where the Sahara event occurred, the growth function now shows an almost ideal shape and reaches growth factors of almost 2 at 75% relative humidity. This clearly different behaviour during different phases within the same measurement period highlights the impossibility to compensate the hygroscopic growth effect with time invariant model parameters. In contrary, the humidity controlled drying of the aerosol during all the phases yields a correction that is time invariant, as it can be observed from the good matching of the corrected SDS011 PM10 data in comparison to the PM2.5 data of the LfU reference station shown in Figure 73. The fact that the SDS011 PM10 data of the device equipped with dryer should preferably be used when calibrating to the PM2.5 data of the reference station, however, must be attributed to an additional deficiency of the low-cost PM sensor, most likely due to its particular collection efficiency characteristics.

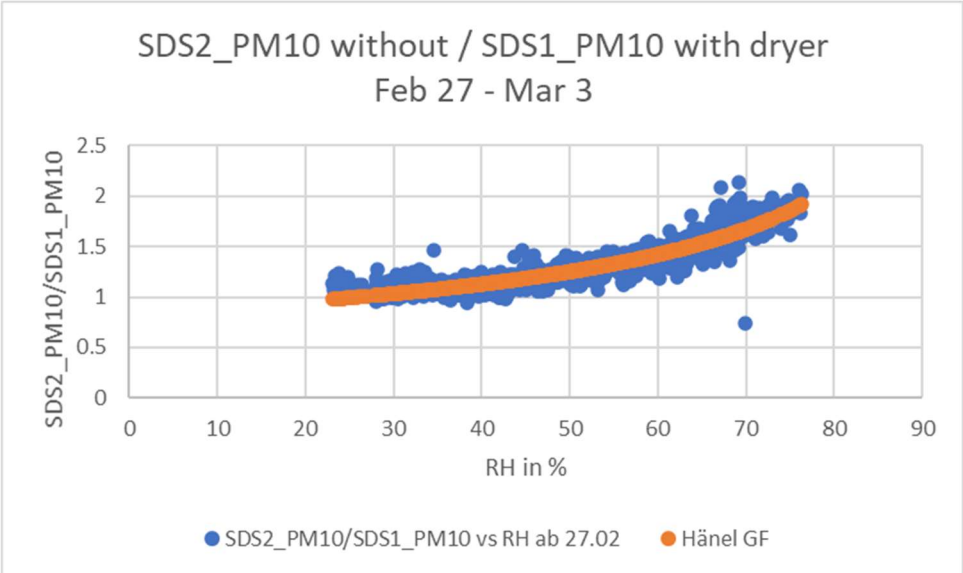

Figure 84: Correlation of the ratio between SDS2_PM10 without and SDS1_PM10 with dryer together with a fitted Hänel growth model during the hygroscopic growth phase February 27th – March 3rd

Discussion and Conclusion

Computational correction method

The idea to correct the humidity influence on a low-cost PM sensor by a computational postprocessing relies on humidity data measured in parallel to the PM-data using a low-cost sensor for the humidity measurement. This correction method uses a growth function model such as the Hänel model (Eq. 2 - Eq. 8). A key challenge with this approach is the fact that errors in the humidity measurement propagate with a high amplification into the growth factor used for correcting the measured PM values. This problem occurs due to the high steepness of the growth function at high humidity values. Therefore, a more costly but accurate and reliable humidity sensor is required.

Furthermore, when analysing the OK Lab network data in Munich as an example, it can be found that 62% of the low-cost humidity sensors are degraded or defective. To our opinion, this problem occurs, since the humidity sensor used in such a low-cost citizen science network is not specified for outdoor use. A humidity sensor that is designed for use in outdoor air would be required instead. An outdoor humidity sensor is protected against the wet water content in air as well as against chemically aggressive dust. We would recommend a part like the HYT221 protected with a protective membrane.

The computational method we used in an exemplary way to correct the humidity influence refers to an inaccuracy that is caused by hygroscopic growth and is based on a respective growth function model. The parameters of this model must be determined from a comparison of the low-cost PM sensor data to the PM data measured by professional equipment using an aerosol dryer (or gravimetric measurement equipment). For the hygroscopic growth model of Hänel /8/, we found an easy way to determine the parameters from measurement data based on a linear regression calculation on the logarithmised data (Eq. 5 - Eq. 7). With the growth function model and the extracted parameters for it, we achieved a moderate improvement of the PM2.5 data in case of a pure hygroscopic growth event. We could confirm the improvement by analysing the coefficient of determination R^2 of a correlation before and after correction with respect to the reference data of a governmental measurement station. During a field measurement experiment executed in Munich, with the duration of one month, the correlation between the corrected low-cost sensor PM2.5 data and the PM2.5 reference data improved moderately to $R^2 = 0.6531$ after correction compared to the uncorrected data with $R^2 = 0.5166$. However, we found that the growth function parameters vary with time. Using the determined correction from an experiment in one month give less improvement when applied to data from another month. We also assume that growth model parameters substantially vary from location to location due to a different composition and property of the aerosol. Therefore, a frequent determination of the growth function model parameters with reference equipment would be required for a computational correction at exactly the location where the low-cost sensor should be used. This requirement will severely limit the use of the investigated computational correction method.

The investigated computational correction method did not work for fog events. Our field measurements confirmed that the investigated low-cost sensor SDS011 is not able to detect fog droplets larger than 5um. In such cases the SDS011 does not report the occurrence of fog adequately. However, it outputs excessively high PM10 values and large PM2.5 values in case the mass distribution of the fog droplets includes sizes smaller than 5um. Since fog events may occur at various levels of relative humidity, the growth models derived from hygroscopic growth events are not valid for fog events. Therefore, fog events cannot be corrected with the investigated computational humidity correction method.

During a Sahara dust event that accidentally happened during the field measurement periods, where dust was deposit over the ground, containing particles with a mass distribution spread over a wide size range and a maximum at 25um, we could confirm that the SDS011 low-cost PM sensor was not able

to detect the fraction of the mass distribution that reached into the PM10 collection efficiency characteristic whereas this fraction was clearly detected by the higher-cost sensor OPC-N3 we operated in parallel.

Correction method using a low-cost aerosol dryer

As an alternative approach for correcting the humidity influence, we designed a low-cost thermal dryer (Figure 23). For the control of the dryer, we used the humidity information in the exhaust air of the SDS011. This however required an irreversible modification of the SDS011 sensor. For this purpose, we integrated a HYT221 temperature/humidity sensor into the exhaust chamber of the SDS011. To regulate the dryer, we used an electronic switch for turning on and off the heating coil whenever the measured humidity in the exhausted air crossed the 35% threshold. The value of 35% was determined to include the efflorescence point of most of the salts contained in urban aerosols. This threshold adjustment was validated with experiments. From the field measurements we could confirm that the dryer control worked properly, and the relative humidity stayed close to 35% during operation.

Based on the low-cost dryer developed, we build a Twin-SDS measurement box that contained two SDS011 sensors, one SDS011 thermally isolated and equipped with the dryer and an additional one without thermal isolation and an inlet tube of same size as that of the dryer. During the co-location measurement in Munich, we also included a humidity sensor into the measurement box.

Using an ultrasonic fog generator and generating high mass concentrations, we were able to confirm an efficiency factor of 2 in reducing the PM10 values during the operation of the dryer. In the field experiments with lower mass concentrations however, we found a surprisingly high efficiency of the dryer. The dryer not only removed the humidity influence during hygroscopic growth event but also removed the influence of fog almost completely for both the PM10 and PM2.5 data output by the SDS011.

When analysing the data measured with the Twin-SDS measurement box with high temporal resolution, we could identify oscillations resulting from the modulation of particle growth induced by the oscillation of the thermal energy when the dryer switches on and off. During the experiments, the maximum electrical energy supplied to the dryer was adjusted to 10W. We found that the oscillation effect can advantageously be used to monitor the dryer efficiency. In contrast, when data are averaged over a timeframe larger than 30 minutes, the oscillations will be filtered out and are no longer visible in the measurement results.

An interesting finding using the low-cost dryer was the fact, that a computational compensation of hygroscopic growth effects of the SDS not equipped with the dryer was possible using the measurement data of the SDS011 equipped with the dryer. The SDS011 equipped with the dryer therefore could be used much like reference equipment. In essence, the SDS011 without the dryer measures the wet aerosol and the SDS011 equipped with the dryer measures the dry aerosol. The ratio of both is equivalent to the growth function. The use of the Hänel growth function works well for the compensation and the fitting of the model function into the measured data. After correction, a correlation of $R^2 = 0.99$ was achieved for the PM2.5 data of a single hygroscopic growth event. Again however, this correction approach clearly showed a failure when fitting the model function to data measured during fog events. This confirms once more that the computational correction of the humidity influence during fog events cannot be corrected using a computational correction method. In contrast, the correction method using the thermal low-cost aerosol dryer worked properly for various fog events that occurred during the field measurements.

During the co-location field measurement, executed in Munich, we compared the results of a separate Twin-SDS measurement box equipped with a SD011 with dryer and a SDS011 without dryer to the

results of a governmental measurement station for air quality operated by the Landesamt für Umwelt (LfU) in Bavaria. In the experiment we concentrated on measuring the PM2.5 mass concentration, since we were not able to install the Twin-SDS measurement box in immediate vicinity to the reference station but only at a distance of 550m. During this co-location experiment we also were able to record a strong fog event, a Sahara dust event, and a phase during which hygroscopic growth occurred. The outcome of the co-location experiment clearly showed a significant improvement in the correlation between the SDS011 data and the data of the reference equipment with respect to its coefficient of determination R^2 for the SDS011 equipped with the dryer. The very interesting outcome however was, that an almost perfect match between the PM10 output across the whole measurement period of the SDS011 equipped with the dryer and the PM2.5 measurement of the reference station was achieved, after calibrating the SDS011 PM10 signal to the PM2.5 signal of the reference station. Particularly the Sahara dust event helped to understand this phenomenon. It seems to be related to the fact that the PM2.5 collection efficiency characteristic of the SDS011 does not reach up to the fraction with diameters larger than 1.5um that is required to measure PM2.5 correctly. Interestingly this fraction seems to be contained in the signal that is output as PM10 by the SDS011 sensor. The coefficient of determination that could be achieved during a correlation of the PM10 signal of a SDS011 equipped with the dryer, the reference station was $R^2 = 0.911$ and the achieved RMS error was just 3.02ug/m^3.

The fog event and the hygroscopic growth event recorded in Munich showed the same properties as the fog events and hygroscopic growth events analysed in Stuttgart. A key result however was that neither the fog event nor the hygroscopic growth event adversely affected the good matching of the obtained signals from the SD011 equipped with dryer to the LfU reference station. Therefore, we can conclude that the low-cost dryer could completely remove both the fog event and the hygroscopic growth event also with respect to the co-location matching result. Whereas the computational correction results for the humidity influence only worked during time-limited growth phases also in the co-location experiment, we could proof the effective correction of the humidity influence over the whole timeframe of the co-location experiment for the SDS011 equipped with the low-cost dryer.

Comparison of both correction methods

From the result of this research work we conclude that the investigated computational correction of the humidity influence in case of the SDS011 low-cost PM sensor only works for PM2.5 during limited phases of hygroscopic growth and only achieves a moderate improvement. The method works only when the hygroscopic growth function model was adapted to the local and seasonal properties of the ambient aerosol using reference equipment shortly before deployment of the correction and requires a highly accurate humidity sensor. It seems not to be possible to use generally valid parameters for a growth function model to achieve a universal correction. Therefore, the computational correction of the humidity influence seems not to be an appropriate approach for a large sensor network measuring PM.

In contrast, the use of a low-cost dryer in conjunction with measuring the humidity in the exhaust air of the low-cost PM sensor seems to be a promising approach for humidity influence regardless of being caused by fog events or hygroscopic growth events. All our experiments showed a high efficiency of the designed low-cost dryer to correct the humidity influences of both types. This humidity correction approach will of course increase the cost of the sensor node and will make the sensor node bulkier. It also requires a modification of the PM-sensor to integrate the humidity sensor. However, it will substantially increase the quality of the measured data in a way that justifies the higher cost and the larger size of a PM-sensor node. The use of a low-cost dryer in a future low-cost PM-sensor node will still be cheaper by orders of magnitude compared to professional equipment.

We also believe that the results obtained in this work can be transferred to a certain degree to low-cost sensors other than the SDS011 if the mechanical fixturing of the dryer can be achieved and an internal humidity sensor is either available or can be installed. The result may be transferred to more costly sensors such as the Alphasense PM sensors. In this case of the Alphasense PM sensors the calibration offers more flexibility since the sensors also output the number concentration spectrum. Therefore, we anticipate an even better matching of the results to reference instrument when using a low-cost dryer as presented for the SDS011 in this work.

Literature

/1/ Website of the citizen science network “luftdaten.info” developed by the OK Lab Stuttgart

/2/ Budde M. et al., Potential and Limitations of the Low-Cost SDS011 Particle Sensor for Monitoring Urban Air Quality, Proceedings of the 3rd International Conference on Atmospheric Dust - DUST2018

/3/ Budde, M. et al, Suitability of the Low-Cost SDS011 Particle Sensor for Urban PM-Monitoring, Scientific Research Abstracts Vol. 8, p. 11, 2018 ISSN 2464-9147 (Online)

/4/ LUBW (2017), Messungen mit dem Feinstaubsensor SDS011 - Ein Vergleich mit einem eignungsgeprüften Feinstaubanalysator, LUBW Landesanstalt für Umwelt, Messungen und Naturschutz Baden-Württemberg Karlsruhe, Referat 63 – Messsystemtechnik Referat 14 – Marktüberwachung, Qualitätssicherung

/5/ Olga Laskina et al.; Size Matters in the Water Uptake and Hygroscopic Growth of Atmospherically Relevant Multicomponent Aerosol Particles; J. Phys. Chem.A2015, 119, 4489−4497

/6/ Annett Skupin; Optische und mikrophysikalische Charakterisierung von urbanem Aerosol bei (hoher) Umgebungsfeuchte; PH.D. Thesis, Univ. Leipzig, 2013

/7/ Charles O. Stanier et al.; A Method for the In Situ Measurement of Fine Aerosol Water Content of Ambient Aerosols: The Dry-Ambient Aerosol Size Spectrometer (DAASS); Aerosol Science and Technology, 38(S1):215–228, 2004

/8/ Hänel, G. (1976). Aerosol Particles as Functions of the Relative Humidity at Thermodynamic Equilibrium with the Surrounding Moist Air. In "Advances in Geophysics" (H. E. Landsberg, and J. Van Mieghem, Eds.), Vol. 19, pp. 74–189. Academic Press, New York, London.

/9/ Sutyajeet Soneja et al.; Humidity and Gravimetric Equivalency Adjustments for Nephelometer-Based Particulate Matter Measurements of Emissions from Solid Biomass Fuel Use in Cookstoves; Int. J. Environ. Res. Public Health 2014, 11, 6400-6416

/10/ Database archive of luftdaten.info sensor data: http://archive.luftdaten.info

/11/ Norbert Streibl; Influence of Humidity on the Accuracy of Low-Cost Particulate Matter Sensors; http://dx.doi.org/10.13140/RG.2.2.21095.75683

/12/ Hinds, William C.; Properties, behaviour, and measurement of airborne particles; Wiley Interscience, 1998

/13/ Bianca Kroseberg; Modifikation eines Feinstaubsensors zur Kompensation der Feuchtigkeitsabhängigkeit; Bachelorarbeit an der Universität Regensburg; 14. April 2021

Appendix

Arduino Code for the Twin-SDS-Measurement Box

```
#define LEN 9
#define windowSize 10
#define gate 5
#define HYT939_ADDR 0x28
#define TFACTOR 99.2909
#define TDELTA 40.0
#define HFACTOR 163.83
#define rhThres 35


#include <SoftwareSerial.h>
#include <SPI.h>
#include <SD.h>
#include <Wire.h>
#include "RTClib.h"
#include <SoftwareSerial.h>

RTC_PCF8523 rtc;

int dryerOn;

unsigned char incomingByte;
unsigned char buf[10];

int serActive = 0;

float aveArr2_5[windowSize];
float aveArr10[windowSize];
int PM2_5Val = 0;
int PM10Val = 0;
float PM2_5ave = 0;
float PM10ave = 0;
int loopCnt = 1;
String timeStr;
char fileName[15] = "datalog.txt";
File myFile;


void setup() {
  Serial.begin(9600);
  Serial1.begin(9600);
  Serial2.begin(9600);

  pinMode(gate, OUTPUT);


  if (! rtc.begin()) {
    Serial.println("Couldn't find RTC");
    while (1);
  }
  if (! rtc.initialized()) {
    Serial.println("RTC is NOT running!");
    // following line sets the RTC to the date & time this sketch was compiled
    rtc.adjust(DateTime(F(__DATE__), F(__TIME__)));
    // This line sets the RTC with an explicit date & time, for example to set
    // January 21, 2014 at 3am you would call:
    //rtc.adjust(DateTime(2017, 1, 21, 3, 0, 0));
  }
  //rtc.adjust(DateTime(F(__DATE__), F(__TIME__)));

  pinMode(10, OUTPUT); // SD Card CS
  pinMode(9, OUTPUT); // status LED
  digitalWrite(9, HIGH);  // status not ready

  if (!SD.begin(10)) {
    Serial.println("SDcard not ready\n");
    return;
  }


  if (!SD.exists(fileName)) {
    myFile = SD.open(fileName, FILE_WRITE);
    myFile.println("###");
```

```
    myFile.flush();
  }
  else {
    myFile = SD.open(fileName, FILE_WRITE);
    myFile.println("-----");
    myFile.flush();
  }
  pinMode(9, LOW); // status ok

  Serial.println("Wait for averaged data ...");
}


void getTime() {
    DateTime now = rtc.now();   // Real time clock may not be called in SDS011 read routine
(interrupt conflict?)
    timeStr = String(now.day()) + '.' + String(now.month())  + '.' + String(now.year()) + ' ' +
String(now.hour()) + ':' + String(now.minute()) + ':' + String(now.second());
}

float runAve(float aveArr[], float x, int n) {
  float sum=0;
  int i;

  for (i=0; i<n-1; i++) {
    aveArr[i] = aveArr[i+1];
  }
  aveArr[n-1] = x;

  for (i=0; i<n; i++) {
    sum = sum + aveArr[i];
  }

  sum = sum/n;
  return sum;
}

void loop() {
  unsigned char checksum = 0;

  unsigned int traw;
  unsigned int hraw;
  double temp;
  double hum;
  int i;
  unsigned char buffer[4];


  // read hyt221
  Wire.beginTransmission(HYT939_ADDR); // transmit to device #44 (0x2c)
  Wire.endTransmission(); // stop transmitting
  delay(100);
  Wire.requestFrom(HYT939_ADDR, 4,true);
  i=0;
  while(Wire.available()) {
    char c = Wire.read(); // receive a byte as character
    buffer[i]=c;
    i++;
  }
  traw=buffer[2]*256+buffer[3];
  hraw=buffer[0]*256+buffer[1];
  traw&=0xfffc;
  hraw&=0x3fff;
  traw=traw/4;
  temp=(double)traw/TFACTOR;
  temp=temp-TDELTA;
  hum=(double)hraw/HFACTOR;

  //humidity control
  if (hum > rhThres) {
    digitalWrite(gate, HIGH); //turn on dryer
    dryerOn = 1;
  }
  if (hum < rhThres) {
    digitalWrite(gate, LOW); //turn off dryer
    dryerOn = 0;
  }
```

```
// read two SDS
while (serActive == 0) {
  checksum = 0;
  if (Serial1.available()>0) {
    do {
      incomingByte = Serial1.read();
    } while(incomingByte != 0xAA);
    delay(100); //this number is critical, all 9 following bytes must have arrived
    for (i=0; i<9; i++) {
      buf[i] = Serial1.read();
    }
    /*
    for (i=0;i<9;i++) {
      Serial.println(buf[i], HEX);
    }
    Serial.println();
    */
    if ((buf[0] == 0xC0) && (buf[8] == 0xAB)) {
      for (i=1; i<=6; i++) {
        checksum = checksum + buf[i];
      }
      if (checksum == buf[7]) {
        PM2_5Val=((buf[2]<<8) + buf[1]);
        PM10Val=((buf[4]<<8) + buf[3]);
        PM2_5ave = runAve(aveArr2_5, PM2_5Val/10.0, windowSize);
        PM10ave = runAve(aveArr10, PM10Val/10.0, windowSize);

        if (loopCnt == windowSize) {
          getTime();
          Serial.print(serActive);
          Serial.print(' ');
          Serial.print(timeStr);
          Serial.print(" PM10: ");
          Serial.print(PM10ave);
          Serial.print(" ug/m3 ");
          Serial.print("PM2.5: ");
          Serial.print(PM2_5ave);
          Serial.print(" ug/m3");
          myFile.print(timeStr);
          myFile.print("\t");
          myFile.print(PM10ave);
          myFile.print("\t");
          myFile.print(PM2_5ave);
          loopCnt = 1;
          serActive = 1;
        }
        else {
          loopCnt++;
        }
      }
      else {
        Serial.println("checksum Error");
      }
    }
    else {
      Serial.println(" frame error");
    }
  }
}

while (serActive == 1) {
  checksum = 0;
  if (Serial2.available()>0) {
    do {
      incomingByte = Serial2.read();
    } while(incomingByte != 0xAA);
    delay(100); //this number is critical, all 9 following bytes must have arrived
    for (i=0; i<9; i++) {
      buf[i] = Serial2.read();
    }
    /*
    for (i=0;i<9;i++) {
      Serial.println(buf[i], HEX);
    }
    Serial.println();
    */
    if ((buf[0] == 0xC0) && (buf[8] == 0xAB)) {
      for (i=1; i<=6; i++) {
```

```
          checksum = checksum + buf[i];
        }
        if (checksum == buf[7]) {
          PM2_5Val=((buf[2]<<8) + buf[1]);
          PM10Val=((buf[4]<<8) + buf[3]);
          PM2_5ave = runAve(aveArr2_5, PM2_5Val/10.0, windowSize);
          PM10ave = runAve(aveArr10, PM10Val/10.0, windowSize);

          if (loopCnt == windowSize) {
            getTime();
            Serial.print(' ');
            Serial.print(serActive);
            Serial.print(" PM10: ");
            Serial.print(PM10ave);
            Serial.print(" ug/m3 ");
            Serial.print("PM2.5: ");
            Serial.print(PM2_5ave);
            Serial.print(" ug/m3");
            myFile.print("\t");
            myFile.print(PM10ave);
            myFile.print("\t");
            myFile.print(PM2_5ave);
            loopCnt = 1;
            serActive = 0;
          }
          else {
            loopCnt++;
          }
        }
        else {
          Serial.println("checksum Error");
        }
      }
      else {
        Serial.println(" frame error");
      }
    }
  }

  Serial.print(' ');
  Serial.print(temp);
  Serial.print(' ');
  Serial.print(hum);
  Serial.print(' ');
  Serial.print(dryerOn);
  Serial.println();

  myFile.print('\t');
  myFile.print(temp);
  myFile.print('\t');
  myFile.print(hum);
  myFile.print('\t');
  myFile.print(dryerOn);
  myFile.println();
  myFile.flush();

}
```